THE ROLES OF LZAP IN VERTEBRATE EMBRYOGENESIS AND HEAD AND NECK CARCINOGENESIS

By

Dan Liu

Dissertation

Submitted to Faculty of the

Graduate School of Vanderbilt University

In partial fulfillment of the requirements

for the degree of

DOCTOR OF PHILOSOPHY

In

Cancer Biology

December, 2012

Nashville, Tennessee

Approved:

Professor Albert B. Reynolds

Professor David K. Cortez

Professor Harold L. Moses

Professor Wendell G. Yarbrough

ORIGINAL PUBLICATIONS

1. **Liu D**, Wang WD, Melville DB, Cha YI, Yin Z, Issaeva N, et al. Tumor suppressor LZAP regulates cell cycle progression, doming, and zebrafish epiboly. ***Dev Dyn***. 2011;240:1613-25.
2. An H, Lu X, **Liu D**, Yarbrough WG. LZAP inhibits p38 MAPK (p38) phosphorylation and activity by facilitating p38 association with the wild-type p53 induced phosphatase 1 (WIP1). ***PLoS ONE***. 2011;6:e16427.
3. Law JH, Whigham AS, Wirth PS, **Liu D**, Pham MQ, Vadivelu S, et al. Human-in-mouse modeling of primary head and neck squamous cell carcinoma. ***Laryngoscope***. 2009;119:2315-23.

Dedicated to

My loving family and friends, especially my father, Zeyin Liu, and my mother, Junping Liu,

who contributed tremendously to this work from the very beginning,

even though they cannot read English.

ACKNOWLEDGEMENTS

At the endpoint of my graduate studies, I realize that for every accomplishment that I have made in my life and career, numerous people have put their greatest efforts into it, extended their valuable assistance in the preparation and completion of this work. Thank you for helping me to achieve my dream as a Ph.D. candidate for the past five years. The journey has been fraught with failed experiments and long hours, but also filled with moments of accomplishment and true joy. Thank you for supporting me through the journey and you deserve my earnest acknowledgements.

First and foremost, I am heartily thankful to my Ph.D. mentor, Dr. Wendell G. Yarbrough, a creative, brilliant and humorous head and neck physician and scientist. He led me into the field of cancer research and supported my research interest. From the initial to the final stage of my graduate study, he has been on my side over the past few years as a patient teacher, an effective helper and a sincere friend. More importantly, Dr. Yarbrough encouraged his students the time and resources to research and grow independently in a free atmosphere of his lab. Dr. Yarbrough has not only provided me with abundant opportunities to participate in various aspects of academic research, but is also very instructive and supportive in helping me build up and ultimately move forward my career. I am grateful to him for the opportunity to be his graduate student, to work, grow and mature under his guidance.

I also would like to thank my dissertation committee members: Dr. Al Reynolds, Dr. Hal Moses, and Dr. David Cortez for their guidance and encouragement to help me getting to this point. They are great instructors and overseers, who have influenced me greatly with their scientific passion and perspectives. Together, my respect and gratitude to this amazing formation of my thesis committee cannot be adequately expressed here.

I am also delighted to work with Dr. Ela Knapik and her lab colleagues. She has taught me how to work on the new zebrafish models challenged by new experimental techniques and new biological thoughts. Their dedication and enthusiasm to science and help as collaborators greatly facilitated our project and contributed greatly to my first first-author publication.

Thank you to all the past and current members of the Yarbrough lab team who moved from Vanderbilt to Yale. It has been a great pleasure working with and learning from you over the past few years. Dr. Natalia Issaeva is an incredible teacher and I am so thankful for her patience and willingness to teach me everything from experiment design to data interpretation in the field of DNA damage response. I am also appreciative of Dr. Hanbing An and Xinyuan Lu. Without them, my long journey dedicated to LZAP would have been more lonely and difficult. I enjoyed the moments during lab meetings when we discussed experiment ideas as a group. Brandee Brown and Mi Zou are the hands of the Yarbrough lab. Brandee serves as the lab manager and is in charge of the operation and maintenance of the whole lab. Mi, who recently became our new lab manager, is very nice in helping our experiment set up or solving technical problems. I am also grateful to other past and current lab members' help and contributions to my projects. They are: Zhirong Yin, Sergey Ivanov, Alexander Panaccione, Andrew Sewell, Jonathon Law, Sangeetha Vadivelu, and Yong Cha.

I am indebted to many other wonderful collaborators, colleagues and staff from Vanderbilt who support me. They are: Jin Chen, Wender Wang, David Melville, Asel Biktasova, Chris Barton, Chung-I Li, Shyr Yu and Tracy Tveit. I am grateful to their help and contributions to my graduate studies. Financial funding of my research was provided by NIH grants # 2 RO1 DE013173 (Wendell Yarbrough) and funds from the Bill Wilkerson Center for Otolaryngology and Communication Sciences and the Department of Otolaryngology, and through an endowment to the Barry Baker Laboratory for Head and Neck Oncology at Vanderbilt University.

Lastly, I would like to thank my friends and family, especially my parents for their unlimited love and their support and encouragement for my study abroad. I want to thank all of my friends in Nashville for their company and friendship during the past five years. Had they not been a part of my life, it would not have been an experience that was so much easier and enjoyable than I ever thought possible! Thank you!

TABLE OF CONTENTS

LIST OF TABLES

LIST OF FIGURES

LIST OF ABBREVIATIONS

ATM	ataxia telangiectasia mutated
ATR	ATM- and Rad3-related
DDR	DNA damage response
DNA-PK	DNA-dependent protein kinase
DSB	double strand break
DMSO	dimethyl sulfoxide
dpf	days post-fertilization
ES	embryonic stem
FACS	fluorescence-activated cell sorting
HDAC	deacetylase
H&E	hematoxylin and eosin
HNSCC	Head and Neck Squamous Cell Carcinoma
HP	hematopoietic
hpf	hours post-fertilization
HPV	human papillomavirus
hr	hour(s)
IB	immunoblotting
Ig	immunoglobulin
IP	immunoprecipitation
IR	ionizing radiation
KO	knockout
LZAP	LXXLL/leucine zipper-containing ARF-binding protein
MAPK	mitogen activated protein kinase
MBT	midblastula transition

MDM2	murine double minute 2
MEF	mouse embryonic fibroblast
min	minutes
MO	morpholino
mtp53	mutant p53
NCL	nucleolin
NF-κB	nuclear factor-kappa B
NLS	nuclear localization signal
NPM	nucleophosmin
PFTα	Pifithrin-α
PFTμ	Pifithrin-μ
PI	propidium iodine
PIKK	phosphoinositide kinase-related kinase
SCC	Squamous Cell Carcinoma
SD	standard deviation
TAD	Transactivation Domains
TBE	Tris-borate-EDTA
TMA	tumor microarray
TNFα	tumor necrosis factor-α
UTR	untranslated region
Wip1	wild-type p53-induced phosphatase
wtp53	wild-type p53

CHAPTER I

INTRODUCTION

Overview

Head and Neck Squamous Cell Carcinoma (HNSCC) accounts for more than 90% of all head and neck cancers and is the sixth most common cancer worldwide with approximately 50,000 cases occurring annually in the United States. Exploring molecular contributors to HNSCC, we have previously reported that expression of LZAP is lost in about 30% of HNSCC. LZAP (also called CDK5rap3 or C53) was first described as a binding partner of the 35kDa CDK5 activator binding protein $p35^{Nck5a}$ in 2000 (Ching et al., 2000). Activity of CDK5rap3 in association with $p35^{Nck5a}$ has not been further characterized and is not likely to represent its major activity since expression of CDK5 and $p35^{Nck5a}$ is restricted to neurons while LZAP is ubiquitously but variably expressed in all tissues we tested (Ching et al., 2000; Wang et al., 2006). Consistent with alternative roles for CDK5rap3, we have identified this protein as a novel binding partner for the tumor suppressor ARF (alternative reading frame) through an unbiased yeast two-hybrid screen approach in 2006. Based on these data, we renamed this protein LZAP for LXXLL/leucine zipper-containing ARF-binding protein. LZAP is a highly conserved protein in vertebrates, invertebrates and plants, but homologues do not exist in yeast and bacteria. Inside the cell, LZAP localizes to cytoplasmic and nuclear compartments. Database search and literature to date to identify homologs and conserved domains revealed that LZAP shares no significant amino acid homology with any other known proteins and has no conserved functional domains, except for putative leucine zipper (amino acid 357-385) and LXXLL motifs. However, we previously demonstrated that LZAP loss promotes tumor growth *in vivo* and that LZAP is lost in ~30% of human HNSCC (Wang et al., 2007a). We have targeted LZAP in mice and our preliminary findings suggest that mice with targeted LZAP are susceptible to lung tumor formation (unpublished data). Collectively, these data suggest that

LZAP functions as a tumor suppressor. Molecular mechanisms of LZAP activities continue to emerge. We and others have described LZAP functions to regulate activities of ARF, p53, p38 MAPK, NF-κB, Wip1, Chk1 and Chk2.

Mechanisms of LZAP activity

LZAP and ARF

The tumor suppressor ARF is a product of the *INK4a/ARF* locus, which encodes $p16^{INK4a}$ and $p14^{ARF}$ ($p19^{ARF}$ in mice), two unrelated tumor suppressors (Quelle et al., 1995). While $p16^{INK4a}$ prevents phosphorylation of the Rb (retinoblastoma protein), which is important for its growth suppressive functions, the activity of ARF is linked to its interaction and inhibition of MDM2 (HDM2 in human), the major negative regulator of the human tumor suppressor p53 (Pomerantz et al., 1998; Zhang et al., 1998). ARF expression can be induced by multiple oncogenic stimuli, resulting in a p53-dependent cell cycle arrest and/or apoptosis (Weber, 2000). As such, ARF functions as a major cellular defense protecting the cells with excessive proliferative signaling and consequently, many human tumor types are detected with loss of ARF expression. ARF has been shown to counteract the p53-inhibitor functions of MDM2 and at least two models have been proposed (Weber et al., 1999; Zhang and Xiong, 1999). First, ARF disrupts HDM2 binding to p53 and sequesters HDM2 in the nucleolus (Tao and Levine, 1999). Second, ARF binds and forms a ternary complex with HDM2 and p53 in the nucleus, and inhibits HDM2's ubiquitination and transcriptional inhibition of p53 (Zhang and Xiong, 2001).

In addition to the p53-dependent activities of ARF, emerging data suggests that ARF may be involved in cellular processes independent of p53, including cell cycle arrest, ribosomal biogenesis and apoptosis (Donehower et al., 1992; Kamijo et al., 1999). If all tumor suppressive functions of ARF were attributed solely to functional p53, the tumor phenotypes of $p53^{-/-}$ mice would be more severe and encompass the $ARF^{-/-}$ tumorigenesis phenotype. However, distinct

differences are observed during tumor formation in $ARF^{-/-}$ mice compared to $p53^{-/-}$ mice (Donehower et al., 1992; Kamijo et al., 1999). For example, a substantial percentage of $ARF^{-/-}$ mice spontaneously develop carcinomas and neurogenic tumors which are rarely observed in $p53^{-/-}$ mice, and therefore might be p53 unrelated. Additional supporting evidence came from oncogene-induced lymphoma in p53/ARF double KO mice, which develop tumors earlier and are more resistant to therapy compared to lymphoma derived from either p53 or ARF single KO mice (Schmitt et al., 1999). These data suggest that loss of p53 and ARF may have similar, but not identical effects on tumor formation. The mechanisms by which ARF enhances tumor formation independent of p53 are not well known, thus studying the regulators of ARF is of great importance for a full spectrum of ARF tumor suppressive functions.

It has been reported and well characterized that regulation of ARF transcription can by activated by inappropriate hyperproliferative oncogenic signaling, such as that provided by E1A, ras, myc and E2F-1 (Bates et al., 1998; Palmero et al., 1998; Zindy et al., 1998; de Stanchina et al., 1998). However, more recent studies suggest that ARF can also be regulated post-translationally. The ARF tumor suppressor is subject to proteasome-mediated degradation after N-terminal polyubiquitination (Kuo et al., 2004). Furthermore, the nucleolar protein nucleophosmin (NPM) sequesters ARF in the nucleolus, by competitive binding with HDM2 through the same domain, thus impairing ARF-mediated p53 stabilization and activity (Korgaonkar et al., 2005). Several other ARF-binding partners have been identified, such as E2F-1, HIF-1α and a novel protein, CARF (Eymin et al., 2001; Fatyol and Szalay, 2001; Hasan et al., 2002). Most of these binding partners do not regulate ARF activity toward p53, either positively or negatively (Vivo et al., 2001; Hasan et al., 2002). To identify ARF-interacting proteins that may be involved in the regulation of ARF activity, we used a yeast two-hybrid system and screened for binding partners. LZAP was a novel human protein that bound ARF and was identified from the screen. Binding of LZAP to ARF was confirmed in mammalian cells both *in vitro* and *in vivo*. The identified protein

proved to be highly similar to the rat protein C53, which was previously identified as a p35-associated protein, the precursor of the CDK5 activating subunit (Ching et al., 2000). Our lab has previously shown that this leucine Zipper-containing ARF-binding Protein (LZAP) directly and specifically binds to the N-terminal region of human ARF, and that this interaction is induced by oncogenic stimulation. Upon direct binding to ARF, LZAP reverses ARF inhibition of HDM2's p53 ubiquitination activity, but despite of its ability to restore HDM2-mediated p53 ubiquitination in the presence of ARF, LZAP does not decrease p53 stability. Surprisingly, LZAP results in further augmentation of p53 transcriptional activity. Ectopic expression of LZAP plasmids in mammalian cells induces p53-dependent G1 cell cycle arrest. But a similar pattern of p53 activation is observed in ARF null cells. These findings suggest that LZAP regulates p53 through unknown ARF-independent mechanism(s) that are independent of ARF.

LZAP and the p53 pathway

The tumor suppressor protein 53, is one of the two major tumor suppressors implicated in human cancers (Weinberg, 1995) and is frequently mutated in HNSCC. Major tumor suppressor activities of p53 include induction of apoptosis and inhibition of cellular proliferation mediated through p53's transcriptional activity and by a mitochondria pathway. Because p53 regulates cellular proliferation and apoptosis, p53 activity within the cell is tightly controlled at multiple levels.

Mutations that alter p53 activity occur in approximately 50% of human cancers, including HNSCC, and have been associated with poor overall survival in HNSCC (Soussi et al., 2006; Poeta et al., 2007). Excluding mutations or loss of expression, the molecular pathways responsible for inhibition of p53 activity in cancer remain to be fully elucidated; however, themes observed in many cancers impact p53 protein modification and/or p53 protein stability (Ko and Prives, 1996). Both the human papilloma virus (HPV) E6 protein and the endogenous HDM2

protein are oncogenes that serve as p53 ubiquitin ligases and play a critical role in targeting p53 for degradation (Scheffner et al., 1993; Kubbutat et al., 1997). Most tumors with amplified or overexpressed HDM2 or with HPV E6 expression do not acquire p53 mutations and maintain expression of wild-type p53 suggesting that inactivation of p53 by E6 or HDM2 sufficiently inhibits p53 to support tumorigenesis (Leach et al., 1993; Braakhuis et al., 2004). HDM2 is the major cellular regulator of p53 stability acting as a p53 E3 ubiquitin ligase resulting in p53 degradation that is dependent on the 26S proteasome (Lavin and Gueven, 2006). Because of its central role in regulation of p53, HDM2 activity is also regulated at multiple levels. As part of a negative feedback loop, p53 increases HDM2 transcription, and post-transcriptional modification of p53 and HDM2 modulate the ability of HDM2 to bind p53. ARF is the major protein inhibitor of HDM2 activity and is thought to primarily protect against inappropriate mitogenic stimulation and therefore tumorigenesis (Zindy et al., 2003; Views, 2004). ARF binds HDM2 and inhibits its p53 E3 ubiquitin ligase activity while simultaneously reversing HDM2's inhibition of p53 transactivation (Zhang et al., 1998; Zhang and Xiong, 2001). ARF expression is induced by multiple oncogenic stimuli resulting in p53-dependent cell cycle arrest and/or apoptosis (Sherr, 1998; Sherr and Weber, 2000). In this capacity, ARF directs a major cellular defense protecting the organism from cells with excessive proliferative signaling, and as a result, many human tumor types, including HNSCC, have frequent loss of ARF expression.

Although p53 protein stability is largely controlled by HDM2, it is also tightly controlled through a myriad of post-translational modifications including ubiquitination, phosphorylation, acetylation and sumoylation. As opposed to the p53 inhibitory role of ubiquitination, phosphorylation stabilizes and activates p53 (Lavin and Gueven, 2006). Phosphorylation of p53occurs by at least 19 kinases targeting 17 distinct serine or threonine residues (Dai and Gu, 2010). Phosphorylation of most residues of p53 results in stabilization, nuclear accumulation, and increased transcriptional activity. p53 phosphorylation is concentrated at the N-terminus of the

protein, which is responsible for transactivation and binding to HDM2, and at the C-terminal regulatory domain. Phosphorylation of Ser15 (Ser18 in mice) is the most commonly described modification of p53 and may serve as an initiator that potentiates further phosphorylation at Thr18 and Ser20 (Lavin and Gueven, 2006). Ser15, Thr18, and Ser20 are key residues for activation of p53 in response to DNA damage or cellular stress triggering recruitment of acetyl transferases, inhibition of MDM2 binding, and stabilization of p53. These residues in the N-terminus of p53 are phosphorylated by the DNA damage response proteins ATM/ATR, by the stress activated protein kinase p38 MAPK, and by DNA damage-associated checkpoint kinases Chk1/2 (Lavin and Gueven, 2006; Dai and Gu, 2010).

We have shown that LZAP further activates p53 in the presence of ARF (Wang et al., 2006). LZAP binds ARF, co-localizes with ARF, and forms a ternary complex with ARF, HDM2 and p53. Expression of LZAP in the presence of ARF further enhances p53-mediated expression of the cyclin-dependent kinase inhibitor $p21^{Cip1}$ and enhances the ARF-mediated G1 cell cycle arrest. Mechanistically LZAP was found to stabilize p53 protein in the presence of HDM2 through inhibition of p53 nuclear export (Wang et al., 2006). Remarkably, we also found that in the absence of ARF, LZAP increases p53 transcriptional activity with resultant G1 cell cycle arrest. Because LZAP does not inhibit proliferation in cells lacking p53 activity , LZAP mediated cell cycle arrest is dependent on p53 (Wang et al., 2006). These data reveal that LZAP activates p53 in the presence and absence of ARF. The mechanism of LZAP activity in the absence of ARF was previously not described, but could be explained by novel LZAP-binding partners (see preliminary data).

LZAP and the NF-κB pathway

Nuclear factor-kappa B (NF-κB) was discovered in the mid-1980s as a sequence-specific DNA-binding protein that recognizes a DNA element in the mouse immunoglobulin (Ig) κ gene intronic

enhancer (Sen and Baltimore, 1986). It has been the focus of intense investigation since its discovery, chiefly because of the pleiotropic effects and vital roles in immunity, inflammation, stress response and tumorigenesis. Aberrant regulation of NF-κB signaling pathways is implicated in a wide range of human diseases, such as cancer, AIDS (Acquired Immune Deficiency Syndrome), diabetes, and viral infections (Kumar et al., 2004).

In mammals, there are five NF-κB/REL genes that encode seven proteins: RelA, cRel, RelB, NF-κB1 (also known as p50/p105) and NF-κB2 (also known as p52/100) (Fig. 1.1). All members of the family share a conserved sequence motif, the Rel homology domain (RHD) that spans nearly 300 amino acids and is responsible for homo/heterodimerization, DNA-binding and nuclear localization. Post translational modifications of amino acids within the RHD alter both DNA binding and transactivation properties of NF-κB. Only RelA, c-Rel and RelB contain transactivation domains (TAD) necessitating their presence within transcriptionally active NF-κB, while the other two family members, p50 and p52 lack TAD and functioning primarily as DNA-binding subunits in the complex. Among various NF-κB homo/heterodimers, the ubiquitously expressed RelA/p50 heterodimer is the most abundant form, and is responsible for most NF-κB function in different cell types, thus this heterodimer is often referred as NF-κB in general. Figure 1.1 is a schematic representation of Rel family members, as well as IκB family members that primarily function in NF-κB regulation.

The role of NF-κB as a tumor promoter/oncogene in the development of cancer was suspected because v-Rel, the viral homologue of c-Rel, causes aggressive tumors in chickens (Gilmore, 1999). It later became obvious that NF-κB, or more precisely the RelA/p50 heterodimer which comprises the most studied form of NF-κB, is activated in various tumor types and that activation of NF-κB promotes many aspects of oncogenesis including anchorage independent growth, angiogenesis, and proliferation while protecting tumor cells from apoptosis (Rayet and Ge, 1999;

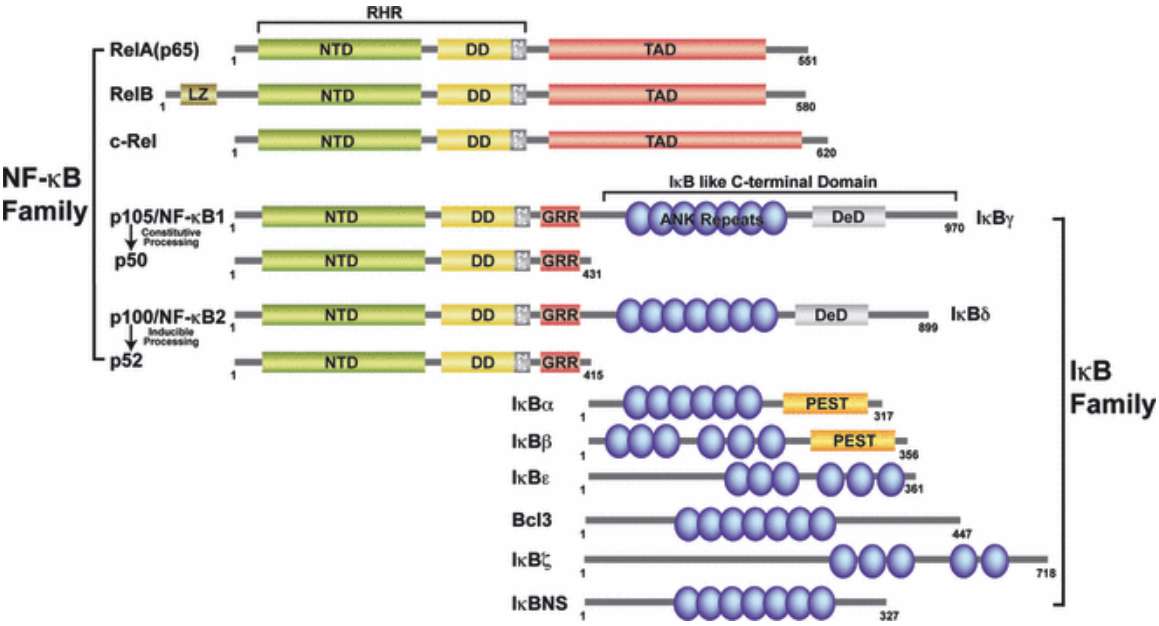

Figure 1.1. Members of the NF-κB and IκB Protein Families
NF-κB family is characterized by having the Rel homology region (RHR) shown in green and yellow. IκB proteins are characterized by the presence of ankyrin repeat domain (ARD) shown in blue.

Baldwin, 2001). NF-κB activation has been described in head and neck squamous cell carcinoma (HNSCC) with aberrant regulation of multiple NF-κB responsive genes identified by gene expression profiling of these cancers (Dong et al., 2001). The regulation of many genes that is controlled by NF-κB includes those involved in development, inflammation, immune response, proliferation, apoptosis, cellular transformation, angiogenesis and differentiation (Orlowski and Baldwin, 2002). The realization that NF-κB inhibits cellular apoptosis in response to cytokines led to investigation regarding its role in resistance to chemotherapy. Exposure of cancer cells to IR and chemotherapeutic agents was found to activate NF-κB. Inhibition of NF-κB, using a stabilized and mutated IκBα, termed IκB-super repressor (IκB-SR), remarkably increases the apoptotic response to these same cytotoxic agents (Baldwin, 2001). Recently, inhibition of NF-κB has evolved as a novel therapeutic target for cancer treatment. Using HNSCC cell lines, inhibition of NF-κB was found to increase cell sensitivity to radiation resulting in increased cell death (Kato et al., 2000). This enhanced chemo/radiotherapy-induced apoptosis in the presence of NF-κB inhibition is p53 independent (Baldwin, 2001). These data suggest that NF-κB activity may protect cancer cells from many of the commonly used therapeutic agents.

NF-κB activity is maintained under basal levels in unstressed cells, primarily through the inactivation by IκB proteins. IκB binds to the RHD and masks the nuclear localization signals (NLS) of NF-κB. In response to many different intracellular or extracellular signals such as TNFα and IL-1, the upstream IκB kinases (IKKα/β/γ) phosphorylate IκB and target it for ubiquitination and degradation dependent on the 26S proteasome. This degradation of IκB results in nuclear translocation of NF-κB. Like many other transcriptional factors such as p53, the DNA binding and transcriptional activities of NF-κB is regulated by multiple post-translational modifications to RelA, such as acetylation and phosphorylation (Gu and Roeder, 1997). Three types of distinct NF-κB activation signaling pathways have been described that have been called as the "canonical", "non-canonical or alternative" and "atypical" pathways. The canonical pathway is

well characterized by TNFα induced NF-κB activation. Upon TNFα stimulation, IKKβ/γ complex is activated and then phosphorylates IκBα, which promotes its recognition by an E3 ubiquitin ligase resulting in proteasome-mediated degradation. However, the alternative pathway is preferentially activated by a subset of other cytokines such as lymphotoxin β (LTβ), induce NF-κB activation through a different mechanism, primarily through IKKα activity resulting in RelB/p52 phosphorylation and processing to produce its active form, the RelB/p52 heterodimer. The resultant complex translocates into nucleus and initiates transcription of various target genes. Both pathways described above converge to activate the IKK complex and are dependent on its kinase activity. The more recently described "atypical" pathway suggests that some stresses, such as DNA damage induced by IR or doxorubicin, activate NF-κB independent of the upstream IKK kinases (Tergaonkar et al., 2003). For example, doxorubicin-induced degradation of IκB does not require phosphorylation of IκB, and thus is independent of IKKα/β activity (Tergaonkar et al., 2003). Although NF-κB is one of the most intensively studied transcription factors, and multiple regulatory pathways have been well illustrated, many facets of the delicate regulation of NF-κB remain unexplored. Novel mechanisms that regulate NF-κB activity are likely to be important in tumorigenesis and/or response of tumors to therapy.

We have shown that LZAP expression markedly inhibits RelA activity even in the presence of the NF-κB stimulating cytokines, TNFα and IL-1, or RelA overexpression. In fact, LZAP is as effective at inhibiting RelA transcription as IκB-SR. Conversely, loss of LZAP increases both basal and cytokine-induced RelA transcriptional activity. Functionally, decreased expression of LZAP increases expression of MMP-9 and increases cellular invasion, both dependent on NF-κB (Wang et al., 2007a). These data suggest that LZAP is a potent NF-κB inhibitor and that endogenous LZAP inhibits both basal and activated NF-κB.

Mechanistically, LZAP does not alter RelA DNA binding or nuclear localization suggesting that LZAP inhibition of RelA is mediated by physical interaction with or post-translational modification of RelA. We showed that LZAP binds RelA and that LZAP is found on chromatin at RelA promoters (MCP-1 and IL-8), and that LZAP loss in primary HNSCC is associated with increased IL-8 expression in the tumor (Wang et al., 2007a). LZAP expression is associated with decreased phosphorylation at S536 of RelA, and conversely, inhibition of LZAP expression increases phosphorylation at this same critical site. LZAP expression is also associated with increased histone deacetylases (HDACs) binding to RelA and with deacetylation of histones at RelA responsive promoters (MCP-1, IL-8). Collectively, these data suggest that LZAP regulation of NF-κB activity requires LZAP association with RelA and modification of RelA phosphorylation status.

LZAP and Chk1/2

To date, there is a single publication describing LZAP activity towards the checkpoint kinases Chk1 and Chk2 (hereafter called Chk1/2) (Jiang et al., 2009). Passage through the G2/M checkpoint depends on activation of the CDK1/cyclin B complex and is tightly regulated by Chk1/2 through CDC25. Recent evidence indicates that in response to DNA damage, additional pathways also impact the G2/M checkpoint through regulation of CDC25, such as the p38 kinases (Bulavin et al., 2002a). Endogenous and exogenous stresses, such as replication fork collapse or IR, result in DNA damage and activation of the apical serine/threonine protein kinases belonging to the PIKK family, including ATM, ATR and DNA-PK. Activated PIKKs in turn phosphorylate and activate the downstream checkpoint kinases Chk1/2. Although both Chk1 and Chk2 can phosphorylate and inhibit CDC25, Chk1 seems to be the primary kinase responsible for the G2/M checkpoint (Graves et al., 2000). Chk1/2-mediated phosphorylation of CDC25C at S216 is required for its recruitment of 14-3-3. Binding of 14-3-3 to CDC25C, either directly or through

cytoplasmic sequestration, inhibits CDC25C binding to the CDK1/cyclin B complexes (Bulavin et al., 2002a).

Jiang et. al. reported that during DNA damage response, LZAP inhibits Chk1/2 phosphorylation and activation. By counteracting Chk1, LZAP activates CDC25C resulting in downstream CDK1 activation (Jiang et al., 2009) (Fig. 1.2). It is well known that Chk1/2 are phosphorylated and activated after DNA damage by ATM and ATR. Expression of LZAP is associated with decreased phosphorylation and inhibition of Chk1/2, but this effect is not mediated through decreasing the activities of their upstream kinases. Since checkpoint kinases are inhibited by LZAP, their activity toward CDC25C is similarly inhibited, resulting in activation of CDK1 and inappropriate or early progression into mitosis (Jiang et al., 2009). Conversely, Jiang et. al. have shown that knockdown of LZAP inhibits of CDK1 and delays mitotic entry (Jiang et al., 2009). These results are consistent with an earlier report by the same group that LZAP increases sensitivity to genotoxins related to inappropriate progression through the G2/M checkpoint (Jiang et al., 2005). These data show that LZAP binds and inhibits Chk1 resulting in dysregulation of cell cycle progression, but Chk1 and Chk2 kinases phosphorylate and regulate targets in addition to CDK1, including p53. Mechanistically, it remains unclear how LZAP alters Chk1/2 phosphorylation and activity.

LZAP and p38 MAPK

The p38 mitogen-activated protein kinase (MAPK) family (p38α/β/γ/δ) together with the c-Jun N-terminal kinase (JNK) family belong to the stress-activated protein kinases (SAPKs) that primarily respond to cellular stress (osmotic, heat shock, DNA damage etc.) and/or cytokines (Waskiewicz and Cooper, 1995; Bulavin and Fornace, 2004). Both p38α and p38β are ubiquitously expressed, but expression patterns suggest that p38α is more abundant in most cell types, including HNSCC cell lines, and p38α has been most extensively studied (Junttila et al.,

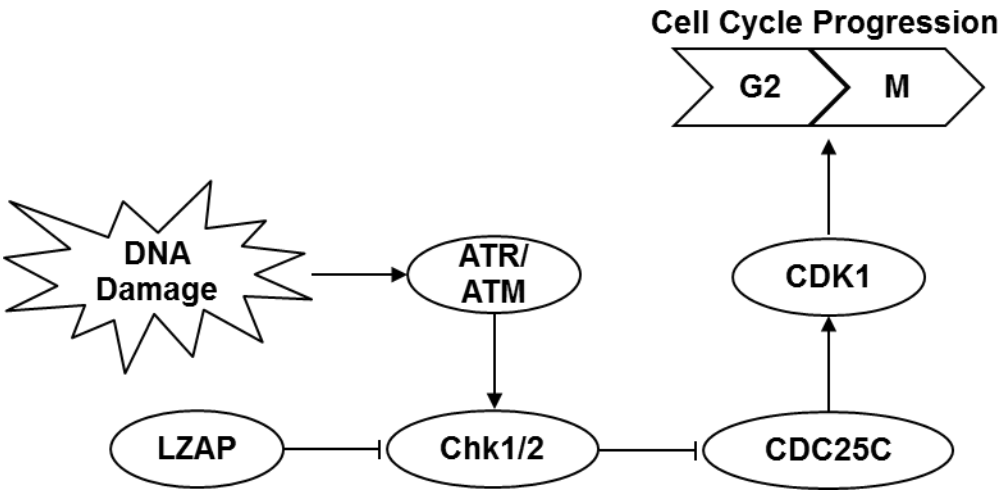

Figure 1.2. LZAP Inhibits Checkpoint Kinases
LZAP inhibits Chk1 and Chk2 causing activation of CDC25C and CDK1. Simplified, LZAP is an activator of CDK1 through inhibition of checkpoint kinases. Arrows indicate activation and T shapes indicate inhibition.

2007; Wagner and Nebreda, 2009). The other three isoforms, p38β/γ/δ, have more restricted patterns of expression and have relatively low expression levels.

p38 is activated by many extracellular stimuli through a classic MAPK kinase kinase (MAP3K)-MAPK kinase (MKK) signaling pathway. The major upstream activating kinases that are responsible for activation of p38 are MKK3 and MKK6, although other mechanisms such as MKK4 and auto-phosphorylation may also contribute to p38 activation (Cuenda and Rousseau, 2007). p38 activity regulates a wide range of substrates including transcription factors, such as p53, activating transcription factor 2 (ATF2) and NF-κB (Raingeaud et al., 1996; Bulavin et al., 1999; Saccani et al., 2002). Interestingly, the pleiotropic biologic effects of p38 activity have suggested that p38 can function both as a tumor suppressor and a tumor promoter.

Studies have focused on p38 tumor suppressor-like activities, mediated through cell cycle arrest, senescence, and apoptosis in many different cell types (Bulavin and Fornace, 2004). p38 engages multiple genes and pathways to regulate cell cycle arrest at both the G1/S and G2/M checkpoint (Bulavin and Fornace, 2004; Wagner and Nebreda, 2009). p38-mediated degradation of the G1 cyclin D1 contributes to G1 arrest (Thoms et al., 2007). p53 is also a direct substrate of p38 kinase activity, which can be phosphorylated by p38 on Ser33 and Ser46, inducing transcription of the $p21^{Cip1}$, with resultant inhibition of both G1 and G2 CDKs (Bulavin and Fornace, 2004). In addition to cell cycle inhibition through increasing p21 expression, p38 directly inhibits G2/M progression by phosphorylating and inhibiting the phosphatases required for activation of CDK1, namely CDC25B and CDC25A (Bulavin et al., 2001; Bulavin and Fornace, 2004). The role of p38 in cell senescence is supported by the observation that $p38^{-/-}$ MEFs can bypass replicative senescence in culture, a behavior that reminiscent of $p53^{-/-}$ and $ARF^{-/-}$ MEFs which are immortal in culture (Donehower et al., 1992; Kamijo et al., 1997; Hui et al., 2007). p38 induces apoptosis by transcriptional and post-transcriptional mechanisms, which may affect death receptors or

mitochondria-dependent apoptotic pathways through regulation on Bcl-2 proteins and p53 (Bulavin and Fornace, 2004). However, several studies have described pro-survival roles for p38, which are partially mediated by the induction of cell differentiation or by anti-apoptotic inflammatory signals (Wagner and Nebreda, 2009). p38 knockout mice models support p38 as a tumor suppressor where livers from conditional p38 knockout mice develop more tumor mass and increased tumor size *in vivo* in a diethylnitrosamine-induced hepatocellular carcinoma model (Hui et al., 2007). Ironically, existing evidence suggests p38 possesses opposing roles as an oncoprotein. Increased p38 activity is observed in many types of human cancers including lymphoma, breast cancer and HNSCC (Neve et al., 2002; Elenitoba-Johnson et al., 2003; Riebe et al., 2007). In HNSCC cell lines, inhibition of p38 decreases both MMP expression and cell invasion (Junttila et al., 2007; Riebe et al., 2007). In addition, $p38^{+/-}$ heterozygous mice are protected from lung metastases compared to wild-type mice (Matsuo et al., 2006). The oncogenic activities of p38 include protection of cells from apoptosis, as well as acceleration of cell proliferation, invasion, inflammation, and angiogenesis (Engelberg, 2004). The dual role of p38 in tumorigenesis is difficult to explain given sufficient conflicting data supporting both roles. It has been suggested that whether p38 functions as a tumor suppressor or oncogene likely depends on cellular context or tumor type, stage and perhaps most importantly, on the accompanying pathway activation or inactivation.

To better understand LZAP biological activities and to gain mechanistic insight, additional LZAP binding partners have been sought. A Scan Site Search (http://scansite.mit.edu/) using LZAP sequence revealed that LZAP contains sites predicted to bind to the common MAPK domain-docking domain (D domain). *In vivo* binding assays reveals interaction of LZAP with p38α MAPK, and immunofluorescent staining of expressed proteins shows p38α co-localizes with LZAP in the nucleus. LZAP expression is associated with a dose dependent decrease in p38

phosphorylation and activity, both at basal level and following cytokine stimulation. Conversely, siRNA-mediated loss of LZAP increases p38 phosphorylation and activity after cytokine treatment indicating that LZAP regulates p38 phosphorylation at basal levels. Mechanistically, LZAP does not decrease p38 phosphorylation of p38 based on inhibition of upstream kinases MKK3 or MKK6.

LZAP and Wip1 phosphatase

Our data describing LZAP regulation of RelA and p38 phosphorylation combined with data from others showing that LZAP decreases Chk1/2 phosphorylation suggest that a common effect of LZAP expression is to decrease phosphorylation of its bound proteins. A search of the literature identified two phosphatases (Wip1 and PP2A) that are responsible for dephosphorylation of RelA at Ser536 (Chew et al., 2009). Remarkably, Wip1 substrates include p38 and Chk1/2, which remarkably, are also LZAP regulated binding partners (Lu et al., 2008).

Aberrant or excessive kinase signaling is considered a hallmark of cancers, including HNSCC (Pomerantz and Grandis, 2004). Because kinases were initially thought to be more specific than phosphatases, kinases were viewed as more appropriate targets for anti-cancer therapies and have been more intensely studied (Lammers and Lavi, 2007). Compared to kinases, phosphatases have been less intensely studied and characterized, even though they are greatly implicated in tumorigenesis. Protein phosphatases can be broadly categorized based on their substrate specificity into tyrosine phosphatases or serine/threonine phosphatases. Metal-dependent protein phosphatases (PPM) are a subset of serine/threonine kinases distinguished by their requirement of divalent cations such as Mg^{2+} or Mn^{2+} for their activities and by their insensitivity to inhibition by the phosphatases inhibitor okadaic acid (Lammers and Lavi, 2007). A single family of phosphatases, PP2C, comprises the PPM group. Because the PP2C family members WIP1 and PPM1B are implicated in our future work, and these phosphatases have been implicated in

tumorigenesis, our focus will be limited to this phosphatase subgroup (Tamura et al., 2006; Lammers and Lavi, 2007). Regulation of PP2C activity is thought to be primarily through regulation of protein levels, post-translational modification, and subcellular compartmentalization (Lammers and Lavi, 2007).

Wip1 (also known as PPM1D and PP2Cδ) was identified in a screen to detect p53-responsive genes and named because it is a wild-type p53-induced phosphatase (Fiscella et al., 1997). Wip1 is a member of the PP2C family of serine/threonine phosphatases and has been extensively studied largely because of its role as an inhibitor of p53 working through a negative feedback loop. Many proteins have been identified as Wip1 substrates and common substrate recognition sequences have also been identified. The majority of Wip1 targets contain either TXY motifs, where X can be any amino acid or S/TQ motifs. The S/TQ motifs containing proteins that Wip1 targets for dephosphorylation are all phosphorylation targets of ATM or ATR, including p53, Chk1, Chk2, ATM, MDM2 and γH2AX (Lu et al., 2008; Cha et al., 2010). p53 is the most well-known and well-studied Wip1 target and inhibition of p53 by Wip1 occurs through five mechanisms (Fig. 1.3). The most direct mechanism through which Wip1 inactivates p53 is through dephosphorylation of p53 at Ser15 (Lu et al., 2005). Additionally, Wip1 dephosphorylates MDM2 at Ser395, an ATM phosphorylation site, leading to MDM2 activation (Lu et al., 2007). Additionally, Wip1 dephosphorylates and inactivates p38 kinase activity thereby inhibiting p53 activating phosphorylation on Ser33 and Ser46 (Takekawa et al., 2000). Finally, Wip1 dephosphorylates and inactivates both ATM and its target Chk2 (Lu et al., 2005; Shreeram et al., 2006). ATM and Chk kinases phosphorylate p53 on Ser15 and Ser20 respectively, resulting in activation and stabilization of p53 (Banin, 1998; Shieh et al., 2000). Collectively, these data suggest that the major target of Wip1 is p53 with resultant destabilization and inactivation of p53 by dephosphorylating p53 directly or indirectly through p53 regulatory proteins. The biologic consequences of p53 inactivation lead to diminished cell cycle arrest and apoptosis in response to

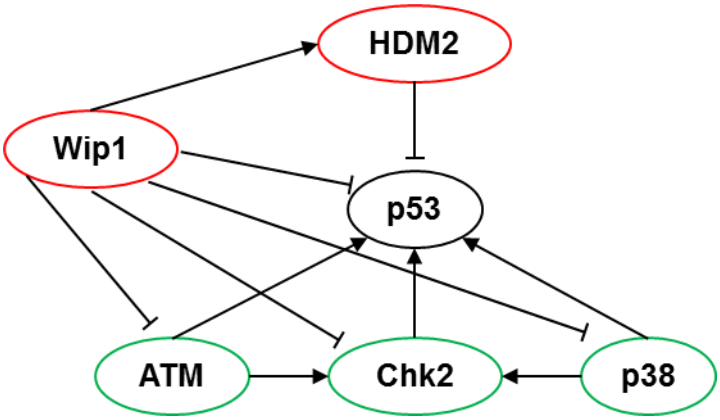

Figure 1.3. p53 is a major target of the Wip1 phosphatase
Wip1 inhibits p53 through direct dephosphorylation of p53 and through dephosphorylation of p53 activators and inhibitors. p53 inhibitors (MDM2 and Wip1) are represented in red oval and p53 activators (p38, Chk2, and ATM) are represented in green oval. Note that dephosphorylation of MDM2 at serine 395 by Wip1 is an activating event. In contrast, dephosphorylation of p53, ATM, Chk2, and p38 by Wip1 are inhibitory. Black arrows represent activation and red T shapes represent inhibition.

DNA damage or oncogenic stress. Although p53 is considered the major Wip1 target, there are many other cancer-related Wip1 targets (Takekawa et al., 2000). Wip1 exerts oncogenic activity through direct targeting and inhibition of p38 and Chk kinases to promote cell cycle progression (Bulavin et al., 2002a; Bulavin and Fornace, 2004). Additionally, MEFs derived from $Wip1^{-/-}$ knockout mice have decreased rates of proliferation and arrest at the G2/M transition, suggesting the role of Wip1 in promoting cell cycle progression (Choi et al., 2002). In addition, Wip1 knockout mice have increased ARF and p16 transcription and expression, suggesting that Wip1 also promotes cellular proliferation through inhibition of ARF and $p16^{INK4a}$ (Bulavin et al., 2004).

Given the direct and indirect targets of Wip1 (p53, ATM, Chk1, Chk2, MDM2, ARF, and p16), Wip1 has been implicated as an oncogene. Expression data from human cancers also revealed that the Wip1 gene is amplified in many tumor types including pancreas, lung, liver, bladder and breast cancers (Kallioniemi et al., 1994; Ried et al., 1994; Wong et al., 1999). RNA expression data from some primary human cells revealed that increased RNA expression of Wip1 correlates with chromosomal amplification (Bulavin et al., 2002b). Despite reports on Wip1 gene amplification, Wip1 protein expression data from tumors is lacking. Murine models have provided critical evidence in support of Wip1 as an oncogene. For instance, Wip1 knockout mice are partially resistant to tumor development (Harrison et al., 2004; Lu et al., 2008). $Wip1^{-/-}$ mice are resistant to ErbB2- or Ras-induced mammary tumor formation (Bulavin et al., 2004). Conversely, mammary-specific expression of Wip1 in mice increases sensitivity to ErbB2 mammary tumor formation, and Wip1 expressing tumor cells proliferate faster relative to cells from mice expressing ErbB2 alone (Demidov et al., 2007). Taken together, these data suggest that Wip1 alone is weakly oncogenic, but can collaborate and enhance tumor formation driven by other oncogenes.

It is established that p53 regulates Wip1 expression transcriptionally; however, no protein regulators of Wip1 activity or substrate specificity have been previously described. Since our data revealed that LZAP decreased p38 and RelA phosphorylation LZAP activity toward Wip1 was explored. We determined LZAP interaction with Wip1 by IP, both *in vitro* and *in vivo*. Following co-expression of LZAP and Wip1, immunofluorescent staining revealed that Wip1 co-localizes with LZAP in the nucleus.

Based on a review of the reported Wip1 targets, we found that LZAP shares a large pool of targets with Wip1 (Table 1). The roles of LZAP and Wip1 in the regulation of RelA, Chk1/2, p53, MDM2, and ARF are detailed (Table 1). Two cohorts of LZAP/Wip1 targets can be identified based on differences in phosphorylation and activity as a result of LZAP and Wip1. Explanations as to why LZAP and Wip1 activity toward some targets is congruent, while activity to other targets diverges are largely unknown; however, tone possibility is that direct protein-protein interaction between LZAP and the target may determine LZAP activity toward the target. Our preliminary and reported data suggest that LZAP binds to Wip1 and some Wip1 substrates, such as p38, Chk1/2 and RelA, but not others, such as p53 and MDM2 (Wang et al., 2006, 2007a; Jiang et al., 2009; An et al., 2011). Noticeably, if LZAP is capable of binding to the Wip1 substrates, LZAP and Wip1 have parallel effects on substrate activity; however, if LZAP does not bind to the Wip1 substrate, as is the case for p53 and MDM2, LZAP has opposite effect on substrate activity compared to Wip1 (Table 1). Thus, we intuitively suspect that LZAP regulation of Wip1 activity depends on LZAP ability to bind specific Wip1 substrates. In this model, LZAP binding to a Wip1 substrate would direct Wip1 toward that substrate as indicated by increased association between Wip1 and the substrate. This would increase substrate dephosphorylation by Wip1 as we reported with p38 (An et al., 2011). If LZAP cannot bind to the Wip1 substrate, then LZAP expression could have no effect on dephosphorylation of the substrate. However, our data suggest that if LZAP cannot bind to the Wip1 substrate, it has discordant activity toward the

Table 1. LZAP and Wip1 targets

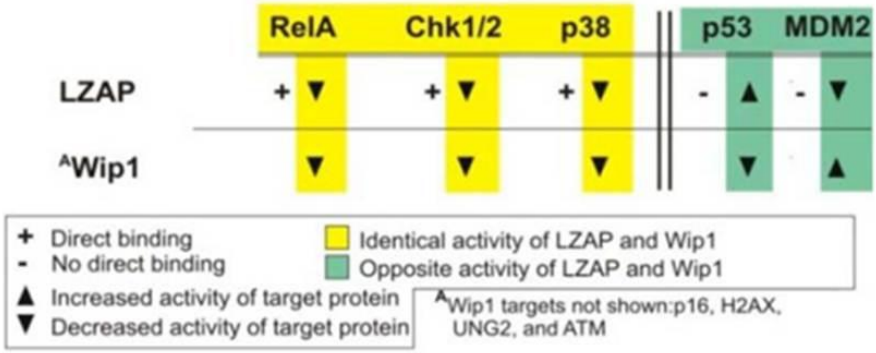

substrate compared to Wip1. These data indicate that LZAP has Wip1 independent effects on the substrate regulation. For example, we have shown that without direct binding to p53, LZAP can enhance p53 phosphorylation and activation. These data suggest that LZAP may regulate Wip1 activity. LZAP may enhance Wip1 activity to dephosphorylate oncogenic targets (e.g. MDM2) while simultaneously suppressing Wip1's major oncogenic activity to inhibit p53. Given the opposing activities of LZAP and Wip1 toward p53 and many other common targets, it is likely that these aspects contribute to their disparate roles in tumorigenesis, LZAP as a tumor suppressor and Wip1 as an oncoprotein.

Regulation of LZAP

To date, little is known about regulation of LZAP in normal or tumor tissues. We and others have shown that LZAP is ubiquitously expressed in all human and mouse tissues tested, including pancreas, brain, liver, heart, intestine, spleen, thymus, muscle and lung (unpublished data). However, expression of LZAP is markedly decreased or undetectable in 30% of HNSCC, but mechanisms of LZAP loss are currently unknown (Wang et al., 2007a). When targeting LZAP in a murine model, we observed spontaneous lung tumor formation from heterozygous animals, and in these tumors the wild-type LZAP allele is lost (unpublished data). Human LZAP has two LXXLL motifs and one conserved LXXLL-like LXXFL motif. These motifs are of unknown significance for LZAP activity, although they are implicated to be important for nuclear hormone receptor co-regulator binding to steroid receptors and transcriptional co-activators (Pike et al., 2000; MJ, 2005). Given that LZAP binds to a phosphatase, we explored post-translational modification of LZAP including phosphorylation that may be important for regulation of LZAP activity. We performed ^{32}P *in vivo* labeling autoradiography and ubiquitination assay, suggesting that LZAP is a phosphoprotein and can be ubiquitinated. These data suggest that LZAP biological or biochemical activity may also be under the regulating of its binding partners such as MDM2 or Wip1 (unpublished data).

Summary

Since the first description of LZAP (CDK5Rap3, C53) as a binding partner of the 35kDa CDK5 activator binding protein p35 in 2000, a growing body of literature has demonstrated pleiotropic roles of LZAP. LZAP has emerged as a putative tumor suppressor and important activities and mechanism are beginning to be explored. Functionally, we have discovered that LZAP protein binds to the alternate reading frame protein ARF encoded by the INK4a gene and enhances p53 activity in the presence or absence of ARF. Increased p53 activity following LZAP expression results in expression of the cyclin-dependent kinase inhibitor p21 and G1 cell cycle arrest. LZAP also binds and inhibits RelA resulting in decreased cellular invasion, decreased anchorage independent growth and decreased transcription of selective NF-κB targets including IL-8. *In vivo*, loss of LZAP accelerates tumor xenograft growth and these LZAP-deficient tumors have increased expression of RelA targets and increased vascularity. Mechanistically, we found that LZAP decreases RelA phosphorylation and inhibits NF-κB transcription. Furthermore, other investigators reported that LZAP binds and inhibits the checkpoint kinases, Chk1 and Chk2, which leads to inappropriate or early progression through the G2 and M phases of the cell cycle and increased sensitivity to chemotherapeutic agents. Reliant on its ability to inhibit Chk1/2, LZAP can activate CDC25C and further activate downstream CDK1 resulting in an early mitotic entry. The potential tumor suppressive activity of LZAP have continued to emerge with our discovery that LZAP protein expression is markedly decreased in approximately 30% of HNSCC and loss of LZAP is associated with increased expression of select NF-κB targets. Human tumor and xenograft mouse tumor data, as well as, LZAP activities as an activator of p53 and suppressor of RelA, suggest that LZAP may function as a tumor suppressor; however, validation of LZAP tumor suppressor status has been lacking. To further investigate the functions of LZAP *in vivo*, we generated transgenic mice with targeted LZAP. In these studies, heterozygous ($LZAP^{+/-}$) mice were born and developed normally and are currently being investigated for inflammatory and

tumorigenic phenotypes. LZAP contains no identifiable enzymatic domains or other known motifs with enzymatic activity, suggesting that its activity may be mediated through protein-protein interactions. We noted that without exception, all reported LZAP binding proteins are also targets of the Wip1. Initial exploration of Wip1 as a potential mediator of LZAP activity revealed that LZAP binds Wip1 and increases Wip1 association with p38, and that LZAP ability to inhibit p38 is at least partially dependent on Wip1.

Therefore, the goals of this thesis are to determine the role of LZAP in cell cycle progression, and if LZAP is a bona fide tumor suppressor, to define major mechanisms explaining LZAP activity and regulation, and to identify the role of LZAP regulated proteins (especially p53) in tumorigenesis associated with LZAP loss.

CHAPTER II

LZAP IS REQUIRED FOR EARLY EMBRYOGENESIS IN MICE AND ZEBRAFISH

The majority of the work presented in this chapter is published with the title "Tumor Suppressor LZAP Regulates Cell Cycle Progression Doming and Zebrafish Epiboly" in *Developmental Dynamics*, Jun 2011 (Liu et al., 2011).

Abstract

LZAP is a putative tumor suppressor whose expression is lost in 30% of HNSCC. LZAP interacts with many proteins (e.g. ARF, RelA, p38, Wip1, Chk1, Chk2) and its activities include regulation of cell cycle progression and response to therapeutic agents. To further investigate the functions of LZAP *in vivo*, we targeted LZAP in mice. However, homozygous knockout of LZAP in mice ($LZAP^{-/-}$) resulted in early embryonic lethality. In fish and amphibians, the initial stages of embryonic development rely on rapid, synchronized cell cleavage of the fertilized egg, upon completion of cleavage cells undergo a set of morphogenetic movements collectively referred to as epiboly and gastrulation, providing a good model to examine earliest cell behaviors *in vivo*. Here, we explore developmental roles of the *lzap* gene during zebrafish morphogenesis. LZAP is highly conserved among vertebrates, suggesting that its functional domains may be required for cell or organism survival. LZAP is maternally deposited so that before initiation of zygotic transcription, LZAP is present. While LZAP is initially ubiquitously and equally expressed during early development, expression of LZAP later becomes more prominent in the pharyngeal arches, aero-digestive tract, and brain. Antisense morpholino-mediated depletion of LZAP results in delay of cell synchronized cleavage and apoptosis during blastomere formation, resulting in fewer, larger cells. Cell cycle analyses suggest that LZAP loss in early embryonic cells causes a G2/M arrest. Furthermore, LZAP-deficient embryos failed to initiate epiboly—the earliest

morphogenetic movement in animal development—which is dependent on cell-cell and cell-matrix adhesion and likely on other signaling events that have not be described. Our results strongly implicate LZAP in regulation of embryonic cell cycle progression, and suggest that LZAP may alter adhesion and/or signaling critical for migratory activity of epithelial cell sheets during early development. These functions provide further insight into LZAP activity that may contribute not only to development, but also to tumor formation.

Introduction

LZAP (also called CDK5Rap3 or C53) was first discovered as a binding partner of the 35-kDa CDK5 activator binding protein p35 (Ching et al., 2000). Activity of LZAP in association with p35 has not been further characterized and this interaction is likely not required for major LZAP activities because in mammals, CDK5 and p35 expression is restricted to central nervous system neurons. LZAP is ubiquitously, but variably expressed in all organs tested, including pancreas, brain, liver, heart, intestine, spleen, thymus, muscle, and lung (Ching et al., 2000; Wang et al., 2006). Functionally, the LZAP protein binds to the Alternate Reading Frame protein of the INK4a gene locus ARF ($p14^{ARF}$ in humans and $p19^{ARF}$ in mice) and enhances p53 transcriptional activity in the presence or absence of ARF. Increased p53 activity following LZAP expression results in expression of the cyclin-dependent kinase inhibitor p21 and G1 cell cycle arrest (Wang et al., 2006). LZAP also binds and inhibits RelA resulting in decreased cellular invasion, decreased anchorage independent growth and decreased transcription of selective NF-κB targets including IL-8 (Wang et al., 2007a). Furthermore, LZAP binds and inhibits the checkpoint kinases, Chk1and Chk2, which leads to inappropriate or early progression through the G2 and M phase of the cell cycle and increased sensitivity to chemotherapeutic agents (Jiang et al., 2005, 2009).

Importantly, LZAP protein expression is markedly decreased in approximately 30% of HNSCC. *In vivo*, loss of LZAP accelerates tumor xenograft growth, and human and xenograft tumors lacking LZAP have increased expression of RelA targets and increased vascularity (Wang et al., 2007a). LZAP contains no identifiable enzymatic domains or other known motifs to suggest activity, indicating that LZAP activity may be mediated through protein–protein interaction.

Loss of LZAP expression in HNSCC and cellular consequences of LZAP activities suggest that LZAP has tumor suppressor-like qualities; however, developmental roles of LZAP remain unexplored. Loss of LZAP renders cells, at least partially, resistant to genotoxin-induced apoptosis possibly through increasing ability to arrest and repair before mitotic entry. LZAP knockdown delays CDK1 activation and mitotic entry possibly related to increased Chk1 and Chk2 activity, and results in dysregulation of cell cycle progression in tumor cell lines (Jiang et al., 2005, 2009).

Mechanisms to explain biological activities of LZAP continue to emerge. We have recently found that LZAP binds and inhibits activity of mitogen-activated protein kinase p38MAPK, suggesting another mechanism through which LZAP could alter proliferation and cell death (An et al., 2011). To further investigate the functions of LZAP *in vivo*, we generated transgenic mice targeting LZAP. In these studies, heterozygous ($LZAP^{+/-}$) mice were born, developed normally, and are currently being analyzed for inflammatory and tumor phenotypes. Of note, live birth of homozygous knockout mice ($LZAP^{-/-}$) has not been observed, suggesting that homozygous loss of LZAP results in embryonic lethality in mice (data not shown).

The absence of live births of $LZAP^{-/-}$ mice led us to explore developmental defects resulting from LZAP loss. Loss of homozygous mice could be attributed to embryonic lethality or placental problems. To begin understanding the role of LZAP in development and distinguish between

embryonic cellular and placental phenotypes, we turned to the zebrafish model. Zebrafish are vertebrates whose eggs are externally fertilized, thus providing an opportunity to examine the earliest cell behaviors in the live embryos. This feature, combined with zebrafish's rapid development and transparent embryos, allows detailed *in vivo* description of epiboly and gastrulation movements (Kane and Kimmel, 1993; Montero et al., 2003; Solnica-Krezel, 2006).

During the first 3 hours post fertilization (hpf) of zebrafish development, the large fertilized egg processes through a series of divisions without increased cytoplasm, referred to as cleavage. Cells are replicating DNA and rapidly dividing, resulting in an increasing number of progressively smaller cells. Approximately 3hpf, zygotic transcription begins, in a process referred to as the midblastula transition (MBT). Cells are not motile before MBT (Kane and Kimmel, 1993), but within an hour after MBT, they form three distinct layers: two extra embryonic lineages—an outer enveloping layer (EVL) and an inner dual layer, consisting of the yolk syncytial layer (YSL) and yolk cytoplasmic layer (YCL)—and the embryo proper between the EVL and the YSL/YCL. These embryonic cells, which are referred to as the deep cell layer (DCL), will give rise to ectoderm, endoderm, and mesoderm through the morphogenetic movements of gastrulation.

Epiboly is the first morphogenetic movement of embryonic cells. It converts a ball of dividing cells into a sheet of cells that spread over the yolk (Arendt and Nübler-Jung, 1999; Solnica-Krezel, 2005). The first visible sign of epiboly appears around 4 hpf with the flattening of the blastoderm and doming of the yolk. As epiboly progresses, cells of EVL and forming epiblast behave as tightly packed epithelia with extended cell–cell interactions and continuous spatial rearrangements (Solnica-Krezel, 2005; Lachnit et al., 2008). Normal physiological cell death is not observed during these stages; however, when the process of epiboly is stalled, developing embryos are unable to initiate gastrulation and die. Although several genes have been implicated in enabling epiboly, e.g., E-cadherin (Kane et al., 2005), G proteins (Lin et al., 2009),

prostaglandin E 2 (Cha et al., 2006), and Pou5f1 (Lachnit et al., 2008), molecular mechanisms and signaling pathways important for epiboly are not well understood.

To begin defining the physiological role of LZAP in embryogenesis, we performed MO-mediated LZAP knockdown in zebrafish embryos. The spatiotemporal expression of *lzap* was determined, revealing maternal deposition and high levels of expression during the initial cleavage stages. In organogenesis, *lzap* was highly expressed in pharyngeal arches, digestive tract, and brain. MO-mediated loss of LZAP function (*lzap* MO) resulted in slowed progression of cell division during blastomere cleavage stages and absence of epiboly in the majority of morphant embryos. Analysis of proliferating cell nuclear antigen (PCNA), phospho-histone H3, and activated Caspase-3 indicated that LZAP loss was associated with decreased proliferation and mitosis but increased apoptosis in zebrafish embryos, at a developmental stage that is not associated with apoptosis. Cell cycle analysis of embryonic cells suggested that loss of LZAP resulted in a G2/M arrest or delayed exit from G2/M. LZAP morphants initiated transcription at the MBT, suggesting that LZAP did not have global effects on gene expression. Hematoxylin and eosin (H&E) histological staining revealed loosely packed blastoderm cells indicative of disrupted cell–cell adhesion. These results strongly suggest that LZAP is essential for cell cycle progression and that loss of LZAP results in poorly adherent cells and inability to initiate epiboly.

Methods

Zebrafish Lines

Zebrafish, AB strain, were raised in the Vanderbilt Zebrafish Core Facility and maintained under standard conditions at 28 ℃ according to the policies and procedures of the Institutional Animal Care and Use Committee of Vanderbilt University. Embryos were obtained by natural spawning and were staged according to (Kimmel et al., 1995).

Cloning of Zebrafish lzap cDNA and Sequence Analysis

A zebrafish LZAP ortholog (NP_001002105) was identified by NCBI Blink search using the homedomain sequence of the mouse LZAP ortholog (NP_084524.1). Total RNA was isolated from one-cell to 120 hr post-fertilization (hpf) wild-type embryos in TRI-Reagent (Sigma). cDNA was synthesized from 48 hpf RNA template by reverse transcription using the iScript cDNA synthesis Kit (Bio-Rad) according to the manufacturer's protocol. Transcripts of *lzap* were amplified by PfuTURBO DNA polymerase (Stratagene) and products were subcloned into pCR-Blunt II-TOPO (Invitrogen). Primers were as follows: *lzap*-coding region forward: 5'-ATGGAGAACATCCAGAATCT-3'; and reverse: 5'-TCACACATGAACTCCCATGA-3'. A second fragment containing the 5'-UTR and 3'-UTR regions were cloned using primers *lzap*-UTR forward: 5'-GTGGAAATGTAAACTTGTGC-3'; and reverse: 5'-TGATGCATATGTGCAGCTTG-3'. The identity of the cloned zebrafish *lzap* gene was verified by sequencing in the forward and reverse directions by the Vanderbilt Sequencing Facility.

Quantitative RT-PCR

Total RNA was extracted from approximately 100 embryos at different embryonic time points using the TRIzol reagent (Sigma). A total of 50 ng of RNA was used per 20 μL reaction and performed by iScript One-Step RT-PCR Kit with SYBR Green on a Bio-Rad iCycler IQ according to the manufacture instructions. Sequences of primers were as follows: *lzap*-3'-UTR forward: 5'-GTGAAGAAGGCGACTTGGTG-3'; and reverse: 5'-TGATGCATATGTGCAGCTTG-3'. *β-actin* was used as a baseline expression using primers forward: 5'-GACTCAGGATGCGGAAACTG-3'; and reverse: 5'-GAAGTCCTGCAAGATCTTCAC-3'. Three independent experiments in triplicates were performed. ΔΔC(T) Method was used to analyze relative gene expression data. *lzap* expression fold change was normalized to *β-actin* and relative quantity was normalized to 1-cell stage.

Morpholino Oligonucleotides and mRNA Microinjections

Antisense morpholino (MO) specifically targeting the 5'-UTR of LZAP was designed and purchased from Gene Tools, LLC (Philomath, OR). An additional MO oligonucleotide was designed to target the ATG start codon. This ATG MO at 8 ng caused the same morphologic phenotype as 5'-UTR MO at 4 ng dose, therefore, we used the later in all presented experiments. The sequences of the morpholino oligonucleotides were: *lzap*-5'-UTR MO: 5'-AAGAATTACTAAAACGACCCCATGC-3' (targets bases -54 to -30); 5-base pair mismatch control morpholino: 5'- AACAATTAGTATAACCACCCCATCC-3', and *lzap*-ATG morpholino: 5'-AGGGAGATTCTGGATGTTCTCCATT-3' (targets bases -1 to 24). A validated MO targeting zebrafish p53 (5'-GCGCCATTGCTTTGCAAGAATTG-3') was obtained from Gene Tools (Robu et al., 2007).

The full-length cDNA of *lzap* was amplified by PCR and subcloned into the pCS2+ expression vector. Additional constructs used in this study were pCS2+-lzap:3HA (3×hemagglutinin tag added to the 3'-end of *lzap* coding sequence) and pCS2+-lzap:CDs (*lzap* cDNA lacking the 5'-UTR subcloned into pCS2+ vector) for rescue experiments. Capped RNA (cRNA) was synthesized from expression constructs using the mMessage mMachine kit (Ambion) according to the manufacturer's instructions and RNA quality was assayed using gel electrophoresis. RNA, MO, or both combined were dissolved in distilled water and injected into the yolk of 1-to 2-cell stage embryos as described (Montero-Balaguer et al., 2006). Effective and specific doses of MOs and cRNA were determined by titration, reporter constructs and rescue experiments. Used concentrations are provided with each experiment.

Whole-Mount In Situ Hybridization

Whole-mount in situ hybridization using Dig-labeled RNA probes was performed as previously described (Barrallo-Gimeno et al., 2004). For probe synthesis, *lzap* was cloned into pCR-Blunt II-

TOPO, the vector was linearized with BamHI and antisense probes were synthesized with T7 RNA polymerase (Ambion). Hybridization and washing were performed at 63 ℃.

Histological and Immunohistochemical Analysis

Staged zebrafish embryos were fixed overnight in 4% paraformaldehyde then embedded in paraffin, sectioned at 5 μm thickness and stained with hematoxylin and eosin (H&E) for histological analysis. To determine cell proliferation, mitotic and apoptotic rates, immunohistochemical stain for proliferating cell nuclear antigen (1:15,000 dilution, Sigma-Aldrich), p-Histone H3 (1:400 dilution, Cell Signaling Technology), and active Caspase-3 (1:300 dilution, BD Pharmingen) were performed respectively as described previously (Yin et al., 2008). The immunostained slides were examined by light microscopy. Cell proliferation, mitosis, and apoptosis were assessed as PCNA, p-Histone H3, and active Caspase-3 labeling index (LI), respectively. For each embryo, the index was defined as the percentage of immune-positive embryonic cells of PCNA, p-Histone H3 or active Caspase-3 in total embryonic cells respectively. For each LI, 20 representative embryos were evaluated at higher power magnification ($\times 40$), and the average was calculated. The data for the PCNA, p-Histone H3, or active Caspase-3 LI were presented as mean $\pm$ standard deviation (SD).

Immunofluorescent Staining and TUNEL Labeling

Whole-mount immunofluorescent staining was performed as described (Pfaff et al., 2007) using polyclonal Ser-10 p-Histone H3 (1:750 dilution, Santa Cruz) and monoclonal α-tubulin (1:500 dilution, Sigma) detected with Alexa Fluor fluorescently conjugated secondary antibody (1:600 dilution, Molecular Probes). For nuclear counterstain, embryos were incubated with TO-PRO-3 (1:1,000 dilution, Molecular Probes) for 30 min. Confocal images were taken with a Zeiss LSM510 inverted confocal microscopy (Vanderbilt Cell Imaging Shared Resource). For TUNEL

staining, embryos were dechorionated and fixed at 6 and 12 hpf and apoptotic cells visualized by in situ cell death detection kit (Roche).

Fluorescence-Activated Cell Sorting Analysis of DNA Content and Nocodazole Treatment

MO-injected zebrafish embryos were transferred from 28 ℃ and manipulated in ice-cold Ca^{2+}-free Ringer solution. For cell cycle inhibition, embryos were treated with nocodazole, 10 μg/ml for 30 min (Sigma). After termination of this treatment, the embryos were washed with Ca^{2+}-free Ringer solution, 0.05% DMSO (Horowitz et al., 1983), then incubated in egg water for 15 or 30 min. Embryos were dechorionated by pronase, and yolks mechanically disrupted. The embryonic cell mass was then trypsinized, and isolated embryonic cells were stained with PI, filtered through Cell Strainer Cap (BD), and cell cycle analyzed by fluorescent flow cytometric analyses as previously described (Yarbrough et al., 2002). Cell clusters and debris were manually excluded leaving only isolated single cells for analyses. Cell cycle analyses were performed on a FACSCalibur machine (Becton Dickinson) and analyzed using CellQuest Pro software.

Statistics

Results in graphs represent mean ± SD or as indicated. Statistical significance was determined by unpaired two-tailed Student's t-test (Excel or Prism Software), with $p < 0.05$ considered as significant.

Results

LZAP Is Highly Conserved Across Species

Using *in silico* data mining of NCBI databases, sequences encoding LZAP orthologs were aligned, revealing that they are highly conserved in multicellular organisms including vertebrates, invertebrates and plants, but not in unicellular yeast and bacteria. The zebrafish *lzap* gene spans 9.3 kb of genomic sequence and is located on zebrafish chromosome 12 (Fig. 2.1A). The full-

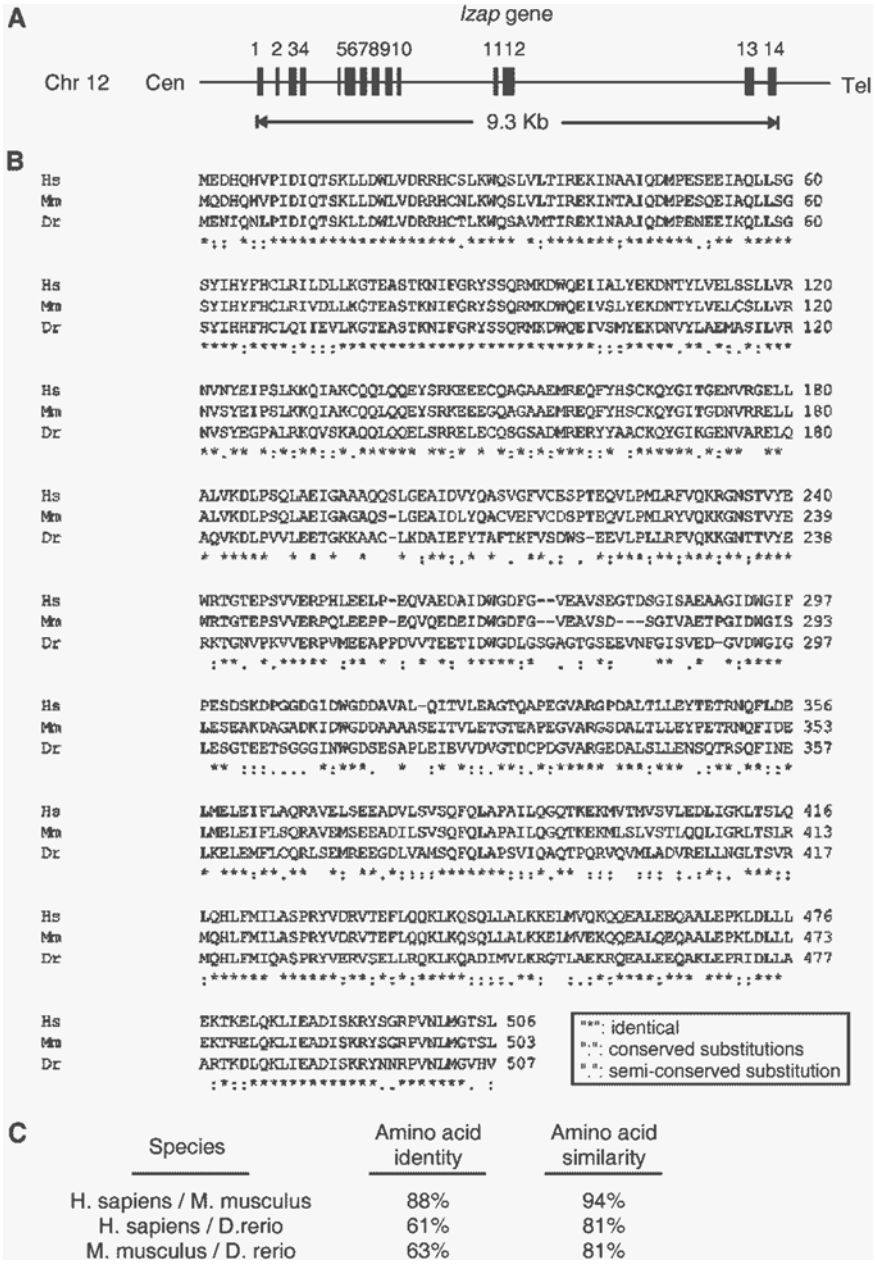

Figure 2.1. *lzap* Is Highly Conserved During Evolution

(A) Gene structure of zebrafish *lzap* located on chromosome 12. Filled boxes represent exons. Cen, centromere; Tel, telomere.

(B) Alignment of human, mouse, and Zebrafish Lzap protein sequences. Amino acid sequences of LZAP orthologs from the NCBI database were aligned and similarity assigned based on the Clustal W algorithm. Hs, Homo sapiens (NP_788276.1); Mm, Mus musculus (NP_084524.1); Dr, Danio rerio (NP_001002105.1). (*) identical; (.) conserved; (:) semi-conserved.

(C) Pairwise comparison of amino acid conservation between human (H. sapiens), mouse (M. musculus), and zebrafish (D. rerio) LZAP.

length cDNA of the *lzap* gene was amplified using gene-specific primers and total RNA from zebrafish wild-type AB strain as template. A 1,524-bp transcript comprised the full-length cDNA and encoded a protein consisting of a predicted 507 amino acid residues. Sequence alignment demonstrated that the zebrafish LZAP protein is highly similar in composition and length to the human and murine orthologs. Similarity between zebrafish LZAP and either human or murine LZAP is greater than 80%, and between murine and human LZAP is more than 90%, indicating that structural, and likely functional aspects of LZAP have been highly conserved during evolution (Fig. 2.1B and C). Sequence alignment suggests that the amino-terminal portion (amino acids 1-122) and carboxyl-terminal (amino acids 412-terminus of LZAP) domain are even more faithfully conserved, suggesting that these areas may represent domains of the LZAP protein that are critical for functions.

Homozygous Floxed LZAP Alleles Results In Embryonic Lethality In Mice

To create the conditional LZAP knockout mouse, the LZAP gene was targeted in murine ES cells through homologous recombination by electroporation using a targeting vector with two loxP sites, one engineered 564 bp 5' of the initiating ATG (155 bp 5' of the predicted proximal promoter) and another in the second intron. The general schema including loxP sites (arrowheads), LZAP gene structure including 14 exons, and LZAP mRNA are shown (Fig. 2.2A). Two recombinant clones (2A2 and 2G5) were selected by PCR and Southern blotting (Fig. 2.2B), injected into blastocysts and resultant F0 chimeric mice crossed with C57Bl/6 mice. Insertion of loxP sites was confirmed on F1 generation mice by PCR and sequencing (Fig. 2.2C and data not shown).

The Neo cassette had been deleted from the 2A2 clone, but not the 2G5 clone before creation of the chimera. The 2G5 clone mice were crossed with ACTFLPe expressing mice expressing FLP1 recombinase under the human *ACTB* promoter (Jackson Laboratory) for removing the Neo

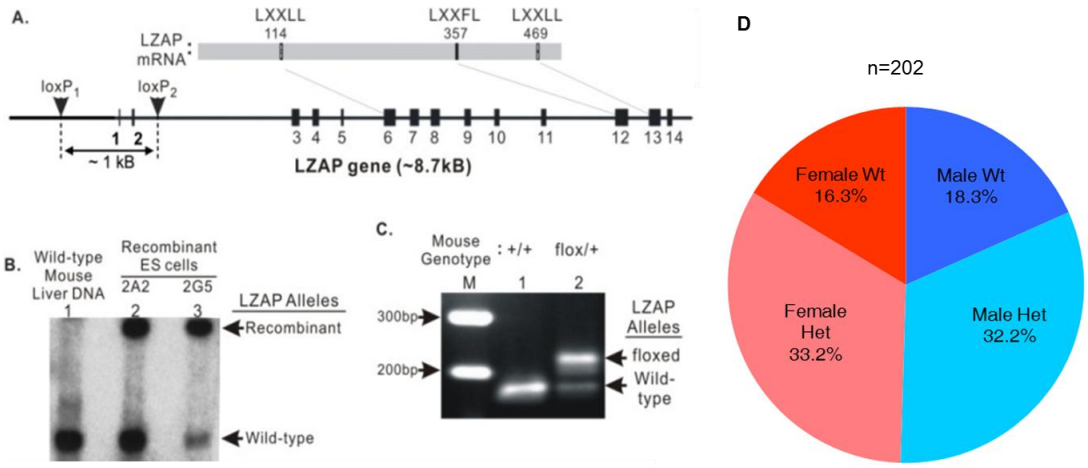

Figure 2.2. Targeting LZAP in Mice

(A) Design of conditional *lzap* allele. Using homologous recombination in murine ES cells, two loxP sites were inserted into the LZAP gene as indicated.

(B) Southern blotting of recombinant ES cells. DNA from wild-type mouse liver (lane 1) or from independent ES cells clones 2A2 and 2G5 after homologous recombination (lane 2 & 3) was digested with HindIII and ScaI, separated by electrophoresis and Southern blotting performed with a [^{32}P]-labeled probe specific to the 1st exon of the LZAP gene.

(C) PCR genotyping of wild-type and LZAP$^{flox/+}$ mice. DNA isolated from tails of mice derived from crosses of 2A2 chimeric mice with C57Bl/6 mice was PCR amplified using primers surrounding loxP$_2$. Floxed and wild-type alleles are indicated (size difference is based on presence or absence of loxP).

(D) Numbers and percentages of wild-type and heterozygous, male and female mice pups that were produced from crosses between heterozygous males and females.

cassette. All data reported were derived from the 2A2 clone unless specified; however, critical results were confirmed using the 2G5 clone in independent experiments. All mice derived from 2A2 and 2G5 clones were bred with EIIa-Cre expressing mice (Jackson Laboratory) to delete the floxed-sequence. Mice heterozygous for LZAP ($LZAP^{+/-}$) were identified in the F1 generation and crossed to generate mice homozygous for loss of both LZAP alleles ($LZAP^{-/-}$); however, of more than 200 mice born to $LZAP^{+/-}$ crosses, no $LZAP^{-/-}$ mice were identified. Wild-type ($LZAP^{+/+}$) and heterozygous ($LZAP^{+/-}$) mice were observed in litters at the normal Mendelian frequency of 1:2 (Fig. 2.2D). There was no obvious sex ratio bias and $LZAP^{+/-}$ mice developed, grew, and reproduced normally. Although not yet thoroughly described, $LZAP^{+/-}$ mice may have skin inflammatory phenotypes that are more severe than normal for the C57BL/6 mice strain. To determine the developmental stage of death for $LZAP^{-/-}$ embryos, dissection of pregnant females from $LZAP^{+/-}$ crosses was performed starting at embryonic day 14.5 (E14.5) and regressing to E5.5 (data not shown). Even at the earliest developmental day examined, no $LZAP^{-/-}$ embryos have been observed. These data suggest that embryonic death in $LZAP^{-/-}$ mice is early during embryonic development.

Based on known LZAP binding partners and activities, explanations of embryonic lethality in $LZAP^{-/-}$ mice were not obvious. Although the phenotype of embryonic lethality was observed in mice derived from independent clones of ES cells after homologous recombination, it was possible that the phenotype was due to aberrant targeting of the LZAP construct or disruption of noncoding RNA, or other unanticipated effects not related directly related to loss of LZAP. Also, in mammals embryonic lethality can be related to placental issues independent of effects on embryonic development. To probe these issues, we examined developmental effects of LZAP loss in *Danio Rerio* (*Dr*, zebrafish). Because development is more easily observed in zebrafish than mice and placental development is not an issue, MO was utilized. MOs decrease protein expression through interruption of translation but do not alter or disrupt gene expression at the

mRNA level. Thus, we used this complementing method in a different species to confirm findings from LZAP$^{-/-}$ mice, and to determine if loss of LZAP expression results in a developmental phenotype and, if so, at what developmental stage.

lzap Is Expressed During Epiboly and Organogenesis

To determine timing and relative magnitude of *lzap* expression during development, quantitative reverse transcriptase-polymerase chain reaction (qRT-PCR) using exon-spanning *lzap*-specific primers was performed on total RNA isolated from whole embryos at developmental stages ranging between one-cell and 5 dpf (Fig. 2.3A). *lzap* is expressed during all developmental stages examined. When normalized to *β-actin*, *lzap* expression decreases during gastrulation. Interestingly, our results indicate that expression of *lzap* is dramatically up-regulated at 12 hpf. Because there is no ideal gene for normalization during very early development (Tang et al., 2007), and *β-actin* expression is low at one-cell stage and increases with development in a time-dependent manner before shield stage (Cao et al., 2004; Duffy et al., 2005), the normalized quantification of expressed *lzap* during very early development (< 6 hpf) may be overestimated. To begin exploring cellular, tissue, and organ localization of *lzap* transcripts, we performed *in situ* hybridization on zebrafish whole-mount embryos representing the same developmental stages as examined by qRT-PCR (Fig. 2.3B–L). Maternal deposition and ubiquitous expression of *lzap* is observed throughout cleavage stages (Fig. 2.3B and C). *lzap* is widely expressed in early epiboly (Fig. 2.3D), but at 12 hpf expression of *lzap* is restricted to the prechordal plate in an area corresponding to hatching gland at Prim stages (Fig. 2.3E–G). *lzap* expression is first detected in the central nervous system, eye, and mesoderm at 24 hpf, and expression persists throughout the second day of development (Fig. 2.3G and H). At 3 dpf, *lzap* transcripts are detectable in the region of the developing pharynx, pharyngeal arches and in the primordia of the gastrointestinal organs (Fig. 2.3I). As development progressed, *lzap* expression persists in the pancreas and gastrointestinal tube, jaw and pharynx region, tectum, and the hindbrain regions (Fig. 2.3J and K).

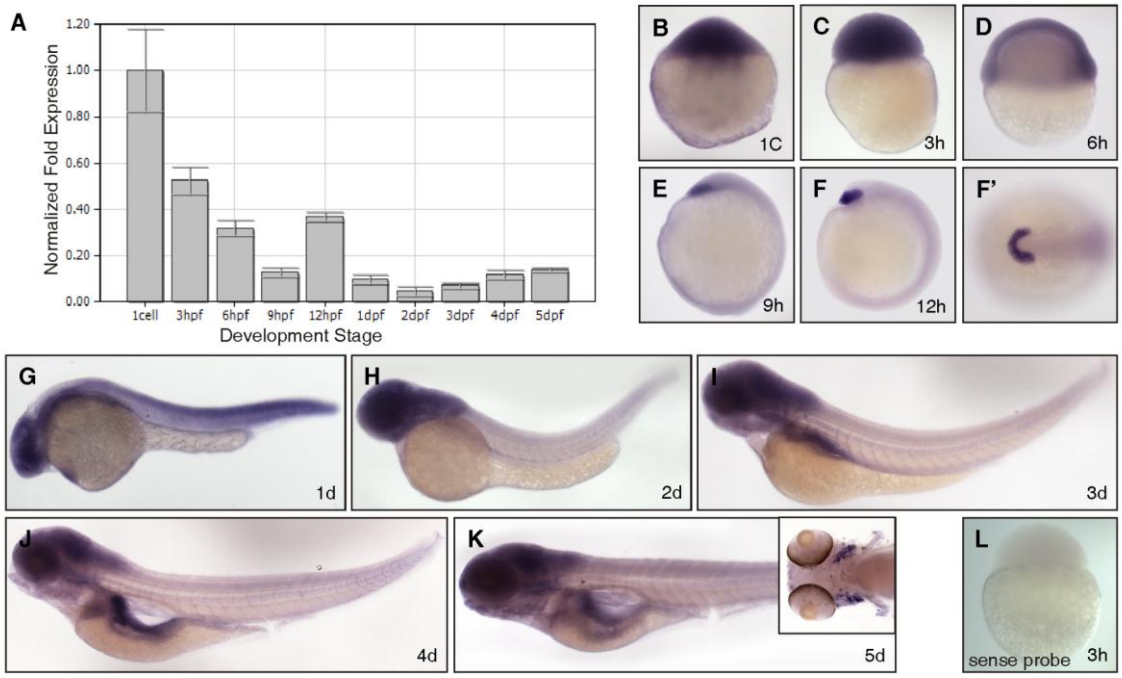

Figure 2.3. *lzap* is Expressed During Epiboly and Organogenesis

(A) Relative expression of *lzap* mRNA in developing fish embryos. *lzap* expression was determined by qRT-PCR at indicated developmental stages and normalized to *β-actin* expression.

(B–K) Representative photographs of lzap expression during development as determined by *in situ* hybridization. Embryos are depicted in lateral view, except for the animal pole view shown in F'.

(B–D) Ubiquitous expression of maternal *lzap* was detected throughout cleavage stages (B,C) and expression was maintained into early epiboly (D).

(E, F) After epiboly from 9–12 hpf, *lzap* expression was concentrated in the precordal plate and areas corresponding to the future hatching gland.

(G, H) At 1 dpf to 2 dpf *lzap* expression was more intense in the central nervous system, eye, and pharyngeal region.

(I) *lzap* staining was visible in the developing pharynx region, pharyngeal arches and in the primordial of the gastrointestinal organs at 3 dpf.

(J, K) *lzap* mRNA was detected at 4–5 dpf (J,K) in the pancreas and gastrointestinal tube, jaw and pharynx region, tectum, gills (see inset, K), and the hindbrain regions.

(L) Negative control with sense probe at 3 hpf reveals no staining.

Specifically, *lzap* expression appears to be present in pharyngeal arch epithelia at 4 and 5 dpf, in structures that will contribute to the epithelia of the future gills (Fig. 2.3K). The 1.6-kb-long antisense RNA probe used for *in situ* hybridization experiments spans the full-length cDNA. The equivalent probe transcribed in the sense orientation was used as a control and does not detect expression (Fig. 2.3L).

Morpholino-Mediated Depletion of LZAP Results in Epiboly Defects

To investigate the function of LZAP during development, we generated loss-of-function zebrafish morphants by injection of antisense oligonucleotides into one-cell stage embryos to block protein translation. The *lzap* morpholino (MO) corresponded to sequences within the 5' untranslated region (UTR) and was designed to target both maternal and zygotic transcripts. A MO corresponding to the *lzap* 5' UTR targeting MO but with a 5-bp mismatch was used as control. Several antibodies recognizing mammalian LZAP were tested for reactivity with zebrafish LZAP protein; however, none recognized zebrafish LZAP by either immunoblotting or immunostaining. In addition, full-length zebrafish LZAP was used to make rabbit polyclonal antibodies. Unfortunately, initial bleeds of the rabbits revealed no specific antibodies. Therefore, to determine effectiveness and specificity of the 5' UTR MO, an expression construct that includes the 5' UTR sequence targeted by the MO, the *lzap* open reading frame, and three HA tags at the C-terminus (*lzap*:3HA, Fig. 2.4A) was used to measure effectiveness of *lzap* MO. Expression of HA-tagged LZAP from the *lzap*:3HA construct is detectable in 89% of injected embryos by 4 hpf without developmental dysmorphology, as assessed by direct immunofluorescence with antibodies against the HA tag. To estimate the minimal effective concentration of MO capable of inhibiting LZAP expression, *in vitro* synthesized *lzap*:3HA mRNA and increasing MO doses (2 ng, 4 ng, or 6 ng) were co-injected, and HA-tagged LZAP expression was determined by immunofluorescence (Fig. 2.4B). Following injection of 2 ng of MO, expression of HA-tagged LZAP is decreased in approximately 50% of injected embryos and is undetectable in the

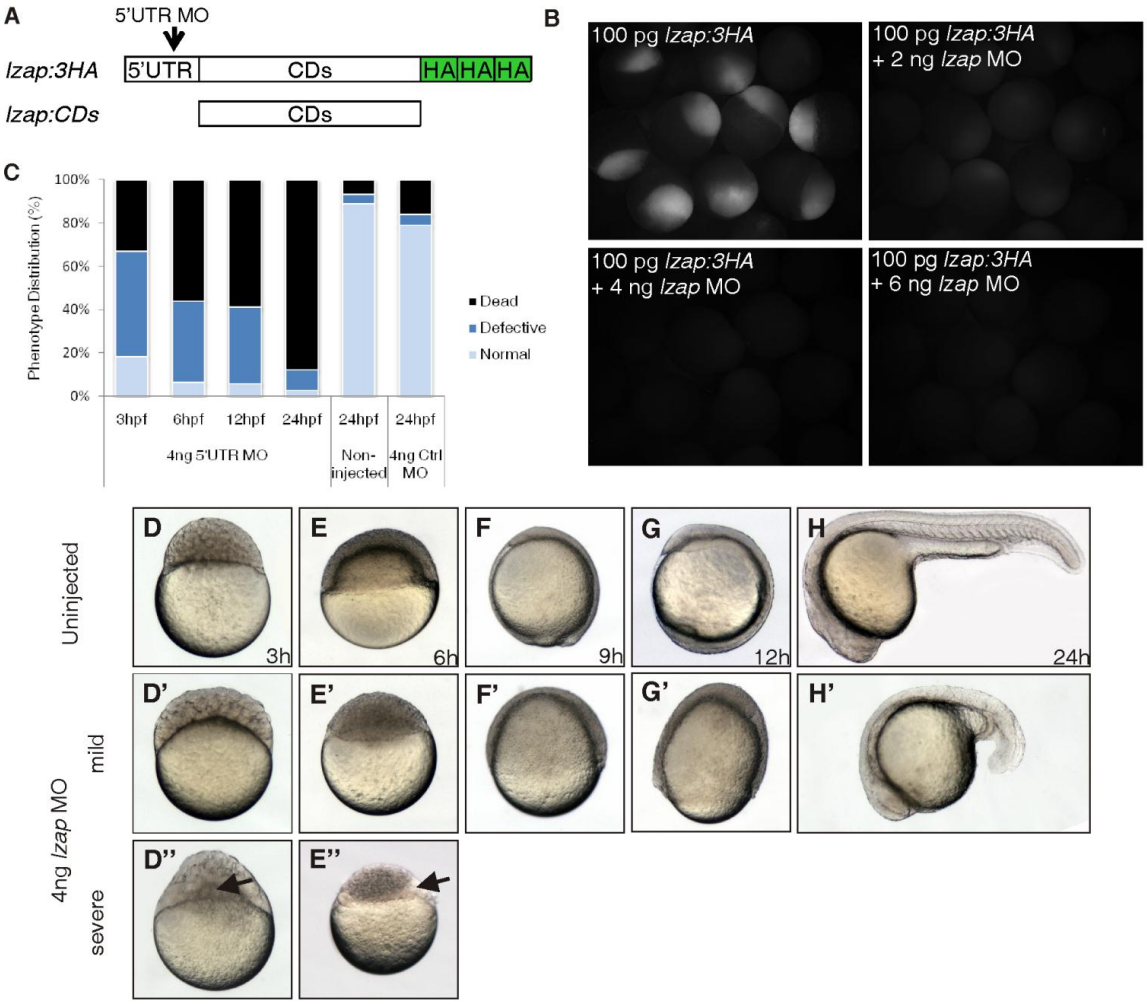

Figure 2.4. Morpholino-mediated Depletion of LZAP Results In Cleavage Stage and Epiboly Defects

(A) Schematic representation of *lzap* RNAs. *lzap:3HA* contains the 5' UTR sequence targeted by the *lzap* MO and was used to confirm MO effectiveness. *lzap:CDs* contains the entire *lzap* coding sequence but lacks the MO target sequence and was used for rescue.

(B) Verification of on-target and dose-dependent effects of *lzap* MO on exogenous LZAP expression. Embryos were injected with *lzap:3HA* singly or with increasing amounts of *lzap* MO visualized by immunofluorescence 4 hpf. No immunofluorescence was observed in control embryos lacking the primary antibody (data not shown).

(C) Schematic showing incidence of developmental defects and nonviable embryos at indicated time points following injection of *lzap* MO, control MO or in embryos without injection.

(D–E") *lzap* specific MO or control was injected and viability and morphology determined by microscopic visualization at indicated times. Results were compared with uninjected embryos. (D–H) Lateral view of uninjected embryos from 3–24 hpf.

(D'–H', D"–E") Lateral view of *lzap* MO injected embryos. Embryos were time matched to uninjected embryos. Arrows indicate persistence of the syncytial layer. Mild and severe phenotypes following injection of *lzap* MO are shown.

remainder. After injection of 4 ng and higher concentrations of *lzap* MO, HA-tagged LZAP could not be detected by immunofluorescence in essentially any injected embryos. Because 4 ng of *lzap* MO was the lowest effective dose that consistently ablates exogenous LZAP expression, it was used in all following experiments.

Consistent with early expression of LZAP (Fig. 2.3), the morphant phenotype was observed before the MBT, the time marking onset of zygotic transcription. At 3 hpf, *lzap* morphants could be categorized as follows: (i) normally developing embryos (18%), (ii) dead embryos (33%), and (iii) abnormal embryos (49%). Abnormal morphant embryos could be further categorized as either mildly or severely abnormal (Fig. 2.4C). At 3 hpf, development of morphant embryos with a mild phenotype lags the wild-type embryos by approximately 40 min, and the severely abnormal morphants are even further delayed (Fig. 2.4D–D”). At 6 hpf, nearly all MO injected embryos present a phenotype, and 56% of injected embryos are dead. Surviving morphant embryos at 6 hr fail to dome, which normally occurs at 4 hpf, and remain at the sphere stage (Fig. 2.4E–E”). In animals with mild phenotype, epiboly proceeds up to the yolk plug closure, albeit at a slower pace than in uninjected controls. Of *lzap* morphant embryos, the severe phenotype is most common with embryos reaching oblong stage (3.7 hpf) (Fig. 2.4E”), where they persist for up to 12 hpf before degenerating. In contrast, the mild category morphants complete gastrulation, undergoing involution, dorsal convergence and limited extension before dying between 12 and 24 hpf. The majority (80%) of the embryos injected with comparable dose of the control MO develop normally (Fig. 2.4C), and no differences were observed between uninjected embryos and embryos injected with control MO.

Epiboly Defects in lzap Morphants Can Be Rescued by Co-injection of lzap mRNA

To exclude off target effects and to verify MO specificity, as well as to implicate LZAP in the extensive developmental delay observed in *lzap* morphants, rescue experiments were performed

using synthetic *lzap*:CDs mRNA that contains full-length *lzap* open reading frame but lacks MO target sequences within the 5' UTR (Fig. 2.4A). Injection of 100 pg of the capped *lzap*:CDs mRNA does not result in developmental dysmorphology (not shown), but co-injection of *lzap*:CDs mRNA with 4 ng of *lzap* MO significantly improves morphants' survival during the first 24 hr of development and accelerates gastrulation to almost normal rates (Fig. 2.5A–F). Morphant rescue with *lzap* mRNA increases the percentage of live embryos from 67% to 94% at 3 hpf, from 44% to 81% at 6 hpf and from 12% to 38% at 24 hpf (Fig. 2.5G). There is a significant loss of embryo viability in the rescued group co-injected with *lzap* MO and *lzap* mRNA between 6 hpf and 24 hpf; however, compared with the *lzap* MO group, embryo viability following *lzap* mRNA remains significantly improved. It is possible that expression of LZAP may inhibit cellular or embryo viability between 6 and 24 hpf. Alternatively, lethality following co-injection of *lzap* MO and mRNA may be due to longer stability of MO compared with co-injected synthetic mRNA. Taken together, these results indicate that the observed phenotypes are due to depletion of LZAP and suggest that endogenous LZAP expression is critical for normal development and survival in the early embryo.

We and others have previously shown that LZAP regulates mitotic entry, cell cycle progression and genotoxin-induced apoptosis, likely through its interaction or regulation proteins involved in apoptosis and cell cycle: p53, p38, Chk1/2 and CDK1 (Jiang et al., 2005; Wang et al., 2006; An et al., 2011). To begin exploring potential cellular mechanisms mediating LZAP function, we analyzed cellular proliferation, mitosis, and apoptosis in *lzap* MO-injected and rescued embryos. At 6 hpf, proliferation of embryonic cells is determined by staining for expression of PCNA, mitosis by staining for phospho-histone H3 (p-Histone H3), and apoptosis by staining for expression of activated (cleaved) Caspease-3. Three groups of uninjected-, 4 ng of MO injected-, and 4 ng of MO / 100 pg of *lzap* RNA co-injected-embryos were collected for analysis at 6 hpf (Fig. 2.5H and 2.6A).

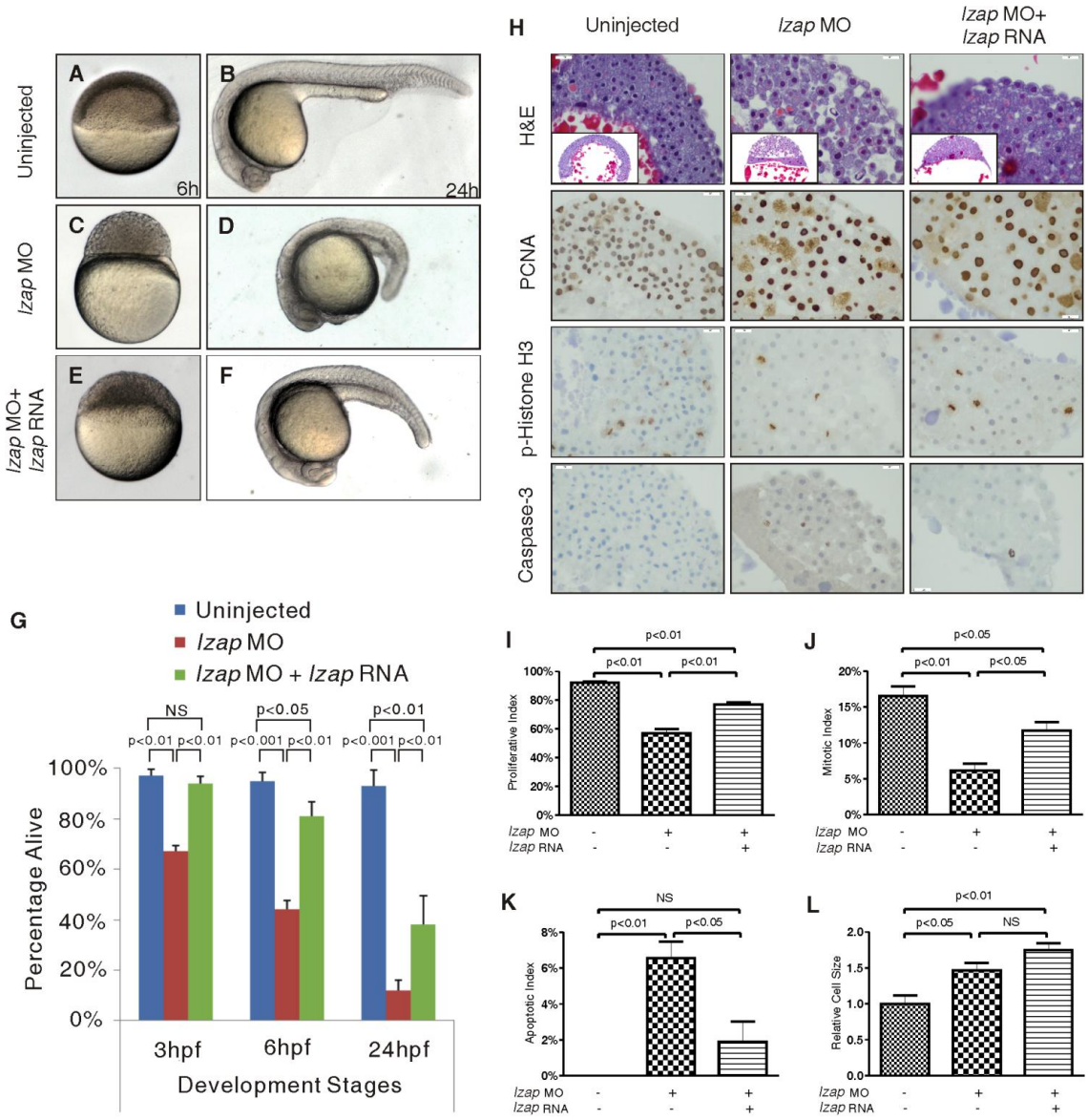

Figure 2.5. Cleavage Stage and Epiboly Defects in *lzap* Morphants are Rescued by Co-injection of *lzap* mRNA

(A–F) Co-injection of *lzap* mRNA with 5'UTR MO partially rescued developmental defects of *lzap* morphants at 6 and 24 hpf.

(G) Schematic showing embryo viability at indicated time points following injection of *lzap* MO with or without *lzap* RNA. Data represent means and standard errors derived from more than 180 embryos from three independent experiments.

(H) *lzap* morphants display proliferative, mitotic, and apoptotic defects that are partially rescued through co-injection of *lzap* mRNA. Embryos were analyzed at 6 hpf by IHC staining using antibodies to PCNA, p-Histone H3, and cleaved Caspase-3 as indicated (original magnification, ×40).

(I–L) Indices for proliferation (I), mitosis (J), and apoptosis (K) were determined by dividing the number of cells staining for PCNA, p-Histone H3, or cleaved Caspase-3, respectively, by the total number of cells. Means and standard error are presented. Data are from sections of 20 independently injected embryos. For relative cell size determination, cell borders were marked on captured hematoxylin stained images and relative area (L) calculated by ImageJ software. Values are normalized to control cells. NS, not significant.

PCNA is a subunit of DNA polymerase that plays a critical role in DNA replication. Cells were scored as proliferating if PCNA staining was detected within the nucleus. Proliferative index was calculated by dividing PCNA-positive cells by total number of cells examined. At 6 hpf, cells PCNA expressing cells were observed throughout embryos in uninjected controls, *lzap* morphants, and *lzap* mRNA rescue groups; however, the proliferative index of *lzap* morphants is significantly decreased compared with controls (92% vs. 56%, $p < 0.01$). Proliferative index is partially restored (56% vs. 77%, $p < 0.01$) following rescue through co-injection of *lzap* mRNA with MO (Fig. 2.5H, 2.5I and 2.6A).

To further support findings of differences in cellular proliferation as indicated by PCNA expression, expression of p-Histone H3 as a marker of mitosis was determined using immunohistochemistry (IHC) and immunostaining. Mitotic index was defined by dividing the number of p-Histone H3-positive cells by the total number of cells examined (Fig. 2.5H, 2.5J and 2.6A). Consistent with proliferation data as measured by PCNA, the mitotic index reveals that mitoses are significantly reduced in *lzap* morphants compared with controls (16% vs. 6%, $p < 0.01$). Rescue by co-injection of *lzap* mRNA significantly increases mitosis compared with *lzap* morphants (6% vs. 11%, $p < 0.05$) but does not restore mitotic index to the level observed in control embryos (11% vs. 16%, $p < 0.05$).

To measure apoptosis within embryos, IHC was performed using antibodies specific to cleaved Caspase-3, and apoptotic index was determined by dividing Caspase-3–positive cell number by total number of cells examined (Fig. 2.5H and K). Consistent with reports which show that during normal development apoptosis is not observed before gastrulation (Yamashita, 2003; Granero-Moltó et al., 2008), no apoptotic cells are detected in control embryos at 6 - 30 hpf (Fig. 2.5H,

2.6B and 2.6C). However, following *lzap* MO injection, 7% of cells express cleaved Caspase-3 as a marker of apoptosis (0% vs. 7%, $p < 0.01$). Co-injection of *lzap* morphants with *lzap* mRNA significantly decreases the apoptotic index from 7% to 2% ($p < 0.05$). The presence of apoptosis in *lzap* morphants at 6 and 12 hpf was confirmed by TUNEL (terminal deoxynucleotidyl transferase–mediated deoxyuridinetriphosphate nick end-labeling) assay (Fig. 2.6C). We have also independently further supported these results in live embryos stained with Acridine Orange, where we observed a specific and abnormal accumulation of dying cells in the central nervous system, eye and mesoderm at 30 hpf in *lzap* morphants (Fig. 2.6B). These data suggest that MO-directed knockdown of LZAP during early and later embryogenesis increases activity of the intrinsic apoptosis pathway resulting in abnormal apoptosis. Although potentially contributing to embryonic lethality, it should be recognized that the relatively low levels of cellular apoptosis observed in *lzap* morphant embryos may not be the sole contributor to embryonic death in *lzap* morphants. Although not explored, it is possible that necrosis may contribute to observed early embryonic death given reports describing necrosis in embryos failing to initiate epiboly, regardless of the precipitating defect responsible for inhibition of epiboly (Kishimoto, 2004; Reim and Brand, 2006).

In addition to cellular phenotypes of proliferation, mitosis, and apoptosis in morphant embryos, histological evaluation reveals a noticeable difference in cell number, cell size, and cell adhesion compared with control embryos (Fig. 2.5H and 2.6A). Relative cell size was quantified in H&E stained control, morphant and rescued embryos by ImageJ software (NIH) at 6 hpf. The mean cell size for morphant embryos is significantly greater when compared with cells from control embryos (1.5-fold; $p < 0.05$) (Fig. 2.5L). Although rescue with *lzap* mRNA partially corrects proliferation, mitosis and apoptosis defects caused by *lzap* MO, expression of *lzap* does not restore the cell size abnormality observed in the morphant embryos. Larger cell size and fewer

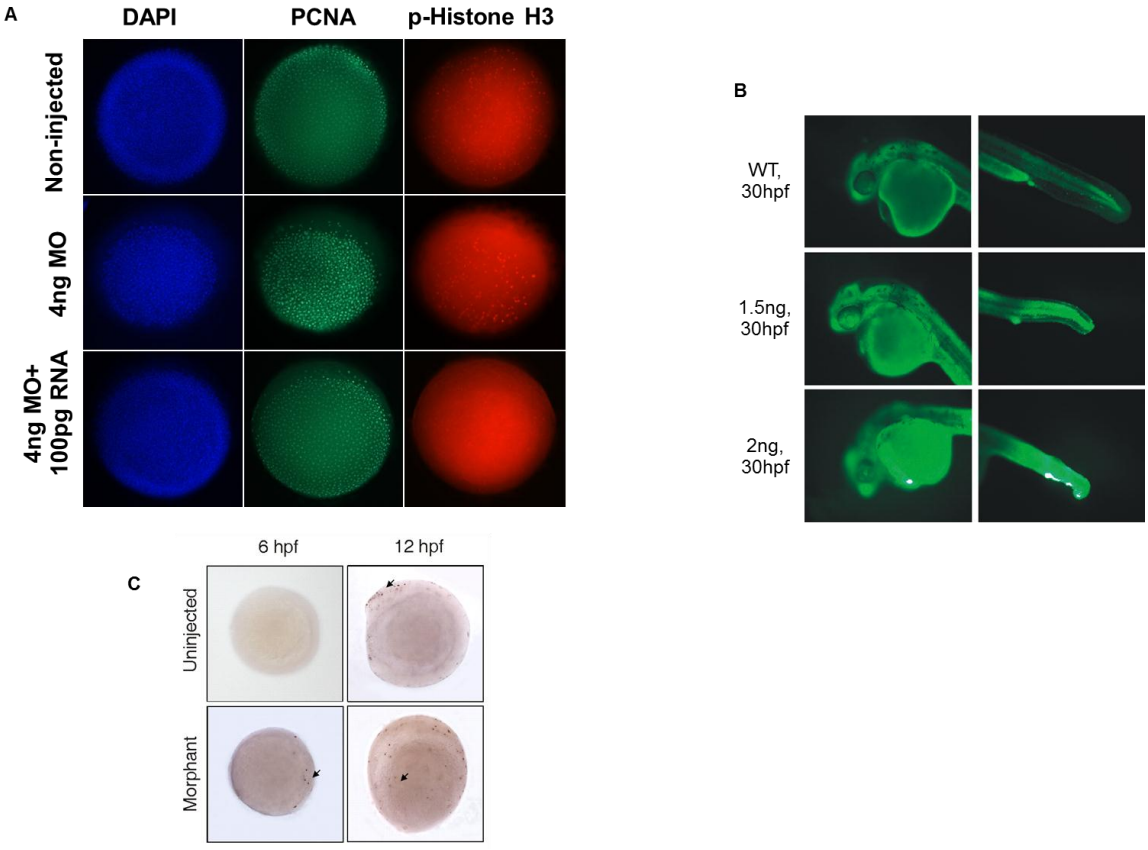

Figure 2.6. *lzap* Morphants Display Proliferative, Mitotic and Apoptotic Defects

(A) Embryos were analyzed at 6 hpf by IF staining using antibodies to PCNA (green) and p-Histone H3 (red). Cells were also stained with DAPI (nuclear staining, blue).

(B) Detection of dying cells by Acridine Orange staining of non-injected and *lzap* MO injected embryos at 30 hpf (lateral views).

(C) TUNEL staining was used to identify apoptotic cells (indicated by arrows) at 6 and 12 hpf. Apoptosis was observed in scattered cells within the embryo after *lzap* depletion, while no apoptosis is detected in uninjected controls. At 12 hpf, apoptotic cells were observed primarily in rostral locations in control embryos, while apoptotic cells were more widely dispersed in *lzap* morphants.

nuclei were observed throughout the first 6 hpf, suggesting that LZAP may be required for normal cell cycle progression or cell cleavage.

Dividing cells before the MBT are not motile, but within an hour after onset of MBT, they begin epiboly and generate a sheet of epithelial-like cells. This cellular layer provides material for morphogenetic movements of gastrulation with resultant formation of germ layers. Motility of these cells has been shown to be dependent on cell adhesion molecules including E-cadherin (Kane et al., 2005; Shimizu et al., 2005). Notably, sections of early *lzap* morphant embryos reveal gaps between cells, which were not observed in controls or in morphants rescued by injection of *lzap* mRNA. Although intercellular spaces in *lzap* morphant embryos could be an artifact of fixation, the fact that they were not observed in control or rescued embryos suggest that loss of *lzap* may alter intercellular adhesion, potentially contributing to abrogation of epiboly. Alternatively, intercellular spaces may be an early manifestation of LZAP-associated cellular defects that decrease cell survival. Together, these data suggest that LZAP may play a role in cell survival, proliferation, cleavage and/or cell adhesion, all of which may be required for epiboly.

LZAP Is Required for Normal Cell Cycle, but Not Zygotic Gene Expression After MBT

The MBT is marked by onset of zygotic gene expression with loss of synchronous cell division. To determine whether onset of zygotic transcription is disrupted by LZAP depletion, we examined several genes that initiate expression after MBT at 6 hpf. As expected, expression of zygotic genes *bmp2b*, *eve1*, and *ntl/brachyury* is initiated in zebrafish embryos in blastomeres at 6 hpf. In older, stage-matched mild *lzap* morphants, expression of these genes that mark onset of the MBT is indistinguishable from control embryos (Fig. 2.7A) (Joly et al., 1993; Schulte-Merker et al., 1994; Sidi et al., 2003; Ramel et al., 2005; Wilm and Solnica-Krezel, 2005). Anterior mesendoderm and hatching gland marker *hgg1*/*cathepsin L* expression is present in the polster of stage-matched mild morphants (Fig. 2.7A) (McFarland et al., 2005); however, the expression

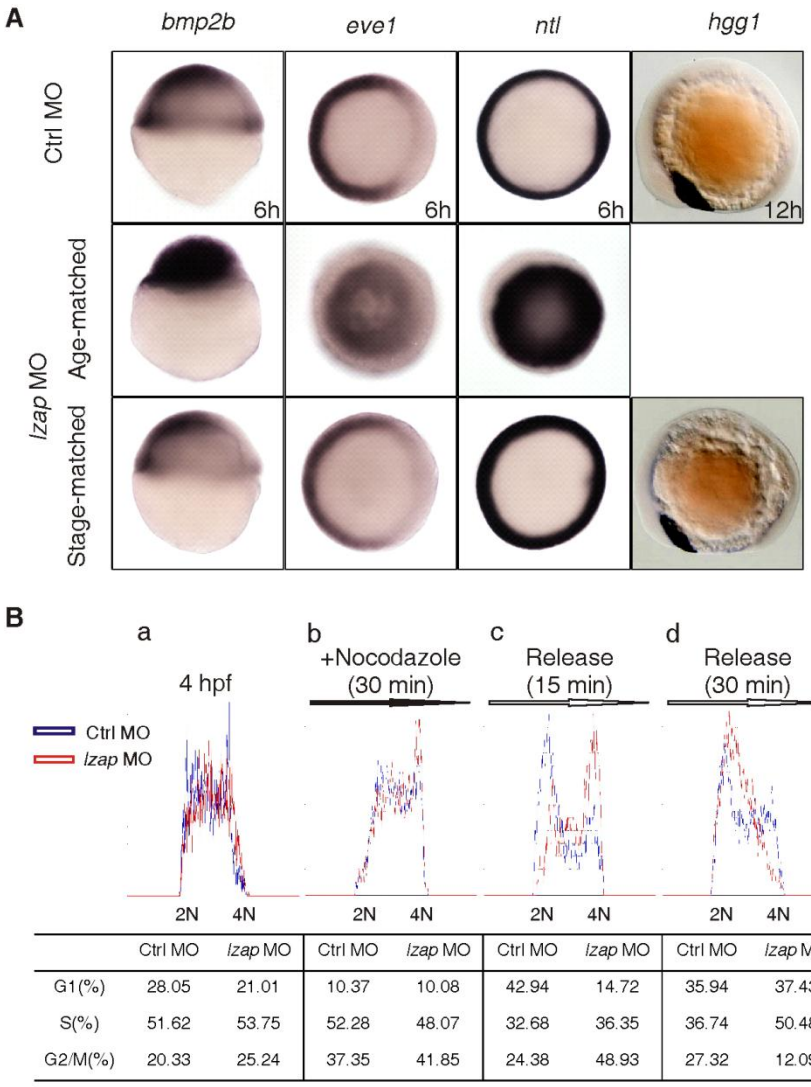

	Ctrl MO	*lzap* MO	Ctrl MO	*lzap* MO	Ctrl MO	*lzap* MO	Ctrl MO	*lzap* MO
G1(%)	28.05	21.01	10.37	10.08	42.94	14.72	35.94	37.43
S(%)	51.62	53.75	52.28	48.07	32.68	36.35	36.74	50.48
G2/M(%)	20.33	25.24	37.35	41.85	24.38	48.93	27.32	12.09

Figure 2.7. Depletion of LZAP Causes Delay in Cell Cycle Progression but Does not Disrupt Zygotic Gene Expression after MBT

(A) The expression of *bmp2b*, *eve1*, *ntl*, and *hgg1* in control and both age-matched and stage-matched lzap morphant embryos were detected by whole-mount in situ hybridization. *bmp2b* expression, lateral view, 6 hpf in control. *eve1* and *ntl* expression, top view, 6 hpf in control. *hgg1* expression, lateral view, 12 hpf in control.

(B) Cell cycle analyses of dissociated zebrafish embryonic cells. DNA content was determine on untreated embryonic cells (a), on cells treated with 10 μg/ml nocodazole for 30 min (b), or on cells treated with nocodazole followed by release for 15 (c) or 30 min (d). Cells were assigned to G1, S, or G2/M based on fluorescent signal and manual gating using CellQuest Pro software. Results in the table represent the mean of at least three independent experiments.

domain is smaller as compared to controls. Collectively, these data suggest that the initiation of zygotic transcription is not disrupted by loss of LZAP.

To investigate changes in cell cycle progression associated with LZAP loss, *lzap* morphant embryos were dissociated and cell cycle position of embryonic cells was determined by flow cytometry after propidium iodide labeling at 4 hpf. As expected based on PCNA staining of early embryos (Fig. 2.5H), control and *lzap* morphant embryos are rapidly proliferating and primarily in S phase (51% vs. 53%). However, histograms of *lzap* morphant cells revealed a potential increase in G2/M and similar decrease in G1 populations relative to control (Fig. 2.7B-a). To better define the possible G2 delay, nocodazole was used to arrest cells in mitosis and cell cycle analyzed. In embryos treated with nocodazole for 30 min, G1 is similar between *lzap* morphants and controls, suggesting that loss of *lzap* does not impact progression through G1. As observed in untreated cells, *lzap* morphants treated with nocodazole have increased percentage of cells in G2/M (Fig. 2.7B-b). Embryos were released from nocodazole block to determine progression from mitosis into G1 and the remainder of the cell cycle. Cell cycle position of control cells following 15 minutes of release from nocodazole block reveal that they progress primarily to G1, whereas *lzap* morphant cells remain predominantly in G2/M (Fig. 2.7B-c). Following a 30-min release, control cells have progressed out of G1 into S and begin repopulating G2/M. In contrast, following 30 min release, *lzap* morphants are primarily in G1 and S, but have not begun to repopulate G2 (Fig. 2.7B-d). Although minor defects in G1 progression of cells derived from *lzap* morphants cannot be excluded, these data are most easily explained by a G2/M arrest associated with *lzap* loss. Analyses also reveal an increased sub-G1 population in *lzap* morphants consistent with increased apoptosis as observed by Caspase-3 staining (Fig. 2.5H).

In parallel, we investigated spindle formation and chromosome alignment by immunofluorescence at three consecutive stages (4h, 6h, 9h) past MBT. We labeled mitotic

spindles using α-tubulin antibody and condensed chromatin at metaphase and early anaphase by p-Histone H3 anti-body (Fig. 2.8A). We also analyzed overall size and shape of nuclei by TO-PRO-3 labeling and confocal imaging of whole-mount preparations. We found that the nuclei are of comparable size and number at 4 hpf in morphants and controls, however, at 6 and 9 hpf the size and number of *lzap* morphant nuclei remain similar to the earlier stage while control nuclei increase in number and decrease in size (Fig. 2.8B). The formation of mitotic spindles is not disturbed by LZAP depletion, and chromosome alignment at metaphase is comparable between morphants and controls at all stages tested. Despite the distinction of nuclear size and number following LZAP loss, there are no gross abnormalities of chromatin morphology such as nuclear strings connecting nuclei or fragmented chromatin. These results suggest that LZAP depletion does not interfere with assembly of mitotic spindles and chromatin condensation or alignment during mitosis.

Discussion

The *lzap* gene structure and protein sequence are highly conserved across multicellular species, which may be a result of its critical developmental role. Here, we present a set of experiments that begin exploring the roles of LZAP during zebrafish development. Given our observations of early embryonic death in *lzap* morphant zebrafish and in LZAP$^{-/-}$ mice, findings related to LZAP role in early embryogenesis likely apply to other species as well.

We show that LZAP is ubiquitously expressed during blastomere cleavage stages and gastrulation. Of interest, homozygous LZAP knockout mice are embryonic lethal, and LZAP$^{-/-}$ embryos could not be found from dissection of pregnant females at or after embryonic day 4.5 (unpublished data). These results are consistent with the phenotype of the zebrafish *lzap* morphant embryos that are lethal at a very early embryonic stage, before initiation of epiboly. Thus, both zebrafish and murine data suggest that LZAP is essential for early embryogenesis.

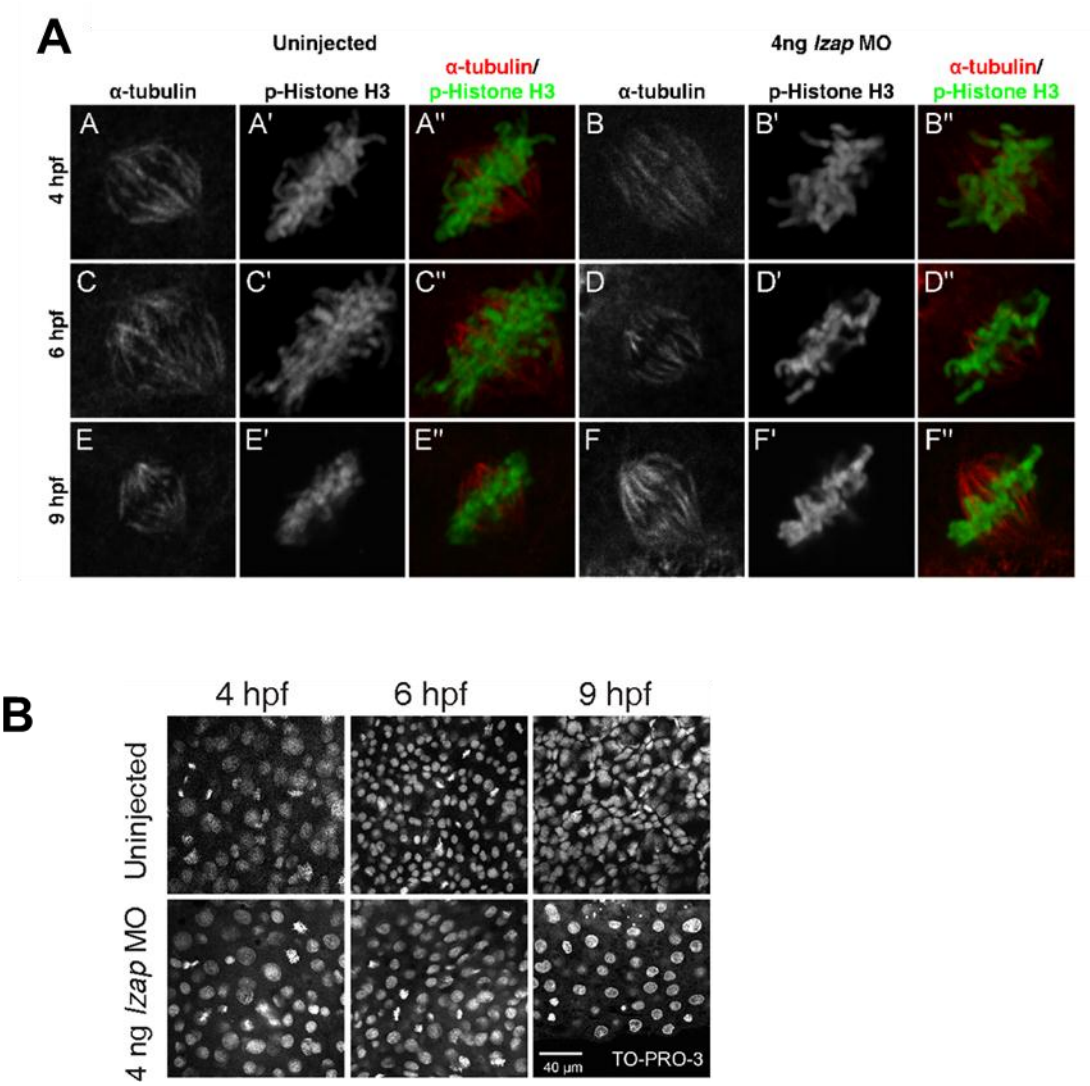

Figure 2.8. Mitotic Spindles and Nuclear Morphology are not Disrupted in *lzap* Morphants

(A) Embryos with and without injection of 4 ng of *lzap* MO were co-immunostained with anti–α tubulin (red) and p-Histone H3 (green) antibodies at 4, 6, and 9 hpf in mitotic cells. Results are representative of observations from more than 100 nuclei for each panel.

(B) Confocal images of whole mount embryos with and without 4 ng *lzap* MO were stained with the nuclear marker TO-PRO-3. Pictures represent 4, 6, and 9 hpf. Scale bar: 40 μm.

We and others have shown that LZAP can bind to or regulate proteins involved in cell cycle progression (e.g., p53, ARF p38, Chk1/2, and CDK1) (Jiang et al., 2005, 2009; Wang et al., 2006). Through these effectors, LZAP has been shown to regulate mitotic entry, G2/M checkpoint, cell cycle progression, and apoptosis. In zebrafish development, we show that loss of *lzap* increases apoptosis and inhibits proliferation likely through inhibition of progression through G2 and M phases of the cell cycle.

Epiboly

Epiboly is the first morphogenetic movement that in zebrafish initiates approximately 1 hr after the MBT with intercalation of the deep blastomeres and animalward movement of the yolk (doming). Actin inhibitors and calcium chelators interrupt epiboly, but few genes have been implicated in this process (Cheng et al., 2004). In *lzap* morphants, despite progression through the MBT with expression of zygotic genes and mesodermal markers, neither doming nor epiboly was observed. Previously, four mutants were identified that arrest epiboly after it is initiated (Kane et al., 1996); however, genes corresponding to these mutants have not been assigned. Depletion of LZAP arrests epiboly before any morphogenetic movements begin suggesting that LZAP is not likely to be altered in these epiboly mutants.

Zebrafish mutants that disrupt development before the MBT have been isolated by mutagenesis strategies then selecting for maternal effect genes; however, most of the genes have yet to be cloned and none of the described mutants mimic the *lzap* morphant phenotype (Dosch et al., 2004; Abrams and Mullins, 2009). Pre-MBT mutants including *irreducible* (*irr*), *indivisible* (*ini*), *atomos* (*aoo*), *cellular island* (*cei*), and *cellular atoll* (*cea*) each failed to initiate cytokinesis, karyokinesis or both, whereas *lzap* morphants do not display abnormalities in cytokinesis or karyokinesis. The large cell morphology observed in *lzap* morphants is reminiscent of the

screeching halt (*srh*) mutant (Wagner et al., 2004). Similar to *srh* mutants, *lzap* morphants zygotically express *ntl, eve1,* and *bmp2b,* in a spatial pattern consistent with failure to progress past the sphere stage in age-matched embryos; however in stage-matched morphants, these genes are expressed in a normal pattern. Unlike *srh*, the *lzap* morphants present normal nuclear morphology, alignment of metaphase chromosomes, and mitotic spindle formation (Fig. 2.8A and B).

The zebrafish *betty boop* mutant (*bbp*) causes arrest of epiboly with constriction and bursting of the yolk cell at 50% epiboly. This defect was linked to an inactivating mutation of MAPKAPK2 (Holloway et al., 2009). MAPKAPK2 is a downstream target of the mitogen activated protein kinase p38 and dominant-negative mutations of p38MAPK recapitulate the *bbp* phenotype. Likewise, mutations in the homeobox transcription factor, Mxtx2, result in a similar phenotype (Bruce et al., 2005; Wilkins et al., 2008). Although yolk bursting was not observed in *lzap* morphants, we have recently found that human LZAP binds and inhibits p38MAPK suggesting that this pathway could be involved in epiboly defects observed in LZAP depleted animals (An et al., 2011).

Cell Cycle

In mammalian cells loss of LZAP results in cell cycle defects. To determine whether cell cycle progression is altered in *lzap* morphants, proliferative and mitotic indices and cell cycle position are determined in cells dissociated from early embryo (Fig. 2.5). Percentages of proliferating and mitotic cells are decreased in *lzap* morphant embryos. Flow cytometric analyses suggested that fewer cells from *lzap* morphants are in G1 and more cells are in G2/M compared to untreated or control embryos, but analyses of unperturbed cells is limited because of the rapid cell cycle at this stage with the majority of cells positioned in S phase (Zamir et al., 1997). Nocodazole treatment and release was used to more finely determine cell cycle effects of LZAP loss (Fig. 2.7B).

Following removal of nocodazole, *lzap* morphants are delayed in exit from the G2/M phase, suggesting that LZAP loss in embryonic cells results in a G2/M delay. Polo-like kinase 1 (Plk1) and SCL-interrupting locus (SIL) are required for progression through mitosis and result in embryonic growth defects (Pfaff et al., 2007; Jeong et al., 2010). Both Plk1 and SIL result in disorganized mitotic spindles as opposed to *lzap* morphants whose spindles are morphologically normal (Fig. 2.8A).

LZAP loss in mammalian cells delays mitotic entry through activation of Chk1 and Chk2 consistent with our findings in unsynchronized cells. However, nocodazole results in a mitotic or spindle checkpoint arrest triggered by unattached kinetochores (Amon, 1999; Musacchio and Hardwick, 2002). Results presented here suggest that in addition to delaying exit from the G2 checkpoint, LZAP may also regulate exit from the spindle checkpoint.

Apoptosis

Of interest, non-mammalian vertebrate embryos do not manifest spontaneous apoptosis before gastrulation; however, apoptotic machinery is present and apoptosis can be induced in zebrafish embryos post MBT by inhibition of protein synthesis or DNA replication (Ikegami et al., 1999; Negron and Lockshin, 2004). Mutation of *grp* and *Mei* in flies results in embryonic death, but apoptosis in these embryos has not been evaluated (Sibon et al., 1997, 1999). Likewise, apoptosis is not examined in *screeching halt* zebrafish mutants (Wagner et al., 2004). Here, we show that *lzap* morphant embryos have a significant proportion of cellular apoptosis as early as 6 hpf (Fig. 2.5H, 2.5K, 2.6B and 2.6C). Despite the ability of LZAP to activate p53 and p53's accepted role as an inducer of cell cycle arrest and apoptosis, concomitant loss of p53 does not affect severity of the *lzap* MO phenotype nor rescue *lzap* morphants. Gaps between cells were commonly observed in 6 hpf *lzap* morphant embryos, less frequently observed in rescued morphants and not observed in control embryos. The mechanism responsible for loss of cell–cell adhesion has not

been explored, but could relate to loss of adhesion molecules or may simply be a marker of impending cell death.

Combined, our data suggest that LZAP function is critical for normal progression through the G2/M of the cell cycle and to prevent apoptosis in early embryos. LZAP also appears to be required for initiation of epiboly. Inhibition of doming and epiboly in *lzap* morphants is exciting and suggest that *lzap* activity is required at or before the earliest stages of cellular and tissue differentiation at a stage that all cells maintain stem cell characteristics. The absence of initiation of doming or epiboly in *lzap* morphants is even more remarkable given that E-cadherin mutants with disrupted cell–cell adhesion still are capable of doming (Kane et al., 2005; Shimizu et al., 2005). LZAP-deficient zebrafish embryos show disrupted development at an earlier time point than fish with mutated E-cadherin, MAPKAPK2, or p38MAPK or than in described epiboly mutants and at a stage where embryonic cells should maintain a pluripotency (Ma et al., 2001). These studies suggest that LZAP may be required for embryonic stem cell maintenance or appropriate cell fate determination.

CHAPTER III

LOSS OF LZAP REPRESENTS A NEW MECHANISM OF P53 INACTIVATION IN HUMAN CANCER

The work presented in this chapter has been submitted to the *Journal of Clinical Investigation*.

Summary

We reported that LZAP has tumor suppressor activity, is lost in a portion of HNSCC and inhibits NF-κB. Here, we show that LZAP downregulation diminishes mutant and wild-type p53 protein expression, even after genotoxic stress. Loss of LZAP decreases p53 translation and destabilizes p53, at least partially due to increased expression of nucleolin (NCL). Importantly, knockdown of LZAP abrogates p53 stabilization induced by ionizing radiation, and downregulation of LZAP protects wild-type p53 cells from radiation while sensitizing cells expressing mutant or no p53. The importance of LZAP loss in tumorigenesis is suggested by correlation of LZAP and p53 levels in HNSCC tumors and by the decreased frequency of p53 mutations found in HNSCCs with low LZAP expression. These data suggest that loss of LZAP represents a novel mechanism of p53 inactivation in human cancer.

Significance

Our findings suggest that loss of LZAP represents a new mechanism of p53 inactivation in human cancers. Regardless of p53 mutational status, LZAP depletion downregulates p53 at multiple levels, even after genotoxic stress. In addition, loss of LZAP mitigates the need for p53 mutation in human tumors. LZAP regulation of p53 is, at least partially, dependent on NCL and LZAP regulates NCL protein levels. Disruption of LZAP activity toward p53 may present a promising therapeutic opportunity, since LZAP depletion decreases levels of both wild-type and mutant p53,

with protection of wild-type, but sensitization of mutant p53 cells to radiation-, or chemotherapy-induced death. Therefore, temporary inhibition of LZAP activity toward p53 for patients with tumors harboring p53 mutations may simultaneously sensitize the tumor and protect normal surrounding tissues from radiation damage.

Introduction

HNSCC accounts for more than 90% of all head and neck cancers and is the sixth most common cancer worldwide, affecting approximately 50,000 people in the United States annually (Siegel et al., 2012). Recently, we reported that expression of LZAP (also known as Cdk5rap3 and C53) protein is decreased in approximately 30% of HNSCC (Wang et al., 2007b), and that LZAP loss is associated with increased anchorage independent growth, cellular invasion, and xenograft tumor growth, suggesting that LZAP has tumor suppressor activity. LZAP has also been proposed as a candidate tumor suppressor in hepatocellular carcinoma, where low LZAP expression was found to be independently associated with poor prognosis, and expression of LZAP in HCC cell lines triggered apoptosis and inhibited both proliferation and xenograft tumor growth (Zhao et al., 2011). Conversely, LZAP expression in hepatocellular carcinoma has been associated with poor prognosis, invasiveness, and metastases (Mak et al., 2011, 2012), with grade and depth of invasion in colon adenocarcinoma (Chen et al., 2011), and LZAP is frequently overexpressed in lung adenocarcinoma (Stav et al., 2007). We and others have described LZAP activity toward ARF (Wang et al., 2006), p38 (An et al., 2011), RelA subunit of NF-κB (Wang et al., 2007b), Chk1 and Chk2 (Jiang et al., 2009), Wip1 (unpublished data). As we have shown, LZAP activates p53 through both ARF-dependent and ARF-independent pathways (Wang et al., 2006); however, detailed mechanisms of LZAP functions, particularly ARF-independent LZAP effects on p53, remain unclear.

p53 is universally or nearly-universally inactivated in human cancers through a variety of mechanisms. p53 is inactivated directly by mutation, or indirectly through binding to viral proteins or as a result of alterations in genes, whose products either activate, stabilize, or carry signals from p53 (Hupp et al., 2000; Vogelstein et al., 2000; Lane and Lain, 2002; Lane and Hupp, 2003). As a protein directing critical cellular processes and a potent inductor of apoptosis, p53 expression is tightly controlled, and the number of p53 regulators continues to increase.

NCL was recently described as a regulator of p53 with activity to alter p53 expression at several levels. First, following DNA damage, NCL was found to bind the 5' UTR of p53 mRNA and suppress p53 translation, and under similar conditions, downregulation of NCL was found to increase p53 protein expression (Takagi et al., 2005). Second, NCL has been reported to destabilize p53 and diminish its activity; however, studies in this area are conflicting, suggesting that depletion of NCL increases p53 protein stability and activity (Yang et al., 2011). Opposingly, NCL, like ARF, has been shown to stabilizes p53 by binding and inhibiting Hdm2 (Saxena et al., 2006). NCL is an extraordinary functionally pleiotropic protein with intrinsic DNA and RNA helicase, nucleic-acid-dependent ATPase and self-cleaving activities that is found in multiple cell compartments, including nucleoli, nucleoplasm, cytoplasm and cell surface (Mongelard and Bouvet, 2007; Tajrishi et al., 2011). NCL functions in transcription and translation, chromatin remodeling, viral infection, and at several steps of DNA and RNA metabolism; however, detailed molecular mechanisms of these activities are not fully understood. Although NCL is upregulated in cancer, autoimmune syndromes, Alzheimer's and Parkinson's diseases, as well as other pathological conditions, very little is known about regulation of its levels or activities.

Current anticancer therapies, including those used to treat head and neck cancer, are associated with severe side effects limiting dose and efficacy. Because these side effects occurring in normal tissues are, at least in part, dependent on the p53-mediated apoptosis, transient downregulation or

suppression of p53 has been explored as a therapeutic strategy to protect normal cells during cancer treatment (Komarov et al., 1999; Botchkarev et al., 2000; Gudkov and Komarova, 2003, 2005; Leonova et al., 2010). Mutations in the TP53 gene occur in around 50% of human tumors including HNSCC and are associated with rapid tumor progression and resistance to anticancer therapy also (Koch et al., 1996; Poeta et al., 2007; Skinner et al., 2012). Emerging data firmly support a gain-of-function roles for mutant p53, suggesting that targeting of mutant p53 may be a promising anticancer treatment strategy (Oren and Rotter, 2010; Rivlin et al., 2011; Blandino et al., 2012). Much effort has been directed to restoring wild-type p53 function in tumor cells expressing mutant p53 (Selivanova et al., 1998; Foster, 1999; Bykov et al., 2002, 2003; Selivanova and Wiman, 2007); however, the strategy of inhibiting both mutant (in cancer cells) and wild-type p53 (in normal surrounding cells) has not been well studied. Transient inhibition of wild-type and mutant p53 with simultaneous sensitization of mutant p53 cancer cells and protection of normal tissues from severe side effects may be useful in combination with radio- and chemo-therapy to target p53 mutant cancers.

Here, we show that depletion of LZAP increases NCL expression and decreases expression of p53, regardless of p53 mutation status or the presence or absence of genotoxic stress. Loss of LZAP alters p53 expression through inhibition of translation and decreased p53 protein stability. LZAP activity toward p53 is independent of ARF, Wip1, and HDM2, all of which are known p53 regulators. In human HNSCC, LZAP and p53 protein levels linearly correlate, and tumors expressing low levels of LZAP have a significantly lower *TP53* mutation incidence compared to tumors with high LZAP. Together, these data suggest that loss of LZAP represents a new pathway for p53 inactivation in human cancer. Depletion of LZAP in cancer cells expressing wtp53 protects them from DNA damage-induced cell death, and loss of even one LZAP allele in normal bone marrow cells derived from LZAP heterozygous mice increases cells resistance to

radiation. In contrast, cells expressing mutant or no p53 are sensitized to radiation and chemotherapeutic drugs treatment upon loss of LZAP.

Methods

Cell Lines, Transfection and Lentiviral Infection

U2OS and Saos-2 human osteosarcoma cells, HCT116 $p53^{+/+}$ and $p53^{-/-}$ colorectal carcinoma cells, JHU012, FaDu and SCC-61 HNSCC cells were cultured in complete growth medium suggested by American Type Culture Collection (ATCC) at 37 ℃ under 5% CO_2. Wild-type, $Wip1^{-/-}$ and $p53^{-/-}/Mdm2^{-/-}$ MEFs were cultured at 37 ℃ under 5% CO_2 in hypoxia (2% O_2).

The U2OS Tet-on cell line was generated following BLOCK-iT Inducible H1 RNAi Kit (Invitrogen) protocol. GenMute transfection reagent (SignaGen) was used for siRNA and plasmid transfection. LZAP, NCL and control (ON-TARGETplus Non-targeting) siRNAs were from Dharmacon. For shRNA-mediated knockdown GIPZ lentiviral shRNA (control non-silencing and human LZAP shRNA) vectors were purchased from Thermo. All cell lines used were confirmed as unique and, where possible, matched to microsatellite profiles using the Cell ID kit from Promega.

p53 luciferase reporters were kind gift from J.A. Pietenpol. GFP-p53 expressing vectors were a gift from G. Selivanova.

Creation of LZAP heterozygous mice

LZAP was targeted in murine embryonic stem cells by homologous recombination using a LZAP floxed construct targeting the first 2 exons of murine LZAP. After selection, clones were screened by PCR and Southern blotting with 2 independent recombinant clones (2A2 and 2G5) identified. Mice were crossed with B6.FVB-Tg(EIIa-cre)C5379Lmgd/J mice (Jackson Laboratories) and

then crossed for 6 generations with C57Bl/6 mice (Jackson Laboratories). Genotype of LZAP mice was confirmed by PCR using primers: 5'-TGTGCCACCACGCAACTTTT-3' and 5'-CATGAAGACAGAACCAAAC-3'.

BM-MNCs Colony Forming Assay

C57Bl/6 wild-type and LZAP heterozygous mice were treated with total body irradiation (6 Gy) or left untreated (four mice in each group). 4 hr after TBI, BM-MNCs were isolated from femurs and tibias of each mouse and plated (4 x 104 cells/ml in 35 mm diameter plates) in MethoCult M3231 medium (StemCell Technologies) supplemented with 10 ng/ml recombinant mouse GM-CSF (StemCell Technologies) and IMDM growth medium (Invitrogen). Colony formation (MEP and GMP) was scored after 7 days of culture at 37 ℃ in the presence of 5% CO_2. MEP and GMP colonies were distinguished based on morphology (condensed MEP and dispersed GMP).

Gene Expression

Total RNA was extracted from the cells using RNeasy Mini Kit (QIAGEN) and reverse-transcribed into cDNA (Bio-Rad). SYBR green (Bio-Rad) real-time quantitative PCR was performed using a CFX96 Real-Time System (Bio-Rad). The following sets of primers were used: *lzap* (5'-CAATGCTGCCATCCAGGACATG-3' and 5'-ATCCGCTGTGAAGAGTATCGGC-3'), *p53* (5'-CCTCAGCATCTTATCCGAGTGG-3' and 5'-TGGATGGTGGTACAGTCAGAGC-3'), and *β-actin* (5'-CACCATTGGCAATGAGCGGTTC-3' and 5'-AGGTCTTTGCGGATGTCCACGT-3'). The expression of mRNA of interest was normalized to the expression of *β-actin*.

RT^2 Profiler PCR Array (Human p53 Signaling Pathway) was performed according to the manufacturer's instructions and analyzed using the vendor's online software (QIAGEN).

DNA Purification and p53 Sequencing

Twenty-nine human HNSCC tumor specimens were obtained from formalin-fixed and paraffin-embedded slides. DNA was extracted using Recover All Total Nucleic Acid Isolation Kit (FFPE) (Ambion). Exons 4-10 of human p53 gene were amplified and sequenced according to the protocol from International Agency for Research on Cancer (IARC).

Immunoprecipitation and Immunoblotting

Cells were lysed in RIPA lysis buffer (Sigma) with proteinase inhibitor cocktail (Roche) and phosphatase inhibitors (Sigma), protein concentration was measured with Bradford protein assay (Bio-Rad). For immunoprecipitation, 1 mg of whole cell extracts was incubated with 2 μg of p53, LZAP or NCL antibodies or rabbit IgG, overnight at 4ºC. 30 μl of slurry of Protein A/G-agarose beads (Santa Cruz) was then added and incubated for 1-2 hrs. Immunocomplexes were centrifuged, washed four times with ice-cold lysis buffer, incubated 10 min. at 70 ℃, centrifuged, separated in NuPAGE 4-12% Bis-Tris Mini Gel (Invitrogen) and transferred to Immobilon PVDF Membranes (Millipore). Immunoblots were incubated with primary antibodies overnight at 4 ℃ followed by fluorescent secondary IRDye 680LT anti-mouse IgG and IRDye 800CW anti-rabbit IgG (LiCore) for 1 hr. Signals were detected by infrared fluorescence (Odyssey).

The following primary antibodies were purchased from Santa Cruz Biotechnology: mouse monoclonal anti-LZAP (ZZ-7), mouse monoclonal anti-NCL (MS-3), rabbit polyclonal anti-NCL (H-250), mouse monoclonal anti-p21 (F-5), mouse monoclonal p53 (DO-1), rabbit polyclonal anti-p53 (FL-393), rabbit polyclonal anti-GAPDH (FL-335), mouse monoclonal anti-β-actin (C-4). Mouse monoclonal anti-MDM2 (2A10) was obtained from Abcam; rabbit polyclonal anti-phospho-p53 (Ser15) was from Cell Signaling; rabbit polyclonal anti-LZAP antibody serum was produced as described (Wang et al., 2007b); rabbit polyclonal anti-LZAP (HPA022141) for IHC staining was obtained from Sigma.

p53 Protein Stability

Cells were treated with 25 μM cycloheximide (Sigma) and collected at indicated time points. Immunoblotting was performed with LZAP and p53 antibodies.

In vivo ^{35}S-protein Labeling

Cells were transfected with control or LZAP siRNAs; 48h after transfection, culture medium was changed to methionine/cysteine-free medium supplemented with EasyTag Express Protein Labeling Mix (PerkinElmer) and cells were incubated for 10 min. Protein extracts were immunoprecipitated with p53 antibody and a newly synthesized p53 protein was analyzed by SDS-PAGE and autoradiography as previously described. SDS-PAGE of whole cell protein extracts followed by autoradiography was used to estimate global rate of translation.

Immunohistochemistry

Specimens were fixed with 10% formalin and embedded in paraffin per routine of the surgical pathology division. Sectioning and immunostaining were performed by the Vanderbilt Translational Pathology Shared Resource using antibodies: LZAP (HPA022141, Sigma) and p53 (DO1, Santa Cruz Biotechnology).

Clonogenic Survival Assay

Clonogenic survival assay was performed as we described before (Gubanova et al., 2012). All experiments were performed in triplicate.

Cell Viability Assay

Cells viability assays were performed using WST-1 cell proliferation reagent (Roche) according to the manufacturer's instructions. All experiments were performed in triplicate.

Human Tumor Tissue

Tumors used for this study were obtained from biopsy or surgical specimens after patient consent and after IRB approval. Prior to lysis for immunoblotting, tumor content was enriched to >75% of total cellular content by macrodissection of frozen sections.

Statistical Analysis

Results are reported as mean ± SEM of three independent experiments. Comparisons were performed by using GraphPad Prism S software unless specifically noted.

Results

LZAP Loss Decreases p53 Protein Levels Regardless of p53 Mutation Status

Targeting of a single LZAP allele by homologous recombination in murine ES cells revealed lower LZAP expression in 2 of 2 independently derived clones (~40% 2A2 and 60% 2G5) (Fig.3.1A). We were surprised that p53 protein levels were similarly decreased in ES cell clones after targeting of LZAP (~40% 2A2, and 50% 2G5) (Fig. 3.1A). To determine if LZAP depletion similarly regulated p53 levels in human cells, two different LZAP siRNAs were transfected into human cancer cell lines carrying wild-type p53 (wtp53) (U2OS - human osteosarcoma, JHU012 and SCC61 - both human HNSCC). Downregulation of LZAP was associated with markedly decreased p53 protein in all lines tested (Fig. 3.1B). These findings were confirmed using U2OS cells stably expressing an LZAP shRNA under control of tetracycline-inducible promoter (Tet-on), where addition of doxycycline resulted in a dose-dependent decrease in LZAP expression that is paralleled by decreased p53 protein levels (Fig. 3.1C).

Since loss of LZAP was associated with marked downregulation of wtp53, effects of LZAP depletion on mutant p53 (mtp53) protein level was explored. p53 null osteosarcoma Saos-2 cells were co-transfected with control or LZAP siRNAs and two different "hot spot" p53 mutants

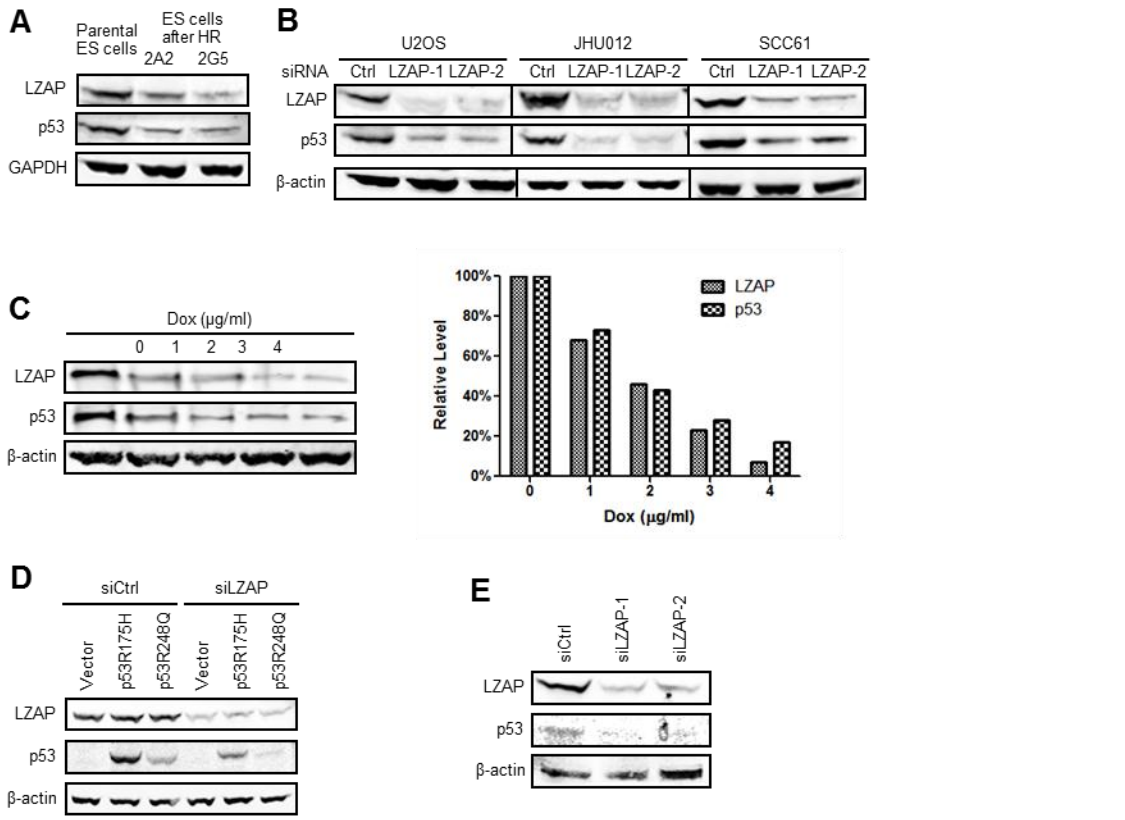

Figure 3.1. LZAP Loss Results in Downregulation of Both Wild-type and Mutant p53

(A) Immunoblot detecting LZAP and p53 in parental ES cells (wild-type) and in ES cell clones (2A2 & 2G5) after homologous recombination targeting LZAP. Immunoblotting of GAPDH serves as loading control.

(B) Immunoblot detecting LZAP and p53 proteins in wtp53 cell lines transfected with control or siRNAs specific to LZAP. Immunoblotting of b-actin serves as loading control.

(C) Left: Immunoblot detecting LZAP and p53 proteins in U2OS cells with doxycycline-regulated (Tet-on) knockdown of LZAP; right: Quantification of LZAP and p53 levels normalized to β-actin.

(D) Immunoblot detecting LZAP and ectopically expressed mutant p53 (R175H and R248Q) in p53 null Saos-2 cells with and without LZAP knockdown.

(E) Immunoblot detecting LZAP and endogenous mutant p53 in SCC-25 cells with and without LZAP knockdown.

(R175H and R248Q) or vector as control. Consistent with findings from cells expressing wtp53, depletion of LZAP downregulated mtp53 proteins in cells ectopically expressing mutant p53 (Fig. 3.1D). These data suggest that LZAP loss downregulates p53 protein levels irrespective of p53 mutation status.

LZAP Loss Inhibits Wild-type p53 Transactivation, Rendering Wild-type p53 Expressing Cells Resistant to Radiation and Chemotherapeutic Drugs

p53 is a primary regulator of cellular response to standard anticancer therapies (e.g. radiation and cytotoxic chemotherapy) (Komarova and Gudkov, 2000; Gudkov and Komarova, 2005, 2007); therefore, transient downregulation or suppression of wtp53 function has been proposed and experimentally confirmed as a strategy to protect normal cells from consequences of radiation or chemotherapy (Komarova and Gudkov, 1998, 2001; Gudkov and Komarova, 2003, 2005).

Since LZAP depletion downregulated p53 (Fig. 3.1), we suspected that LZAP depletion could also protect cells expressing wtp53 from radiation or chemotherapeutic drugs. To determine if biological consequences of LZAP deficiency were dependent on p53 status, isogenic HCT116 cell lines (human colon cancer) with and without p53 (HCT116 $p53^{+/+}$ and HCT116 $p53^{-/-}$, respectively) were infected with control lentivirus or lentivirus driving expression of LZAP shRNA. Cells were plated for clonogenic survival and treated with increasing doses of gamma irradiation. Depletion of LZAP in HCT116 $p53^{+/+}$ cells rendered them more resistant to radiation (Fig. 3.2A and B). In contrast, depletion of LZAP in cells lacking p53 (HCT116 $p53^{-/-}$) enhanced their sensitivity to identical radiation doses (Fig. 3.2A and B).

Limiting p53 activity improves survival of cells following radiation, an effect largely attributed to reduced induction of apoptosis. To determine if LZAP depletion could reduce induction of apoptosis following DNA damage, LZAP was depleted in HCT116 $p53^{+/+}$ cells before exposure

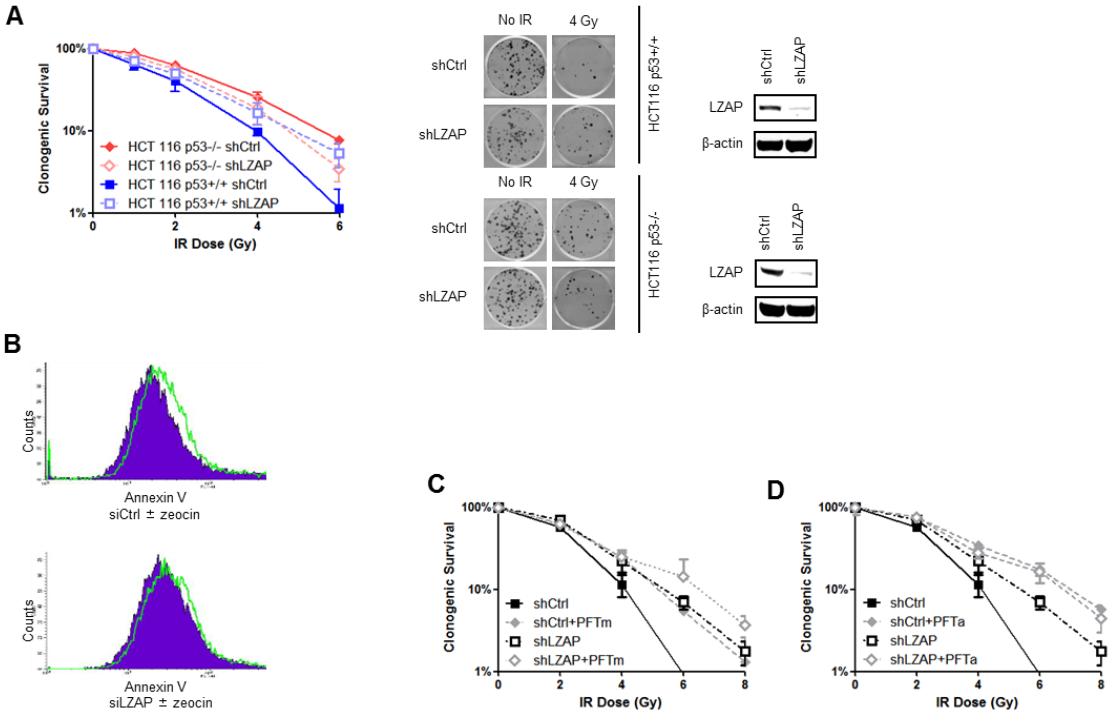

Figure 3.2. LZAP Depletion Protects p53 Wild-type Cells from Radiation but Sensitizes p53 Null Cells to Radiation

(A) Left: Clonogenic survival of isogenic cell lines, HCT116 $p53^{+/+}$ and HCT116 $p53^{-/-}$, after radiation with indicated doses with and without LZAP knockdown. Middle: Representative plates following treatment with 5 Gy showing stained colony at the end of experiment. Right: Immunoblot confirming LZAP downregulation upon shRNAs expression.

(B) Histograms showing annexin V staining in control and LZAP knockdown HCT116 $p53^{+/+}$ cells with and without Zeocin treatment. The percentage of cells with increased annexin V staining after zeocin treatment was determined in control and LZAP knockdown cells and is presented beneath the histograms.

(C) U2OS cells were infected with lentiviral construct expressing empty vector or shLZAP and plated for clonogenic survival. p53 inhibitors PFT-α were added 1 h before exposure to increasing doses of IR. Colonies were stained and counted.

(D) U2OS cells were infected with lentiviral construct expressing empty vector or shLZAP and plated for clonogenic survival. p53 inhibitors PFT-μ were added 1 h before exposure to increasing doses of IR. Colonies were stained and counted.

to the radiomimetic drug zeocin and apoptotic cells were measured by annexin V staining. Compared to control cells, LZAP knockdown reduced the percentage of apoptotic cells following Zeocin treatment by approximately 4-fold (19% vs. 5%) (Fig. 3.2B).

In response to DNA damage, p53 initiates apoptosis through both transcriptional transactivation of specific pro-apoptotic target genes and through a transcription-independent mechanism, involving translocation of p53 to mitochondria. To begin distinguishing which p53 functions are impacted by LZAP loss, small molecular inhibitors of p53, pifithrin-α (PFTα), an inhibitor of p53 transactivation function, and pifithrin-μ (PFTμ), an inhibitor of p53 mitochondrial translocalization, were employed (Komarov et al., 1999; Strom et al., 2006). As expected, LZAP depletion alone or treatment of HCT116 $p53^{+/+}$ cells with either p53 inhibitor singly protected cells from radiation (Fig. 3.2C and D). In addition to radioprotection afforded by PFTμ, depletion of LZAP further improved survival of HCT116 $p53^{+/+}$ cells following radiation (Fig. 3.2C). In contrast, LZAP depletion did not improve survival of HCT116 $p53^{+/+}$ more than treatment with PFTα alone following radiation (Fig. 3.2D). These data suggest that radioprotection following LZAP downregulation likely functions primarily through regulation of p53 transactivation activity.

Stress responsive kinases, ATM and ATR, are rapidly activated after DNA damage and phosphorylate p53 protein at different sites, including Ser15, leading to the disruption of the interaction between p53 and MDM2 with resultant p53 stabilization and activation. Depletion of LZAP by siRNAs reduced levels of Ser15 phosphorylated p53 and total p53 in untreated cells and at several time points following treatment with 5 Gy irradiation (Fig. 3.3A). Despite the overall lower levels of p53 and phospho-Ser15 p53, the timing of p53 induction and p53 phosphorylation at Ser15 after radiation was not altered by LZAP loss, suggesting that LZAP depletion did not affect radiation induction of kinases, but rather decreased initial and stimulated p53 levels.

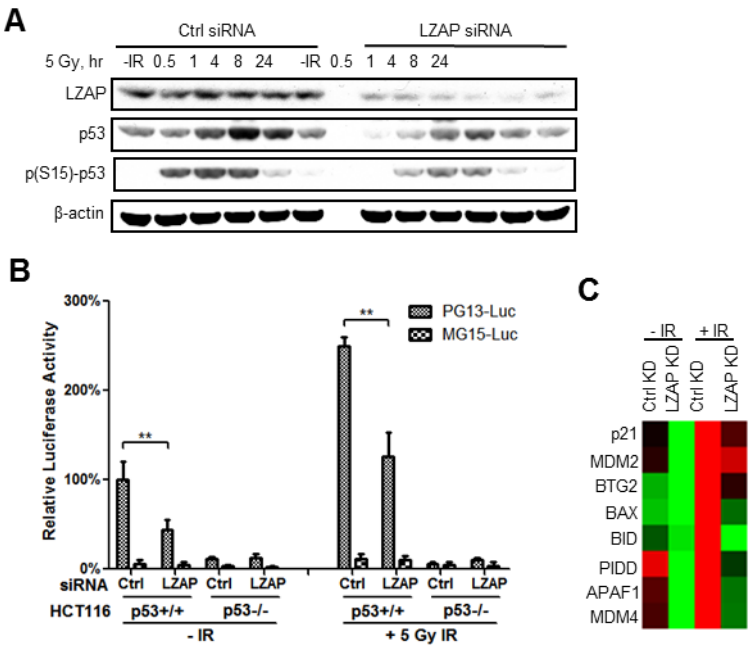

Figure 3.3. LZAP Depletion Inhibits p53 Transcriptional Transactivation

(A) Immunoblot detecting LZAP, total p53 and p(S15)p53 levels in U2OS cells transfected with control or LZAP siRNAs and collected at the indicated time points after 5 Gy radiation.

(B) p53-dependent luciferase activity was determined using the p53 responsive luciferase construct (PG13-Luc) in HCT116 $p53^{+/+}$ cells at basal state and 4 hours after 5 Gy IR with or without siRNA-mediated depletion of LZAP. HCT116$p53^{-/-}$ cells, as well as a mutant luciferase construct not responsive to p53 (MG15-Luc) served as controls.

(C) U2OS cells were transfected with LZAP or control siRNAs. Expression of several p53 responsive genes was determined by p53 Signaling Pathway PCR array in untreated cells or 4 hr after irradiation (5Gy).

To more directly measure the effect of LZAP loss on p53 transactivation, luciferase reporters, containing either p53 responsive elements (PG13-Luc) or mutated p53 responsive elements (MG15-Luc), were transfected into HCT116 $p53^{+/+}$ cells and LZAP levels manipulated by co-transfection with siRNAs. Consistent with findings that depletion of LZAP downregulated p53 and abolished p53 stabilization and phosphorylation after radiation (Fig. 3.3A), LZAP loss diminished p53 transcriptional transactivation activity by approximately 50% in both unstressed and radiated HCT116 $p53^{+/+}$ cells compared to cells transected with control siRNAs (Fig. 3.3B). LZAP loss did not affect the minimal luciferase activity detected following transfection of HCT116 $p53^{-/-}$ cells with p53-reponsive luciferase reporter or transfection of HCT116 $p53^{+/+}$ or $p53^{-/-}$ cells with a luciferase construct containing mutated p53 responsive elements (Fig. 3.3B). To determine if decreased p53 transactivation observed upon LZAP loss affected expression of known p53 target genes, the Human p53 Signaling Pathway PCR array (Qiagen) was used to determine relative mRNA levels of several genes in U2OS cells with and without radiation. Expression of *p21*, *MDM2*, *BTG2*, *BAX*, *BID*, *PIDD*, *APAF-1* and *MDM4* were diminished in cells following LZAP depletion at basal levels and following p53 activation by 4 Gy irradiation (Fig. 3.3C). While depletion of LZAP effectively decreased induction of each p53 target gene following radiation, it was remarkable that loss of LZAP completely inhibited radiation-induced expression of *BID*, *PIDD*, *APAF1* and *MDM4* above basal levels.

LZAP loss sensitized $p53^{-/-}$ cells and protected $p53^{+/+}$ cells following radiation treatment (Fig. 3.2A). To determine if biological consequences of LZAP depletion seen after radiation extended to chemotherapeutic agents having distinct mechanisms of action, cell viability assays were performed following treatment with carboplatin (DNA/DNA and DNA/protein crosslinker), doxorubicin (DNA intercalating agent), and paclitaxel (microtubule stabilizer and anti-mitotic). Regardless of the mechanism of action, loss of LZAP protected HCT116 $p53^{+/+}$ cells and

sensitized isogenic HCT116 $p53^{-/-}$ cells to chemotherapeutic drugs (Fig. 3.4A). Increased sensitivity to these drugs was also observed following LZAP depletion in a human osteosarcoma cells lacking p53 expression (Saos-2) while resistance was observed in similarly treated human osteosarcoma cells that express wtp53 (U2OS) (Fig. 3.4B).

Loss of a Single lzap Allele Protects Murine Bone Marrow Cells from Radiation-induced Cell Death

Depletion of LZAP in cancer cells expressing wtp53 protected them from radiation- or chemotherapy-induced cell death (Fig. 3.2, 3.3 and 3.4); however potential clinical relevance relies on determining the effect of LZAP loss on normal, non-cancer cells. Bone marrow mononuclear cells are exquisitely sensitive to radiation through mechanisms largely attributed to p53-associated apoptosis. Bone marrow sensitivity is the major cause of organismal demise following whole body irradiation and is the major dose-limiting factor for many chemotherapy regimens. Acute bone marrow suppression occurs following total body irradiation; however, p53 inhibition mitigates this syndrome (Komarov et al., 1999; Strom et al., 2006). To begin exploring the effect of LZAP loss on normal cell survival after radiation, wild-type ($LZAP^{+/+}$) and LZAP heterozygous ($LZAP^{+/-}$) mice were irradiated with sublethal doses of total body irradiation (TBI) and clonogenic growth of isolated bone marrow mononuclear cells (BM-MNC) was determined. Mice with homozygous loss of LZAP are not available for study because of early embryonic lethality (less than E4.5 days) as also confirmed in a zebrafish model (Liu et al., 2011). In agreement with observations that p53 was downregulated following LZAP targeting in murine ES cells (Fig. 3.1A), p53 levels in bone marrow cells derived from $LZAP^{+/-}$ mice were lower compared to levels in bone marrow cells from $LZAP^{+/+}$ mice (Fig. 3.5A). Remarkably, upregulation of p53 expression after radiation was dampened in $LZAP^{+/-}$ bone marrow cells compared to wild-type cells (Fig. 3.5A). Radiation did not appreciably alter LZAP levels in either wild-type or LZAP heterozygous bone marrow cells (Fig. 3.5A). To determine if cell survival and

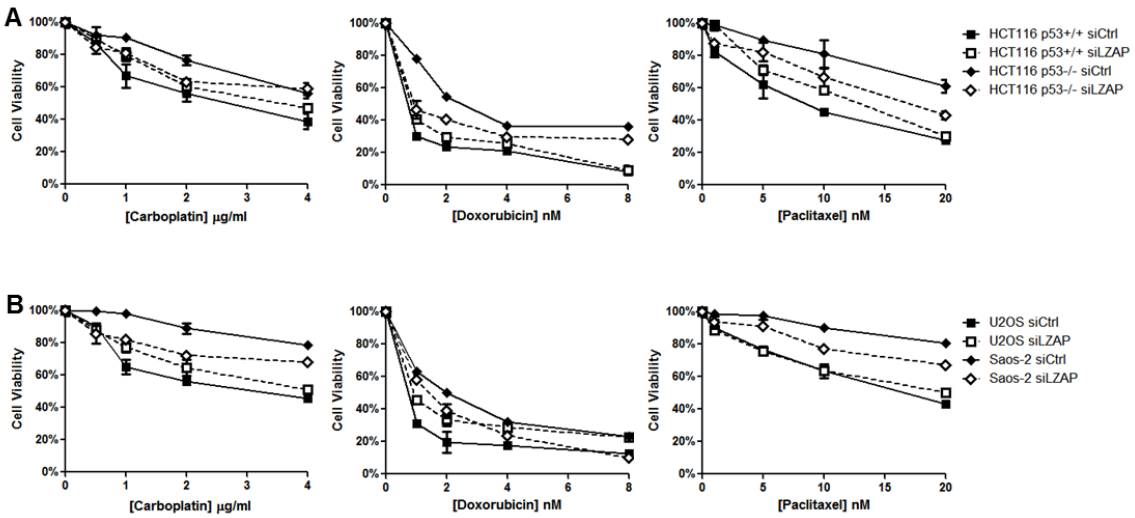

Figure 3.4. LZAP Depletion Alters Cellular Sensitivity to Chemotherapeutic Agents in a p53-dependent Manner

Cell proliferation with and without LZAP knockdown was determined by WST-1 analyses following treatment with the indicated concentration of carboplatin, doxorubicin, and paclitaxel in HCT116 p53+/+ and -/- cells (A) and Saos-2 (p53 null) and U2OS (wtp53) cells (B).

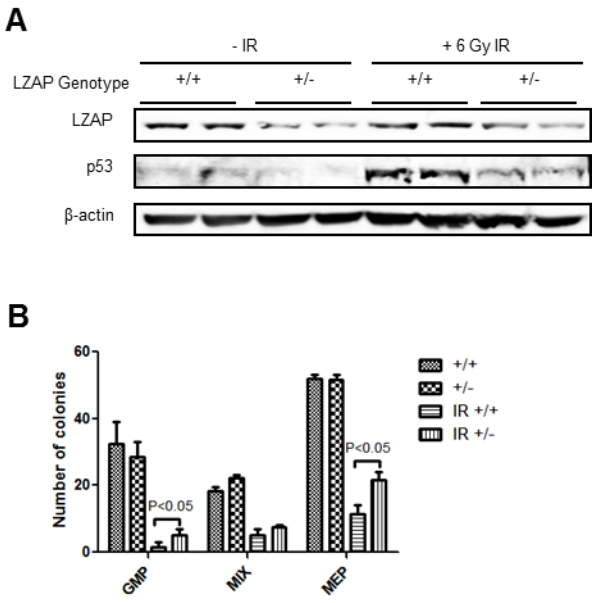

Figure 3.5. Loss of a Single *lzap* Allele Protects Murine Bone Marrow Cells from IR

(A) Immunoblot detecting LZAP and p53 in bone marrow cells derived from $LZAP^{+/+}$ and $LZAP^{+/-}$ mice before and 4 hr after 6 Gy total body irradiation. Immunoblotting of β-actin serves as loading control.

(B) Survival and proliferation of bone marrow progenitor cells derived from untreated wild-type or $LZAP^{+/-}$ mice or littermates treated with 6Gy TBI was determined after 7 days of *in vitro* growth. Granulocyte-macrophage progenitors (GMP) and megakaryocyte-erythroid progenitors (MEP) colonies were identified by colony morphology. Data are presented as mean ± SD (n=4 mice each group).

proliferative capacity differed between BM-MNC derived from wild-type and LZAP$^{+/-}$ mice, BM-MNCs were isolated either after no treatment or 4 hr after total body irradiation. Irradiation decreased colony forming capacity in cells derived from both wild-type and LZAP$^{+/-}$ mice; however, bone marrow progenitor cells derived from LZAP$^{+/-}$ mice of both granulocyte/macrophage (GMP) and megakaryocyte/erythroid (MEP) lineages were significantly protected compared to cells derived from wild-type mice (Fig. 3.5B). These data are consistent with radio- and chemotherapy resistance following LZAP depletion observed in cancer cells expressing wtp53, and suggest that lower LZAP expression driven by loss of a single *lzap* allele in LZAP heterozygous mice is sufficient to render bone marrow mono-nuclear cells more resistant to radiation (Fig. 3.5).

Together, these data suggest that LZAP loss decreases wtp53 levels and inhibits p53 transcriptional transactivation resulting in protection of both cancer and non-cancer wtp53 expressing cells from p53-mediated cell death following exposure to radiation or chemotherapeutic agents.

LZAP Loss Sensitizes Cells Expressing Mutant p53 to Radiation

LZAP depletion correlated with decreased mtp53 protein levels (Fig 3.1D). As opposed to the pro-apoptotic effects of wtp53 in response to therapy, mutations in the *TP53* gene frequently have gain-of-function activity that increases cancer cell therapeutic resistance. Because normal cells will not express mutant p53, inhibition of gain-of-function p53 mutants is an attractive target for anticancer therapy, particularly in combination with radiation and chemotherapy (Oren and Rotter, 2010; Goldstein et al., 2011).

To determine if downregulation of mutant p53 levels following LZAP loss sensitizes cells to radiation, cells were radiated after siRNA-mediated LZAP depletion in p53-null Saos-2 cells

ectopically expressing two different p53 "hot spot" mutants (R175H and R248Q). Clonogenic survival revealed that cells expressing mtp53 were sensitized to radiation upon loss of LZAP (both R175H and R248Q) (Fig. 3.6).

p53 Downregulation in LZAP Depleted Cells is Not Mediated Through ARF, MDM2, or Wip1

To begin exploring potential mechanisms through which LZAP regulates p53 protein levels, dependence on known LZAP binding partners and p53 regulators was tested. We reported that LZAP activates p53 through binding to ARF (Wang et al., 2006); however, neither U2OS nor HCT116 cells express ARF, indicating that ARF is not required for LZAP regulation of p53 levels.

Recently, we reported that LZAP binds and regulates the activity of the wild-type p53-induced phosphatase-1 (Wip1, also called PPM1D) (An et al., 2011). Wip1 dephosphorylates p53 resulting in destabilization and inactivation of p53 (Fiscella et al., 1997), and Wip1 activity sensitizes tumors with inactive p53 to anticancer drugs, while at the same time protects normal tissues via suppressing wtp53 activation (Goloudina et al., 2011). To determine if Wip1 is required for regulation of p53 levels observed upon loss of LZAP, LZAP was depleted by lentiviral shRNA in wild-type and $Wip1^{-/-}$ MEFs. The level of p53 was similarly decreased in cells with and without Wip1 suggesting that Wip1 was not required for p53 regulation by LZAP (Fig. 3.7A).

Although LZAP does not bind HDM2 (Wang et al., 2006), HDM2 is perhaps the most prominent regulator of p53 as indicated by its amplification and overexpression in human cancers and by p53-mediated embryonic lethality observed upon HDM2 deletion. HDM2 binds p53, inhibits its transactivation activity and directly ubiquitinates p53, ultimately leading to its proteasomal degradation. To determine if HDM2 is required for downregulation of p53 protein observed

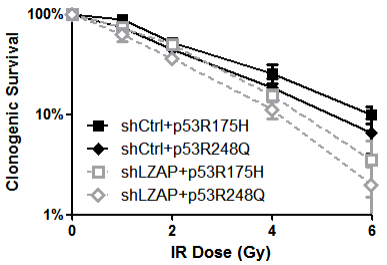

Figure 3.6. LZAP Loss Sensitizes Cells Expressing Mutant p53 to Radiation
Saos-2 cells were co-transfected with siCtrl or siLZAP, and empty vector or p53 mutants R175H or R248Q. Clonogenic survival assay was performed after increasing doses of IR.

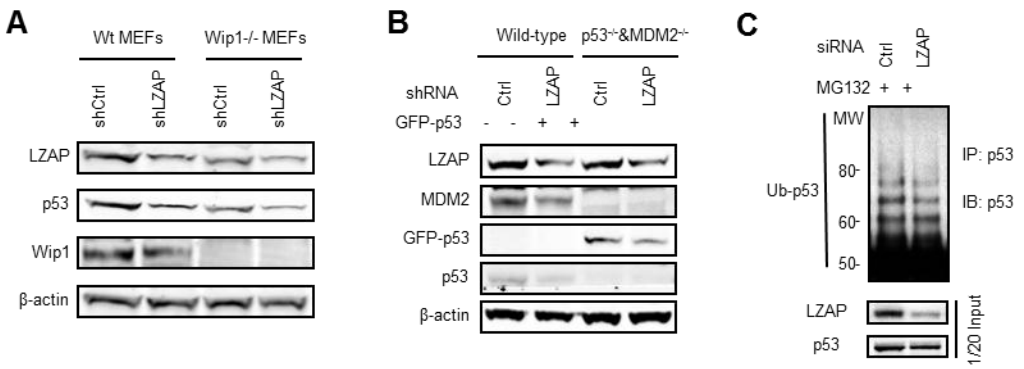

Figure 3.7. p53 Downregulation in LZAP Depleted Cells Does Not Require Mdm2 or Wip1

(A) Immunoblots of LZAP, p53, and Wip1 of lysates derived from wild-type or Wip-1 knockout MEFs with or without LZAP knockdown. Immunoblotting of β-actin serves as loading control.

(B) Immunoblots of LZAP, p53, and MDM2 of lysates derived from wild-type or p53/MDM2 double knockout MEFs transfected with GFP-wtp53 with or without LZAP knockdown. Immunoblotting of b-actin serves as loading control.

(C) Ubiquitination of p53 in U2OS cells with and without LZAP knockdown. p53 ubiquitin ladders were detected by p53 immunoprecipitation and p53 immunoblotting following proteasomal inhibition. Input levels of p53 and LZAP with and without LZAP knockdown are shown (1/20 of input bottom panels).

following LZAP loss, LZAP was depleted by siRNA transfection in wild-type MEFs and MDM2/p53 double null MEFs engineered to ectopically express GFP-wtp53. In cells lacking MDM2, exogenously expressed p53 was efficiently decreased following loss of LZAP (Fig. 3.7B). HDM2 primarily decreases p53 levels through direct ubiquitination that targets p53 for proteasomal degradation. Increased p53 ubiquitination was not observed following proteasomal inhibition in U2OS cells transfected with siRNA targeting LZAP compared to control transfected cells (Fig. 3.7C).

These data suggest that downregulation of p53 protein observed following depletion of LZAP does not require ARF, Wip1, or HDM2.

Depletion of LZAP Downregulates p53 At Multiple Levels

Given that LZAP regulation of p53 was not dependent on ARF, Wip1, or HDM2, *TP53* gene transcription, message translation, and protein stability were explored to better define potential mechanism(s) of p53 downregulation triggered by depletion of LZAP. p53 is important for cellular processes such as cell cycle, differentiation, immune response, metabolism, DNA repair and senescence, and is a potent inducer of apoptosis; therefore, p53 protein levels are tightly regulated by multiple mechanisms (Hupp et al., 2000; Vogelstein et al., 2000). Since protein stability is a major pathway of p53 regulation, the effect of LZAP loss on p53 stability was determined using cycloheximide to inhibit protein synthesis. p53 stability was decreased by approximately 33% (from 57 to 38 min) after siRNA-mediated LZAP depletion (Fig. 3.8A). Co-transfection with a construct driving expression of a siRNA-resistant LZAP restored p53 half-life confirming that loss of LZAP was responsible for p53 destabilization. Interestingly, HDM2 protein level was also decreased after LZAP downregulation in MEFs (Fig. 3.7B) and no induction of p53 ubiquitination was observed in LZAP-depleted U2OS cells (Fig. 3.7C),

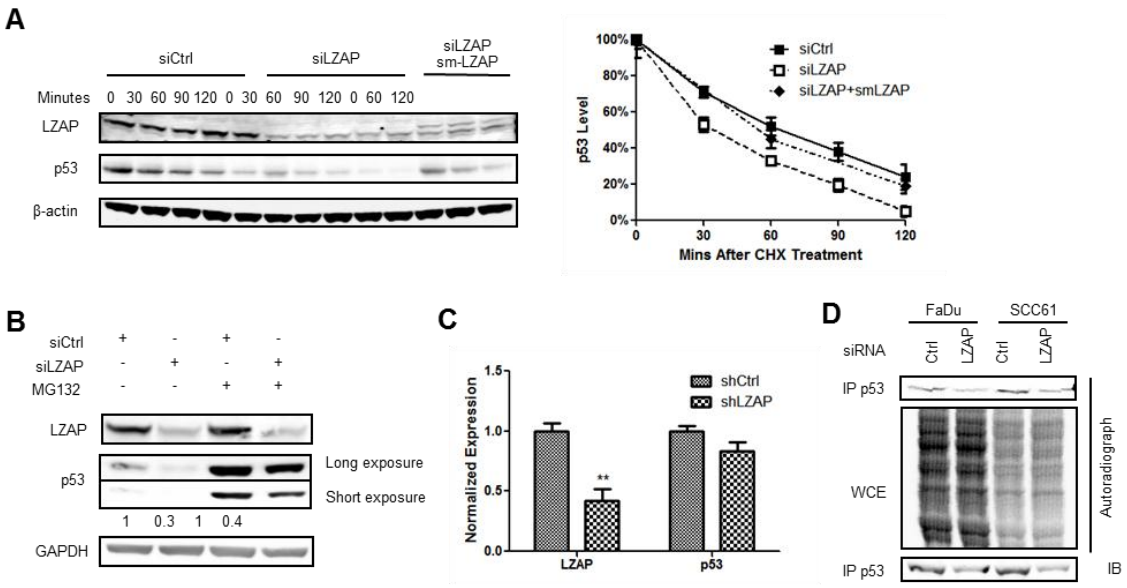

Figure 3.8. LZAP Loss Downregulates p53 Expression at Multiple Levels

(A) LZAP depletion destabilizes p53. Left: Immunoblot detecting LZAP and p53 in U2OS cells with and without LZAP knockdown or in cells with LZAP knockdown and expression of si-RNA resistant LZAP construct (sm-LZAP). Cells were treated with cycloheximide (CHX) for the indicated times. Right: Relative quantification of p53 immunoblots normalized to β-actin.

(B) Proteasomal inhibition only partially restores p53 levels in LZAP depleted cells. Immunoblot detecting p53 and LZAP in U2OS cells with and without LZAP knockdown in the presence or absence of proteasomal inhibitor (MG132). Relative quantification of p53 immunoblots normalized to GAPDH. p53 levels in siRNA control transfected cells were assigned a value of 1 and are compared to similar cells (either with or without MG132) transfected with LZAP siRNA.

(C) *p53* mRNA levels are modestly decreased after LZAP knockdown. qRT-PCR of LZAP and *p53* mRNA in U2OS cells infected by shCtrl or shLZAP normalized to *β-actin*.

(D) LZAP inhibits p53 translation. Translation of p53 in FaDu (mtp53) and SCC61 (wtp53) cells was measured by culturing cells in the present of ^{35}[S]-methionine for 10 min before lysis. Autoradiography of immunoprecipitated p53 (top panel) in cells with and without LZAP knockdown. Autoradiography of whole cell extract (WCE) is a measure of global translation (middle panel). Immunoprecipitation and immunoblotting of p53 demonstrates total p53 levels in cells with and without LZAP knockdown.

suggesting that LZAP regulation of p53 stability is independent of the classic ubiquitin-mediated pathway.

The magnitude of p53 downregulation observed following LZAP depletion (up to 70%) and the inability of the proteasome inhibitor to completely restore p53 in LZAP depleted cells (Fig. 3.8B) suggested that additional mechanism(s) of p53 regulation may be driving LZAP activity toward p53. To determine if LZAP loss regulates p53 other than through protein stability, *TP53* gene transcription and message translation were explored. *TP53* mRNA levels were measured by qRT-PCR with and without LZAP depletion in U2OS cells. LZAP depletion by siRNA resulted in a reproducible small (15%), but not significant decrease of p53 mRNA levels (Fig. 3.8C, $p > 0.05$). However, LZAP depletion dramatically decreased p53 protein level even when ectopic promoters (CMV) were driving p53 transcription (Fig. 3.1D and 3.7B), indicating that p53 transcription is not likely the primary mechanism of p53 regulation by LZAP. To determine if LZAP regulates translation of p53 message, cells were metabolically labeled (^{35}S-methionine) after LZAP depletion. A short metabolic labeling pulse followed by p53 immunoprecipitation and autoradiography revealed that p53 translation was decreased by approximately 70% in unstressed cells independent of p53 mutation status (FaDu expressing mtp53 and SCC-61 expressing wtp53) (Fig. 3.8D). LZAP downregulation did not influence global translation rate as indicated by equivalent ^{35}S incorporation in whole cell lysates derived from cells with and without LZAP knockdown (Fig. 3.8D).

Taken together, these data suggest that loss of LZAP decreases p53 protein stability and slows the rate of TP53 message translation.

LZAP Binds NCL and Modulates NCL Protein Levels

To discover potential protein mediators of LZAP biological activities, LZAP binding partners were identified by mass spectrometry after co-immunoprecipitation using antibodies specific to Flag-tagged LZAP. From potential LZAP-binding proteins identified, NCL was further evaluated because of its reported p53 regulatory activities. Nineteen peptides covering 30.3% of NCL amino acid sequence were identified following LZAP immunoprecipitation (Fig. 3.9), and LZAP and NCL binding was confirmed by reciprocal immunoprecipitation of endogenous proteins from U2OS cell lysate using antibodies specific to either LZAP or NCL (Fig 3.10A). Specificity of LZAP and NCL co-immunoprecipitation was confirmed by immunoprecipitation of identical lysates with non-specific IgG before immunoblotting. Interestingly, NCL regulates p53 at multiple levels. First, it binds the 5' UTR of p53 mRNA, and overexpression of NCL suppresses p53 translation and induction after DNA damage, whereas NCL downregulation increases p53 protein expression (Takagi et al., 2005). Second, depletion of NCL increases p53 protein stability and activity (Yang et al., 2011). Intriguingly, depletion of LZAP in U2OS cells elevated NCL levels even in cells transfected with NCL siRNA (Fig. 3.10B and C). To determine if p53 loss observed after LZAP depletion was dependent on upregulation of NCL, LZAP and NCL were simultaneously depleted by siRNA transfection. As noted above, loss of LZAP partially abrogated the ability of siRNA to deplete NCL; however, incomplete depletion of NCL in LZAP knockdown cells partially restored p53 levels (Fig. 3.10C). Moreover, increased NCL protein expression observed following downregulation of LZAP inversely correlated with decreased p53 protein levels in head and neck cancer cells, irrespective of p53 mutation status (FaDu expressing mtp53 and SCC-61 expressing wtp53) (Fig. 3.10C). Conversely, overexpression of LZAP resulted in substantial decrease in NCL level (Fig. 3.10D).

These data show that LZAP binds to and negatively regulates NCL and that loss of LZAP expression increases NCL protein levels. Importantly, these data suggest that NCL is, at least partially, responsible for LZAP activity to regulate both mutant and wild-type p53.

Figure 3.9. Localization of the peptides identified by mass spectrometry along the NCL protein sequence

The position and length of the peptides are highlighted in gray.

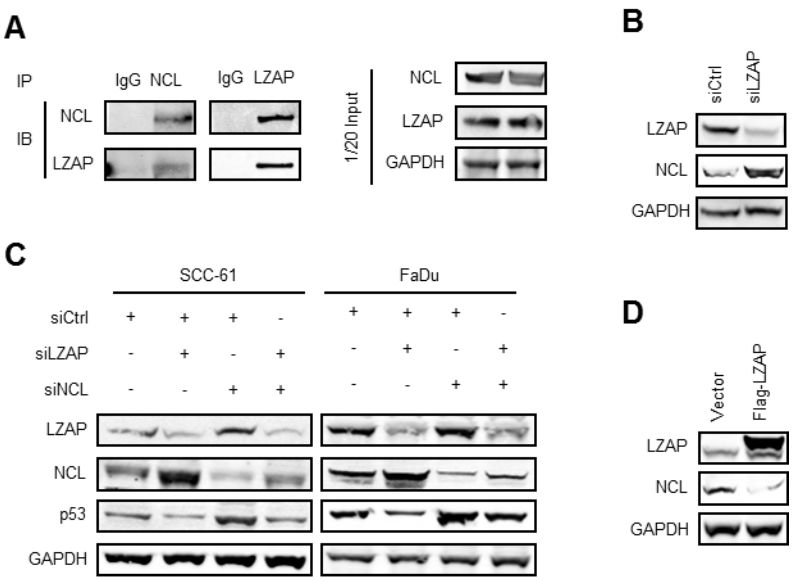

Figure 3.10. LZAP Binds NCL and Negatively Regulates NCL Protein Levels

(A) Co-immunoprecipitation of LZAP and nucleolin. Immunoblots of endogenous LZAP and nucleolin (NCL) after immunoprecipitation with antibodies specific to LZAP or NCL.

(B) Immunoblot detecting LZAP and nucleolin in U2OS cells with and without LZAP knockdown.

(C) Loss of nucleolin at least partially restores p53 expression in LZAP depleted cells. Immunoblots detecting p53 are shown following single knockdown of LZAP or NCL or double knockdown of both LZAP and NCL. Immunoblotting of LZAP and nucleolin confirm knockdown and GAPDH serves as a loading control.

(D) Immunoblot detecting LZAP and NCL in U2OS cells ectopically expressing LZAP. Immunoblotting of GAPDH serves as loading control.

Loss of LZAP Represents a New Mechanism of p53 Inactivation in Head and Neck Cancer

The p53 protein does not function properly in human cancers, being inactivated directly by mutations in the *TP53* gene or indirectly by viral proteins. Alternatively, p53 function can be inhibited by alterations in genes whose products regulate p53 itself or signaling to or from p53 (Hupp et al., 2000; Vogelstein et al., 2000; Lane and Lain, 2002). Altered genes in human cancer that impact p53 function include, but are not limited to: amplification and overexpression of a major negative p53 regulator, HDM2 (Cordon-cardo et al., 1994; Momand et al., 1998); loss of expression of p14ARF, a negative regulator of HDM2 (Iida et al., 2000); overexpression of ΔNp73 (NH2-terminally truncated, transactivation-deficient dominant-negative isoform of p53 homologue p73), which blocks p53 activities (Zaika et al., 2002; Romani et al., 2003; Concin, 2004); mutations in tumor suppressor and phosphatase, PTEN (Mayo et al., 2002); and, disruption of Chk1/2 signaling (Shieh et al., 2000). Our data suggest that depletion of LZAP downregulates steady state p53 levels independent of Wip1, MDM2, or ARF, and inhibits radiation-induced stabilization and activation of wtp53 (Fig. 3.1, 3.2 and 3.7). We previously reported that LZAP protein expression is dramatically decreased in approximately 30% of HNSCC. Combined, findings presented here and previously led us to hypothesize that loss of LZAP may represent a novel mechanism of p53 inactivation in human cancer. To provide support for this hypothesis, human HNSCC (n = 29) (Table 2) were examined to determine if decreased expression of LZAP correlated with decreased expression of p53 protein. Because HPV is recognized to play a role in the pathogenesis of a subset of HNSCCs (e.g. observed in 40-60% oropharynx carcinomas) and HPV inhibits p53 via its E6-mediated degradation, all tumor samples used in these studies were tested for their HPV status as described (Seaman et al., 2010) and shown to be HPV-negative. p53 and LZAP protein levels from immunoblot were quantified and compared between 29 primary tumors. Remarkably, LZAP and p53 levels positively correlated with one another ($R^2 = 0.4$, $p < 0.001$) (Fig. 3.11A, left). If tumors containing mutant

Table 2. Summary of HNSCC patient information.

Number	Age	Gender	Site	Stage	Differentiation	p53 Status	Treatment
1	47	F	Oral Cavity	T4N2	Moderate		S/C/R
2	48	M	Hypopharynx	T1N0	Poor		S/C
3	56	M	Oropharynx	T3N2	Moderate	P80L	S/C
4	48	M	Oropharynx	T4N0	Poor		S/C
5	61	M	Oral Cavity	T4N0	Moderate		S/R
6	66	F	Oral Cavity	T4N0	Poor		S/R
7	77	M	Oral Cavity	T3N0	Moderate		S/R
8	40	M	Oral Cavity	T3N0	Moderate		S/R
9	40	M	Oral Cavity	T3N1	Moderate		S/C/R
10	68	F	Oral Cavity	T2N0	Moderate		S/C
11	64	M	Oral Cavity	T4N0	N/A	S106R	S/R
12	63	F	Oral Cavity	T3N2	Well		S/R
13	57	M	Oropharynx	T2N2	Moderate		S/C
14	68	M	Oral Cavity	T2N2	Poor	G266L	S
15	53	F	Oral Cavity	T4N1	Poor		S/C/R
16	58	F	Oropharynx	T2N0	N/A		S/R
17	57	M	Oral Cavity	T4N0	Moderate		S/R
18	68	F	Oral Cavity	T1N0	Moderate		S
19	45	M	Larynx	T4N2	Moderate	R209^{stop}	S/C
20	59	M	Oral Cavity	T3N2	Well		S/R
21	52	M	Larynx	T2N0	Moderate	P309L, S315F	S/R
22	60	M	Oral Cavity	T2N2	Moderate		S
23	92	F	Oral Cavity	T4N0	Well	G266^{stop}	S
24	59	M	Oropharynx	T2N1	Poor		S/R
25	58	M	Oral Cavity	T4N0	Moderate	S106R	S/R
26	62	M	Oral Cavity	T4N2	Moderate		S/R
27	47	M	Larynx	T3N0	Moderate		S/C/R
28	70	M	Oral Cavity	T1N0	Well		S
29	49	M	Larynx	T4N1	Poor	S106R, K139Q	S/C/R

Note: F - female; M - male
S - surgery; C - chemotherapy; R – radiotherapy
No tumor got distant metastasis and all tumors are HPV negative

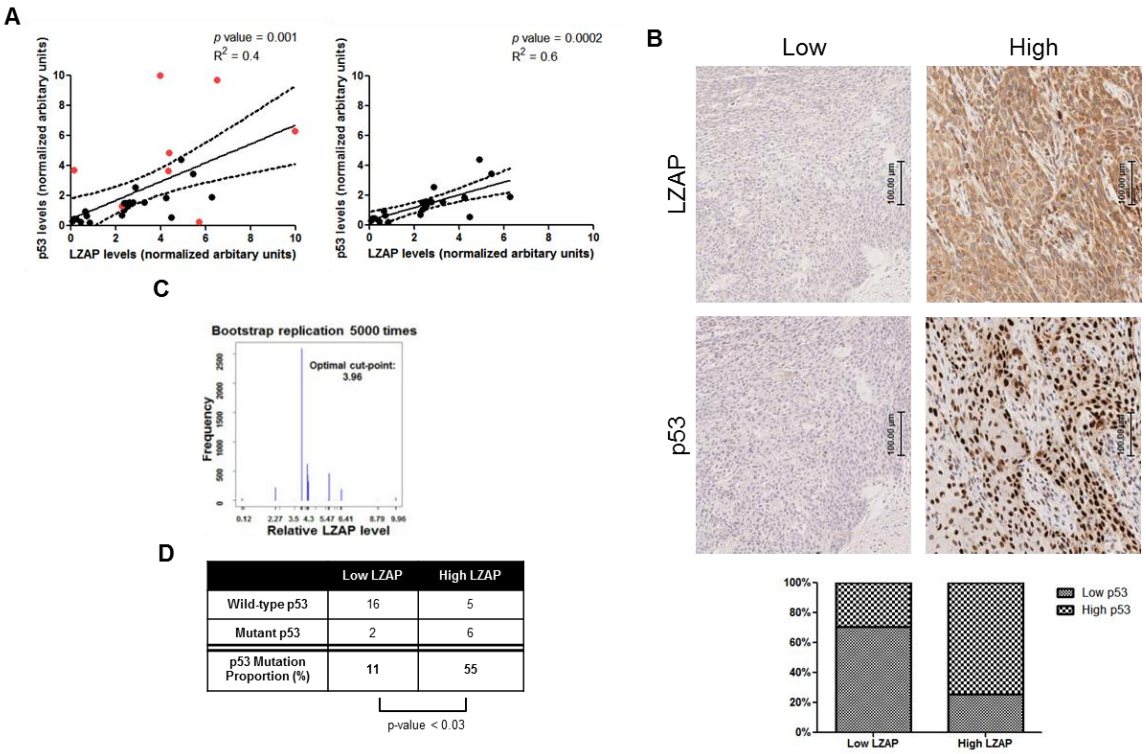

Figure 3.11. LZAP Loss Inactivates p53 in Head and Neck Cancer

(A) Graph of LZAP and p53 levels determined by immunoblot band intensity normalized to GAPDH with best fit (solid line) and 95% confidence (dashed lines) indicated (primary HNSSC, n = 29). Spearman rank correlation p = 0.0004715 (R^2 = 0.4). Exons 4-10 of *TP53* were sequenced; blue dots = wtp53, red dots = mtp53.

(B) Top: Representative photomicrographs of LZAP and p53 IHC in human head and neck squamous cell carcinomas. Bottom: Quantification of IHC (primary HNSSC, n = 29); high LZAP group = strong staining in > 50% of tumors cells, low LZAP group = weak LZAP staining and strong staining in < 50% of tumor cells; similarly high p53 group = strong staining in > 50% of tumors cells, low p53 group = weak p53 staining and strong staining in < 50% of tumor cells The proportions of low and high p53 staining were divided based on low and high LZAP staining. p value < 0.001 analyzed by 2×2 contingency table.

(C) Bootstrap analyses were performed to determine the optimal cut-point of LZAP (3.96) for predicting p53 mutant status. For each Bootstrap replicate, the optimal cut-point of LZAP was determined based on the maximum prediction accuracy (true positive and true negative) which was calculated by using logistic regression.

(D) 29 primary head and neck squamous cell carcinomas were divided into two groups based on an optimal cut-off: "low LZAP" < 3.96 and "high LZAP" > 3.96. The number of cancer samples with wild-type and mutant p53 is indicated. The "low LZAP" group of cancers has a lower proportion of mutated p53 than the "high LZAP" group of cancer ($p<0.03$).

p53 were excluded from analyses, LZAP and p53 levels were even more highly correlated (R^2 = 0.6, $p < 0.0001$) (Fig. 3.11A, right). These findings were confirmed by IHC staining using antibodies specific to LZAP and p53. Only 25% of tumors within "high LZAP" group (strong LZAP IHC in more than 50% of tumor cells) expressed low p53 levels, whereas 71% of "low LZAP" tumors (less than 50% of cells with strong LZAP staining or weak LZAP staining) had low p53 staining intensity ($p < 0.001$) (Fig. 3.11B).

LZAP loss correlated with decreased p53 expression in HNSCC, but to begin determining if the extent of p53 downregulation following LZAP loss is functionally significant, p53 mutation status was determined in 29 head and neck tumors for correlation with LZAP levels. If LZAP-mediated modulation of p53 was functionally significant in tumorigenesis, HNSCCs with low LZAP, and corresponding low p53, should have decreased selection pressure to mutate p53. Among 29 samples 8 tumors expressed mutant *TP53* (Fig. 3.11A, red dots, and Table 2). Segregation of HNSCC into "low LZAP" and "high LZAP" based on optimal LZAP level of 3.96 (Fig. 3.11C), revealed that the incidence of p53 mutations in the low LZAP group was 11% while the incidence of p53 mutations in the high LZAP group was 55% ($p < 0.03$) (Fig. 3.11D).

Together, these data show that LZAP levels correlate with p53 levels in HNSCC. Further, HNSCCs with low LZAP expression display decreased selection pressure to mutant p53, suggesting the loss of LZAP is biologically significant in this tumor type.

Discussion

p53

Previously, we reported that LZAP is lost in about 30% of HNSCC (Wang et al., 2007b). In this study, we discovered that downregulation of LZAP decreased basal p53 protein levels and abrogated p53 accumulation, phosphorylation and transactivation typically observed following

irradiation (Fig. 3.1, 3.2, 3.5 and 3.10). Remarkably, p53 and LZAP protein levels correlated in primary HNSCC, and tumors with downregulated LZAP had decreased pressure to inactivate p53 through mutation (Fig. 3.11). As is typical for many new proteins found to be implicated in cancer, the role of LZAP in cancer development and progression is likely to be dependent on accompanying molecular defects in the tumor, and the complicated nature of these interactions may be beginning to emerge with contradictory reports of LZAP as both an inhibitor of cancer cell growth and invasion and a promoter of cell proliferation and metastasis. Given the importance of known LZAP-binding partners in human cancer (e.g. ARF, p38, Wip1, RelA, Chk1, Chk2) and the dearth of knowledge concerning functional regulation of LZAP through protein-protein interactions or posttranslational modifications, it is also possible that LZAP may play opposing roles in tumor promotion depending on surrounding cellular environment and/or genetic defects co-existing in the tumor. Data reported herein further support LZAP as a tumor suppressor in HNSCC and suggest that activation of p53 is one of its major functions. Squamous cell carcinoma is an epithelial cancer that occurs in organs from different anatomic sites, including the skin, lung, esophagus and urogenital tract. Since SCCs from the head and neck and some other sites share common characteristics (e.g. risk factors, molecular defects and prognostic markers) (Mak et al., 2011), it will be important to determine if LZAP also plays a role in inactivation of p53 in these cancers. In addition larger numbers of HNSCC patients should be examined to determine if LZAP status correlates with prognosis as has been observed for hepatocellular carcinoma (Zhao et al., 2011).

Anticancer Therapies

One very interesting finding of our studies is that LZAP depletion decreased both wild-type and mutant p53 levels (Fig. 3.1 and 3.10) and regulated DNA damage-induced cell death in the p53-dependent manner. Although a treatment strategy of simultaneous temporal downregulation of mutant and wild-type p53 has not been extensively explored, in theory, this strategy should

sensitize tumors with mutant p53 to radiation and chemotherapy and at the same time protect normal, wtp53 expressing tissues. Support for this potential therapeutic strategy was provided by clonogenic survival and proliferation assays revealing that depletion of LZAP in cells with wtp53 expression increased their resistance to radiation and several DNA damaging drugs (Fig 3.2 and 3.4). Remarkably, loss of a single *lzap* allele in mice increased radiation resistance of bone marrow progenitors (Fig. 3.5). In contrast, downregulation of LZAP in cells lacking p53 or expressing mtp53 sensitized cells to DNA damaging agents (Fig. 3.2, 3.4 and 3.6). We focused our study on LZAP activities towards p53, therefore mechanisms of how LZAP depletion alters sensitivity of p53 nulls cells to DNA damage-induced cell death remain to be elucidated. Related to LZAP activity to p53, it is possible that inability of LZAP depleted cells to arrest in G1 phase of cell cycle (Wang et al., 2006; Liu et al., 2011) may increase apoptosis in response to stress signals. Recently, it has been discovered that the immediate activation of p53 upon DNA damage is responsible for toxic side effects, but is not required for the suppression of carcinogenesis (Christophorou et al., 2006). p53 activity is required for prevention of tumors during the period following recovery from DNA damage (Junttila and Evan, 2009), suggesting that temporary inhibition of p53 in normal cells will not increase tumor formation in patients who survive long term. We suggest that transient LZAP depletion or inhibition of LZAP activities toward p53 immediately before and during DNA damaging anticancer therapy could minimize p53-dependent toxicity in normal tissues without decreasing tumor-suppression mediated by p53, which would be activated normally once the temporary inhibition of LZAP activity was relieved.

NCL

Mechanistically, we found that depletion of LZAP downregulated p53 at multiple levels. LZAP has no known enzymatic activity, and diminished p53 levels associated with LZAP depletion were independent of ARF and WIP1 – known LZAP binding proteins, controlling p53, and also independent of MDM2 – a major p53-negative regulator (Fig. 3.7). Interestingly, our data also

suggest that following LZAP depletion, p53 protein was destabilized independent of ubiquitination of p53 (Fig. 3.7C). To identify potential mediators of LZAP activity toward p53, we used mass spectroscopy to determine potential LZAP binding partners. NCL was found and confirmed as an LZAP-associated protein (Fig. 3.9 and 3.10A). Excitingly, we discovered that LZAP regulated NCL protein expression, with depletion of LZAP leading to increased NCL and overexpression of LZAP resulting in decreased NCL protein levels (Fig. 3.10). Further, increased NCL levels observed following LZAP depletion correlated well with decreased p53 protein levels irrespective of p53 mutation status (Fig. 3.10C). These findings are consistent with a described role of NCL as an inhibitor of p53 through decreasing p53 half-life and inhibiting p53 translation.

Elevated expression of NCL has been associated with pathological conditions, including cancer, autoimmunity, viral infection and neurodegenerative processes (Dranovsky et al., 2001; Ugrinova et al., 2007; Call éet al., 2008; Caudle et al., 2009). Despite these links to human disease, little is known about regulation of NCL. The extracellular-regulated kinase (Erk) increases NCL RNA expression and protein half-life in peripheral blood mononuclear cells (Westmark and Malter, 2001), and the RNA binding protein HuR promotes NCL translation, while miR-494 lowers NCL expression by competing with HuR (Tominaga et al., 2011). NCL has been associated with inhibition of HDM2 and p53 stabilization (Saxena et al., 2006), but other studies show that NCL inhibits p53 through both protein destabilization and inhibition of p53 translation (Takagi et al., 2005; Yang et al., 2011). Our data support an inhibitory role of NCL toward p53 specifically after NCL levels were increased following LZAP loss. Although further detailed studies are needed to clarify molecular mechanism(s) and specificity of NCL regulation by LZAP, our data suggest that NCL upregulation following LZAP depletion alters cells sensitivity to DNA damage (e.g. radiation and chemotherapeutic drugs treatment) in a p53-dependent manner.

In summary, these studies have identified a new mechanism of p53 inactivation in human cancer, linking LZAP loss with downregulation of p53 in HNSCC. Remarkably, the pressure to mutate p53 was diminished in HNSCC with low LZAP levels. These data further support LZAP as a tumor suppressor and suggest that loss of LZAP can mitigate p53 activity in tumorigenesis. In the presence of LZAP loss, p53 downregulation was at least partially dependent on LZAP regulation of NCL. LZAP depletion was found to protect normal and tumor cells expressing wtp53 from genotoxic stress, while sensitizing cells without p53 expression or expressing mutant p53 (Fig. 3.12). These findings raise important therapeutic considerations and suggest that strategies or drugs that temporarily inhibit LZAP activity toward p53 may be useful for treating p53 mutant or null cancers while simultaneously protecting normal tissues from DNA damaging therapeutic agents.

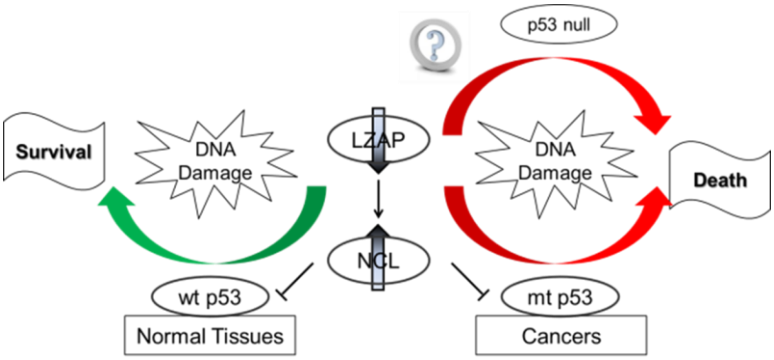

Figure 3.12. Proposed Working Model
Schematic summarizing findings that LZAP loss inactivates p53 in human cancer and modulates cells sensitivity to DNA damage in a p53-dependent manner.

CHAPTER IV

CONCLUSION AND DISCUSSION

Conclusion

LZAP activities are important in development and in tumorigenesis. Understand the biological significance of LZAP and discerning its mechanisms will provide novel insight into normal cellular biology and cancer cell biology. Studies here describe LZAP as a critical regulator of early embryogenesis in zebrafish and mice, and describe LZAP loss as a novel mechanism to decrease p53 activity in human cancer. A clearer understanding of LZAP mechanisms of action and its tumor suppressing function is biologically significant, as results presented here describe a clear opportunity for development of therapeutic strategies for human tumors with LZAP loss or with mutant or null p53.

We discovered LZAP as a novel ARF-binding partner and described LZAP as an activator of p53, both dependent and independent of ARF. Thus, LZAP's tumor suppressor activity is driven by oncogenic stimulation increasing LZAP binding to ARF resulting in p53 activation. We also described that LZAP binds RelA (NF-κB), decreases RelA phosphorylation, inhibits NF-κB transcription, and increases RelA association with HDACs, likely resulting in an inhibitory NF-κB complex on chromatin. Loss of LZAP accelerates tumor cell invasion, as well as xenograft tumor growth and angiogenesis, and is associated with increased expression of select NF-κB targets. Other groups have shown that LZAP accelerates cell death in response to chemotherapeutic agents and alters the G2/M cell cycle checkpoint through inhibition of Chk1 and Chk2. The potential tumor suppressor activities of LZAP have continued to emerge with our description that LZAP expression is lost in 30% of human HNSCC. Human tumor and xenograft mouse tumor data, as well as, LZAP activities as an activator of the p53 pathway and suppressor

of NF-κB activity suggest that LZAP likely functions as a tumor suppressor; however, validation of LZAP tumor suppressor status has been lacking. Recently, we have found and confirmed that LZAP binds the stress activated protein kinase, p38 MAPK. LZAP inhibits p38 phosphorylation and kinase activity, and this LZAP activity is at least partially dependent on the oncogenic phosphatase Wip1. Our preliminary and reported data suggest that LZAP binds Wip1, but variably regulates Wip1 activity toward its substrates possibly dependent on LZAP's ability to bind the substrate, as discussed in the introduction chapter (Table 1). Because LZAP has no conserved enzymatic domains and no known enzymatic activity, potential mediators of LZAP activities were sought by co-immunoprecipitation. We found several potential LZAP-associated proteins including NCL which was explored in this thesis. The number of cancer-centric proteins that LZAP regulates through direct or indirect interactions is remarkable, as we propose in the LZAP network (Fig. 4.1). Interestingly, the majority of LZAP regulated proteins have activities towards p53. Chk1, Chk2 and p38MAPK phosphorylate and activate p53 directly in response to DNA damage, whereas MDM2 and Wip1 are negative regulators of p53. Overexpression of the LZAP-associated protein NCL can suppress p53 translation and destabilize p53 (Fig. 4.1). These findings suggest that the tumor suppressor functions of LZAP can be largely attributed to regulation of p53 tumor suppressor.

To further explore putative tumor suppressor activities of LZAP, we targeted LZAP in mice. However, homozygous LZAP ($LZAP^{-/-}$) knockout in mice resulted in early embryonic lethality, before embryonic day 4.5, which led us to explore developmental defects resulting from LZAP loss. Mice are not the idea model to study the critical functions of LZAP in early embryogenesis, thus, we explored developmental consequences of LZAP loss using zebrafish, which provide an opportunity to examine the earliest cell behaviors in live embryos. LZAP loss using MO in zebrafish results in early embryonic lethality reminiscent of lethality observed in mice. LZAP is

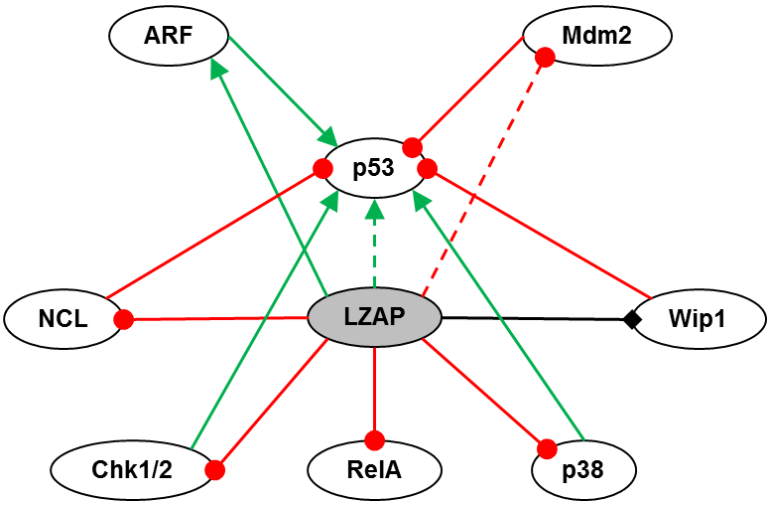

Figure 4.1. Proposed LZAP Network
Schematic summary of LZAP regulated cancer-centric proteins. Proteins are represented by ovals. Solid lines show direct interactions and dashed lines indicate indirect interactions. Green lines represent activating interactions, red lines represent inhibitory interactions, and black arrows represent interactions that can be either inhibitory or activating.

highly conserved at the amino acid level among vertebrates and is maternally deposited. Expression in zebrafish is initially ubiquitous during gastrulation, but later becomes more prominent in the pharyngeal arches, aero-digestive tract, and brain. Antisense MO-mediated depletion of LZAP results in delayed cell divisions and apoptosis during blastomere formation, with resultant fewer, larger cells. Cell cycle analysis in early *lzap* morphant embryonic cells reveals that LZAP loss results in delayed exit from G2/M. Furthermore, LZAP-deficient embryos fail to initiate epiboly—the earliest morphogenetic movement in animal development—which has been shown to be dependent on cell adhesion. Our results strongly implicate LZAP in regulation of cell cycle progression, cell viability and potentially cell adhesion during early development. LZAP also appears to be required for initiation of epiboly. Inhibition of doming and epiboly in *lzap* morphants is exciting and suggest that LZAP activity is required at or before the earliest stages of cellular and tissue differentiation. Loss of LZAP disrupts development at a stage where embryonic cells should maintain a pluripotency, suggesting that LZAP is required for embryonic stem cell maintenance or appropriate cell fate determination.

Here, we also present data supporting a role of LZAP loss as a novel mechanism of inactivation of p53 in human tumors. Downregulation of p53 protein levels and activity following LZAP depletion was observed even after cell exposure to IR. Mechanistically, we found that LZAP regulates p53 at multiple levels (protein translation and protein stability). Since LZAP has no obvious enzymatic domains, LZAP activities described to date are mediated through LZAP associated proteins. To discover potential mediators of ARF-independent LZAP activity toward p53, LZAP binding partners were identified using affinity precipitation and mass spectroscopy. Among others, we identified NCL as an LZAP-associated protein and confirmed endogenous binding between LZAP and NCL in mammalian cells. Excitingly, we discovered that depletion of LZAP resulted in markedly increased NCL protein levels. NCL is an established negative regulator of p53 through both protein destabilization and inhibition of p53 translation. Supporting

a putative role of LZAP as a regulator of p53, we found that low levels of LZAP correlated with decreased p53 protein levels in primary HNSCC. If loss of LZAP indeed represents a new pathway of p53 inactivation in human cancer, tumors with downregulated LZAP would be expected to have decreased pressure to mutate p53. Among primary HNSCCs screened, we found that tumors with "low LZAP" had significantly fewer p53 mutations compared to "high LZAP" specimens. Remarkably, loss of LZAP dramatically reduced both wtp53 and mtp53 protein levels. Mutations of the p53 gene are found in approximately 50% of human tumors and are associated with poor prognosis in many tumors, including HNSCC. Many p53 mutations convey gain-of-function activity that increases resistance to DNA damaging therapy suggesting that inhibition of mutant p53 is a therapeutic strategy to enhance response to conventional chemotherapeutic drugs or radiation. On the other hand, wtp53 activity, while important for prevention of tumor development, is also a driver of injury to non-cancer cells following anticancer therapy. Therefore, transient downregulation or suppression of wtp53 function has long been proposed and experimentally tested as a strategy to protect normal cells during radiation or chemotherapy. Our preliminary data indicate that LZAP loss regulated cell survival after DNA damage dependent on p53-status, with wtp53 cells being protected while mtp53 or null cells were sensitized. This effect was independent of ARF expression. Together, these findings suggest that temporary inhibition of LZAP activity toward p53 could be useful for therapy of p53 mutant tumors by simultaneously sensitizing the tumor to DNA damaging agents (chemotherapy or radiation) while protecting normal surrounding tissue (Fig. 3.12).

Discussion

Our work to study LZAP activity has increased our understanding, but also left many new and exciting areas for future exploration. The diverse roles of LZAP in human cancer and development are only beginning to be explored. Since we have been at the forefront of the LZAP field, we are privileged to speculate about these roles. Here is a partial list of many possibilities.

Does LZAP regulate Wip1 activities, or does Wip1 mediate LZAP activities, or both?

LZAP alters activity of a variety of proteins (p53, Chk1/2, p38, RelA, etc.) which have been implicated of great importance in tumorigenesis (Wang et al., 2006; Jiang et al., 2009; An et al., 2011), and interestingly, these LZAP regulated proteins are also substrates of the Wip1 phosphatase (Takekawa et al., 2000; Fujimoto et al., 2006; Chew et al., 2009). In one of our publications, we found that Wip1 is required for LZAP regulation on p38MAPK and that LZAP increases Wip1 binding to p38 (An et al., 2011), suggesting that Wip1 may also be the mediator of LZAP activity toward proteins whose activity is commonly targeted by both Wip1 and LZAP. Unlike LZAP, which is a putative tumor suppressor, the Wip1 phosphatase has been primarily considered as an oncogenic protein, primarily due to its negative regulation of ARF and p53. In contrast to its dominant oncogenic activities, Wip1 has also been found to dephosphorylate and inhibit oncogenic properties of NF-κB (RelA) signaling, suggesting that Wip1 could also have tumor suppressive. To date, no protein regulators of Wip1 activity or substrate specificity have been described. In table 1, we summarized the common targets of LZAP and Wip1, but we noticed that LZAP directly binds to portion of those. Remarkably, if LZAP binds to Wip1 substrates LZAP and Wip1 have parallel effects on substrate activity; however, if LZAP does not bind to the Wip1 substrate, as is the case for p53 and MDM2, LZAP effect on substrate activity is opposite that of Wip1. Therefore, we hypothesize that LZAP regulation of Wip1 activity depends on LZAP ability to bind those substrates. It is possible that LZAP regulation of Wip1 may reduce much of Wip1 oncogenic activities (e.g. inhibition of p53) while increasing its tumor suppressor activities (e.g. inhibition of RelA).

Our data, particularly findings related to p38, suggest that LZAP may require Wip1 to mediate its effects toward proteins that both LZAP and Wip1 target (e.g. Chk1/2, RelA). Our preliminary data suggest that LZAP and Wip1 bind one another *in vivo* and *in vitro* (data not shown), but the

exact binding domains of each protein remain to be characterized. LZAP truncation mutants will be used to narrow region(s) of LZAP required for Wip1 binding and conserved amino acids within LZAP mutated in attempts to generate LZAP point mutants unable to bind Wip1. LZAP exists as a dimer or polymer (data not shown and Jiang et al., 2009) and polymerization of LZAP may be required for binding to Wip1, which could complicate mapping experiments. Similarly, identification of Wip1 mutants that cannot bind LZAP, but that maintain binding and activity toward Wip1 substrates will be useful to determine the role of LZAP in regulating Wip1 activity.

We believe that creation of LZAP and Wip1 mutant that cannot bind to one another will greatly enhance understanding of the functional relationship between LZAP and Wip1.

LZAP has no reported enzymatic domains or activities, but we and others discovered that it regulates the activities of many associated protein by dephosphorylating them at serine residues. It remains unclear if Wip1 is the only or major mediator of these LZAP activities. Future experiments can determine the role of Wip1 in LZAP-mediated inhibition of RelA and Chk1/2, and LZAP-mediated activation of p53? Based on this work, we may find more potential LZAP regulated proteins and mechanistically explain LZAP activity as a tumor suppressor.

Ultimately we will identify the extent to which Wip1 and LZAP co-regulate one another to promote or inhibit activities important in tumorigenesis.

Does downregulation of LZAP protect organisms from IR?

IR-induced death in mammals is primary due to the induction of apoptosis in radiosensitive organs resulting in two well-described acute radiation syndromes, hematopoietic (HP) syndrome and gastrointestinal tract (GI) syndrome, that result in dose-dependent organismal damage or death (Gudkov and Komarova, 2003). Several lines of evidence reveal that p53 is a major

determinant of IR-induced cell death. First, p53 knockout mice are resistant to IR doses (8-10 Gy) that induce HP syndrome resulting in severe morbidity or mortality (Gudkov and Komarova, 2005). Second, temporary pharmacological inhibition of p53 protects wtp53 expressing cells from radiation and improves survival of wild-type mice through prevention of HP syndrome (Komarov et al., 1999; Strom et al., 2006). p53-induced apoptosis during radiation and chemotherapy is a major cause of severe side effects during the treatment (Botchkarev et al., 2000; Strom et al., 2006), therefore transient downregulation or suppression of p53 function has been suggested as a therapeutic strategy to protect normal cells, and therefore tissues during treatment. However, p53 knockout mice, although being resistant to HP syndrome, at the same time are more sensitive to the higher IR doses (12-20 Gy) that induce GI syndrome, indicating that p53 plays a dual role in response to radiation, inducing apoptosis in hematopoietic tissues, but protecting GI tract cells from cell death at higher radiation doses (Komarova et al., 2004; Kirsch et al., 2010). The mechanisms underlying the protective role of p53 in GI tract is not completely understood, but may be explained the ability of p53 to induce cell cycle arrest or senescence in response to high doses of IR, whereas p53-null cells continue to proliferate leading to mitotic catastrophe and death from unrepaired DNA damage (Gudkov and Komarova, 2003; Komarova et al., 2004).

Our preliminary data suggest that ES cells derived from $LZAP^{+/-}$ mice expressed lower levels of p53 compared to $LZAP^{+/+}$ mice (Fig. 3.1A). Loss of one allele of *lzap* in mice protected bone marrow cells from IR (Fig. 3.5). Remarkably, even after stimulation with radiation, increases in p53 levels and activity was attenuated in bone marrow cells from $LZAP^{+/-}$ mice (Fig. 3.5). Given that p53 is a major driver of apoptosis in bone marrow following IR, we suspected and confirmed that loss of one *lzap* allele in mice protected bone marrow cells from moderate dose of IR (8-10 Gy), suggesting that depletion of LZAP with resultant downregulation of p53 renders cells more resistant to IR.

Several intriguing questions concerning the role of LZAP loss in transgenic mice exist. Because $LZAP^{-/-}$ homozygous knockout mice are not available due to early embryonic lethality, $LZAP^{+/-}$ heterozygous mice, which have been shown to express less LZAP protein in tissues compared to their wild-type siblings, will be used in future experiments. Questions that can be explored include: Will $LZAP^{+/-}$ mice be protected from HP syndrome? And if so, because p53 deficient mice are extremely susceptible to IR-induced carcinogenesis, will mice that survive after radiation have increased or altered tumor incidence, latency or spectrum? Will $LZAP^{+/-}$ mice be sensitized to the IR-induced GI syndrome, as was observed in p53 deficient mice?

Our preliminary results demonstrate that depletion of LZAP in wtp53 cells increased cellular resistance to DNA damaging agents, but has the opposite effect in p53 null and mtp53 cells (Fig 3.2 and 3.4). Given these results it would be interesting to explore if the sensitizing effects of LZAP depletion also occurs *in vivo*. HCT116 $p53^{+/+}$ and $p53^{-/-}$ cell lines can be manipulated for mutant p53 expression and LZAP depletion with controls, and then inoculated into NUDE mice in a xenograft model. Addressing and beginning to understand these questions will provide a much deeper understanding of the role of LZAP downregulation in regulation of cellular sensitivity to IR *in vivo* with potential approaches that could impact clinical cancer care.

What are the molecular mechanisms by which LZAP regulates NCL?

Our preliminary data suggest that depletion of LZAP downregulated p53 at multiple levels, including minimally at the mRNA level, and primarily through increasing p53 translation and protein stability. LZAP effects on p53 occurred regardless of p53 wild-type or mutant status. Interestingly, the proteasome inhibitor MG132, failed to completely restore p53 levels in LZAP depleted cells and LZAP depletion resulted in efficient downregulation of p53 in both MDM2 knockout and wild type MEFs (Fig. 3.7). These data suggest that the classic ubiquitin-proteasome regulation of p53 was not totally responsible for LZAP activity. Neither exogenous nor

endogenous LZAP/p53 complexes were detected in human cells (Wang et al., 2006). Here we showed LZAP bound NCL and depletion of LZAP was associated with upregulation of NCL levels, which correlated well with downregulation of p53 (Fig. 3.10). Although NCL is upregulated in cancer, autoimmune syndromes, Alzheimer's and Parkinson's diseases and other pathological conditions (Caudle et al., 2009), very little is known about regulation of its levels and activities. As such, LZAP may be the first protein regulator of NCL. Therefore, discovery of mechanisms through which LZAP regulates NCL may have broader implications for cancer and other human disease.

The effect of LZAP to alter NCL protein levels will be tested initially by determining NCL stability by using cycloheximide treatment and metabolic labeling with ^{35}S methionine. In addition, because the half-life/stability of NCL and its regulation are not well described, we cannot rule out the possibility that LZAP may affect NCL mRNA expression and/or mRNA stability. Therefore, we determine NCL mRNA levels by qRT-PCR following manipulation of LZAP levels.

NCL is an extraordinary multifunctional protein that is found in multiple cell compartments, including nucleoli, nucleoplasm, cytoplasm and cell surface, with the described roles in transcription and translation, chromatin remodeling and viral infection (Mongelard and Bouvet, 2007; Tajrishi et al., 2011). Detailed molecular mechanisms of many NCL functions are not fully characterized, but subcellular localization of NCL may partially reflect and explain its involvement in different cellular processes. Since a number of stress stimuli have been shown to induce changes in the cellular localization of NCL and since LZAP was in the complex associated with NCL, we are interested in determining whether LZAP alters NCL subcellular localization. Questions that can be addressed include: Do LZAP and NCL co-localize in cells? Does LZAP alter NCL localization or vice versa? Does LZAP alter NCL levels in different compartments?

Does LZAP alter NCL association with other binding partners? Our lab has previously shown that ectopic expressed LZAP primarily localizes to both cytoplasm and nucleus with exclusion from the nucleolus in many cell types, thus there are overlapping compartments for their possible co-localization (Wang et al., 2006).

If we are successful in creating point/deletion mutants of LZAP that are incapable of binding to NCL we will be able to determine to what degree NCL mediates LZAP effects. In particular, we will determine if LZAP mutants incapable of binding NCL will retain ability to regulate p53 levels and activities, and abilities to regulate RelA, p38, Chk1/2 phosphorylation and activity. We also will create a series of NCL mutants and test their LZAP dependency. Identification of LZAP and NCL regions that are important for binding and regulation of activity will create a scientific basis for the future rational design of small molecules that could inhibit LZAP/NCL complex formation and potentially mimic LZAP loss with inhibition of p53.

However, it may be impossible to generate mutants of LZAP (or NCL) that are unable to bind NCL (or LZAP) because of the complicated or extended protein-protein interaction domains or 3D structures. How then can we determine if LZAP depends on NCL given that neither NCL knockout nor transgenic mice have been reported, and no mammalian cell line exists with loss of or inactivating mutations of NCL. Fortunately, we can take an advantage of chicken B lymphocyte (DT40) cells with conditional knockout of NCL (Storck et al., 2009). These cells do not express NCL after 4-hydroxytamoxifen-induced MerCreMer recombinase activity. Once NCL is knocked out, effects of LZAP can be determined.

Here we reported that downregulation of LZAP dramatically increased NCL levels, suggesting that LZAP may be the first protein regulator of NCL. NCL levels, after LZAP knockdown, correlated well, but inversely, with decreased p53 protein levels (Fig. 3.10); however, the exact

mechanisms detailing how LZAP regulates NCL and p53 levels deserves further characterization. NCL binds to the 5' UTR of p53 mRNA and negatively regulates translation of p53 message. Do increased NCL protein levels, as observed following LZAP loss, result in more efficient binding of NCL to the 5' UTR of p53 mRNA? More studies to investigate the molecular mechanisms underlying LZAP regulation of NCL and how this alters p53 levels and signaling will aid the more comprehensively understanding LZAP and NCL effects in cancer and other pathological processes.

Is LZAP loss a more general theme for p53 pathway inactivation in diverse human carcinomas?

The p53 protein does not function properly in human cancers being inactivated directly by mutations in the *TP53* gene or by viral proteins, or indirectly through alterations of genes/proteins which tightly regulate the p53 pathway (Lane, 1998; Hupp et al., 2000; Vogelstein et al., 2000). Our results show that depletion of LZAP downregulated both basal and stimulated p53 levels, and prevented IR-induced p53 stabilization and transcriptional activity (Fig. 3.3). Interestingly, reduced p53 levels in LZAP depleted cells did not depend on ARF, HDM2 or Wip1 (Fig. 3.7). Importantly, we previously reported that LZAP protein expression is lost in approximately 30% of HNSCC (Wang et al., 2007b). Therefore, we hypothesized that loss of LZAP might represent a novel, undescribed pathway to inactivate p53 in human cancer. This hypothesis is supported by data derived from human HNSCC (n = 29) where we demonstrated that LZAP and p53 protein levels correlated. In addition, HNSCCs with low expression of LZAP protein had decreased pressure to inactivate p53 through mutation or loss.

Squamous cell carcinoma (SCC) is an epithelial cancer that occurs in organs from different anatomic sites, including the skin, lungs, esophagus, urinary tract, and cervix. Lung cancer is the leading cause of cancer death in the United States, and approximately 30% of all lung cancers are SCC. Considering that LZAP is downregulated in about 30% of HNSCC and the fact that SCCs

from head and neck and lung show several similarities (e.g. risk factors, molecular characteristics and prognostic markers) (Yan et al., 2011), we are particularly interested to determine if LZAP is also downregulated in lung SCC. Our studies of zebrafish and mouse tissues revealed that LZAP is highly expressed in the gill primordia (in fish) and in lung (in mice); therefore, we are interested to determine if LZAP plays a role in inactivation of p53 in the other major lung cancer histology, adenocarcinoma. Since p53 and LZAP levels correlated by IHC of HNSCC, lung esophageal and other SCC TMAs can be similarly analyzed. After determining if LZAP is lost or downregulated in SCCs from distinct organs, p53 mutations status will be correlated with LZAP expression levels as was done for HNSCC. Such expanded and multi-site TMA studies can help us to determine the spectra of tumors in which LZAP is lost. These studies will identify which tumors may benefit if strategies or drugs that temporarily inhibit LZAP activities toward NCL and/or p53 are developed.

What are the mediator(s) of LZAP activity in p53 null cells?

LZAP depletion renders wtp53 cells more resistant to radiation and DNA damaging drugs, but remarkably LZAP depletion also sensitizes p53 null cells to radio/chemotherapy-induced cell death (Fig. 3.2 and 3.4). These effects are clearly p53-independent because if all LZAP activities in response to DNA damage are mediated by p53, there should not be any obvious difference between p53 null control cells and p53 null LZAP depleted cells. Unlike other tumor suppressors, p53 is rarely deleted or truncated in human cancers. Based on the strong p53-dependent effect of LZAP depletion on DNA damage-induced survival, p53-independent effects of LZAP loss may be less critical for LZAP activity. However, we think it is still important and may help us to understand the full spectrum of LZAP activity. We discovered that depletion of LZAP resulted in remarkable downregulation of $p21^{cip1/waf1}$ not only in HCT116 $p53^{+/+}$ cells, but also in HCT116 $p53^{-/-}$ cells and p53 null Saos-2 cells (data not shown). The cyclin-dependent kinase inhibitor, p21, is a well-known p53 target gene, with a major role in promoting cell cycle arrest in response to

many stimuli (Abbas and Dutta, 2009). Unlike p53 knockout mice, p21 knockout mice are not prone to cancer, suggesting that p53 does not exert its tumor suppressor functions through p21. p21 prevents cell proliferation primarily through inhibiting cyclin/Cdk complexes formation that is required from cell cycle progression. Moreover, loss of p21 has been shown to increase sensitivity to IR, and suppress the development of spontaneous lymphomas (Wang et al., 1997). Therefore, p21 and p21-induced G1 cell cycle arrest are considered to have a protective role following IR-induced DNA damage. Why and how LZAP regulates p21 levels is unclear, but downregulation of p21 in p53 null cells upon LZAP depletion could be one mechanism responsible for sensitization of p53 null cells to radiation following LZAP depletion.

Concluding Remarks

Data presented in this thesis suggest that LZAP is critical for early embryogenesis in zebrafish and mice, and that loss of LZAP is a driver of HNSCC tumorigenesis. This thesis has focused on discovery of mechanisms and biological effects of LZAP in vertebrate development, and on LZAP's function in regulating cancer and normal cell behavior especially sensitivity to DNA damage. We discovered LZAP is critical for normal exit of G2/M of the cell cycle and to prevent apoptosis in early embryos, which may at least partially explain the absence of $LZAP^{-/-}$ mice born following crossing $LZAP^{+/-}$ mice and early embryonic lethality observed in zebrafish following MO depletion. LZAP morphants were unable to survive long enough to initiate the earliest stages of cell movement and differentiation (doming and epiboly). Together these findings suggest that LZAP may be a critical regulator of embryonic stem cell functions such as self-renewal and/or differentiation.

Radiation and DNA damaging chemo-therapies are extensively used as clinical anti-cancer strategies, but their efficacy is limited by toxicity to non-cancer tissues that are at least partially attributed to p53-induced apoptosis in normal cells. Thus, transient downregulation or

suppression of p53 activity has been suggested as a therapeutic strategy to protect normal cells from side effects during anticancer treatment. Mutations in the *TP53* gene occur in approximately half of human tumors and these mutations are associated with aggressive tumor behaviors including resistance to anticancer therapy. Since normal cells do not carry p53 mutations, targeting of mtp53 is a promising anticancer strategy. Although much effort has been expended to restore p53 function to mutant p53 tumors with some success, combined strategy of simultaneous downregulation of both mtp53 in cancerous tissues and wtp53 in normal surrounding tissues has not been extensively addressed, potentially because of lack of a feasible target. Because inhibition of LZAP decreases both wild-type and mutant p53 levels, LZAP may be an ideal target for treating p53 mutant tumors. Our preliminary data suggest that p53 downregulation in LZAP-depleted cells is at least partially due to NCL and that LZAP binds to NCL; therefore, targeting of the LZAP-NCL interaction may be more specific than generalize targeting of LZAP.

Finally, we tested our hypothesis that p53 is inactivated through loss of LZAP in HNSCC, and that cancer cells with downregulated LZAP have reduced pressure to inactivate p53 via mutation. The p53 pathway is inactivated in almost all cancer types. Our work presented here defined LZAP loss as a novel mechanism of p53 inactivation in human cancers. This work will impact several areas of cancer research in both the relatively new LZAP field and the persistently important p53 field.

The results reported herein significantly enhance understanding the role of LZAP in development and tumorigenesis. It is noteworthy that our proposed model begins to provide some structure to understand the diverse functions of LZAP and its other regulated proteins. The p53 LZAP axis seems to be a major driver of LZAP activity and may overshadow other activities, especially in cells with wtp53. Further development and characterization of the detailed mechanisms of how LZAP regulates p53 and NCL will provide further insight into the LZAP activities, as well as the

regulation of p53 pathway, and thus would likely have a broad experimental impact. Owing to the complexity of LZAP interaction with its various binding proteins and the complicated genetic landscape of cancers, additional studies applying our findings to more tumor models and other cancer types such as primary non-small cell lung cancer will help to determine appropriate tumors that will benefit from LZAP inhibitory strategies.

LIST OF REFERENCES

Abbas, T., and Dutta, A. (2009). p21 in cancer: intricate networks and multiple activities. Nature Reviews Cancer *9*, 400–414.

Abrams, E.W., and Mullins, M.C. (2009). Early zebrafish development: it's in the maternal genes. Current Opinion in Genetics & Development *19*, 396–403.

Amon, a (1999). The spindle checkpoint. Current Opinion in Genetics & Development *9*, 69–75.

An, H., Lu, X., Liu, D., and Yarbrough, W.G. (2011). LZAP inhibits p38 MAPK (p38) phosphorylation and activity by facilitating p38 association with the wild-type p53 induced phosphatase 1 (WIP1). PloS One *6*, e16427.

Arendt, D., and Nübler-Jung, K. (1999). Rearranging gastrulation in the name of yolk: evolution of gastrulation in yolk-rich amniote eggs. Mechanisms of Development *81*, 3–22.

Baldwin, A.S. (2001). NF- κ B in defense and disease Control of oncogenesis and cancer therapy resistance by the transcription factor NF-κB. *107*, 241–246.

Banin, S. (1998). Enhanced Phosphorylation of p53 by ATM in Response to DNA Damage. Science *281*, 1674–1677.

Barrallo-Gimeno, A., Holzschuh, J., Driever, W., and Knapik, E.W. (2004). Neural crest survival and differentiation in zebrafish depends on mont blanc/tfap2a gene function. Development (Cambridge, England) *131*, 1463–1477.

Bates, S., Phillips, a C., Clark, P. a, Stott, F., Peters, G., Ludwig, R.L., and Vousden, K.H. (1998). p14ARF links the tumour suppressors RB and p53. Nature *395*, 124–125.

Blandino, G., Deppert, W., Hainaut, P., Levine, a, Lozano, G., Olivier, M., Rotter, V., Wiman, K., and Oren, M. (2012). Mutant p53 protein, master regulator of human malignancies: a report on the Fifth Mutant p53 Workshop. Cell Death and Differentiation *19*, 180–183.

Botchkarev, V.A., Komarova, E.A., Siebenhaar, F., Botchkareva, N.V., Komarov, P.G., Maurer, M., Gilchrest, B.A., and Gudkov, A.V. (2000). p53 Is Essential for Chemotherapy-induced Hair Loss p53 Is Essential for Chemotherapy-induced Hair Loss 1. 5002–5006.

Braakhuis, B.J.M., Snijders, P.J.F., Keune, W.-J.H., Meijer, C.J.L.M., Ruijter-Schippers, H.J., Leemans, C.R., and Brakenhoff, R.H. (2004). Genetic Patterns in Head and Neck Cancers That Contain or Lack Transcriptionally Active Human Papillomavirus. JNCI Journal of the National Cancer Institute *96*, 998–1006.

Bruce, A.E.E., Howley, C., Dixon Fox, M., and Ho, R.K. (2005). T-box gene eomesodermin and the homeobox-containing Mix/Bix gene mtx2 regulate epiboly movements in the zebrafish. Developmental Dynamics : an Official Publication of the American Association of Anatomists *233*, 105–114.

Bulavin, D.V., Amundson, S. a, and Fornace, A.J. (2002a). p38 and Chk1 kinases: different conductors for the G(2)/M checkpoint symphony. Current Opinion in Genetics & Development *12*, 92–97.

Bulavin, D.V., Demidov, O.N., Saito, S., Kauraniemi, P., Phillips, C., Amundson, S. a, Ambrosino, C., Sauter, G., Nebreda, A.R., Anderson, C.W., et al. (2002b). Amplification of PPM1D in human tumors abrogates p53 tumor-suppressor activity. Nature Genetics *31*, 210–215.

Bulavin, D.V., and Fornace, A.J. (2004). p38 MAP Kinase ' s Emerging Role as a Tumor Suppressor. Advances in Cancer Research 95–118.

Bulavin, D.V., Higashimoto, Y., Popoff, I.J., Gaarde, W. a, Basrur, V., Potapova, O., Appella, E., and Fornace, a J. (2001). Initiation of a G2/M checkpoint after ultraviolet radiation requires p38 kinase. Nature *411*, 102–107.

Bulavin, D.V., Phillips, C., Nannenga, B., Timofeev, O., Donehower, L. a, Anderson, C.W., Appella, E., and Fornace, A.J. (2004). Inactivation of the Wip1 phosphatase inhibits mammary tumorigenesis through p38 MAPK-mediated activation of the p16(Ink4a)-p19(Arf) pathway. Nature Genetics *36*, 343–350.

Bulavin, D.V., Saito, S., Hollander, M.C., Sakaguchi, K., Anderson, C.W., Appella, E., and Fornace, a J. (1999). Phosphorylation of human p53 by p38 kinase coordinates N-terminal phosphorylation and apoptosis in response to UV radiation. The EMBO Journal *18*, 6845–6854.

Bykov, V.J.N., Issaeva, N., Shilov, A., Hultcrantz, M., Pugacheva, E., Chumakov, P., Bergman, J., Wiman, K.G., and Selivanova, G. (2002). Restoration of the tumor suppressor function to mutant p53 by a low-molecular-weight compound. Nature Medicine *8*, 282–288.

Bykov, V.J.N., Selivanova, G., and Wiman, K.G. (2003). Small molecules that reactivate mutant p53. European Journal of Cancer *39*, 1828–1834.

Callé, A., Ugrinova, I., Epstein, A.L., Bouvet, P., Diaz, J.-J., and Greco, A. (2008). Nucleolin is required for an efficient herpes simplex virus type 1 infection. Journal of Virology *82*, 4762–4773.

Cao, Y., Zhao, J., Sun, Z., Zhao, Z., Postlethwait, J., and Meng, A. (2004). fgf17b, a novel member of Fgf family, helps patterning zebrafish embryos. Developmental Biology *271*, 130–143.

Caudle, W.M., Kitsou, E., Li, J., Bradner, J., and Zhang, J. (2009). A role for a novel protein, nucleolin, in Parkinson's disease. Neuroscience Letters *459*, 11–15.

Cha, H., Lowe, J.M., Li, H., Lee, J.-S., Belova, G.I., Bulavin, D.V., and Fornace, A.J. (2010). Wip1 directly dephosphorylates gamma-H2AX and attenuates the DNA damage response. Cancer Research *70*, 4112–4122.

Cha, Y.I., Kim, S.-H., Sepich, D., Buchanan, F.G., Solnica-Krezel, L., and DuBois, R.N. (2006). Cyclooxygenase-1-derived PGE2 promotes cell motility via the G-protein-coupled EP4 receptor during vertebrate gastrulation. Genes & Development *20*, 77–86.

Chen, J., Shi, Y., Li, Z., Yu, H., Han, Y., Wang, X., Sun, K., Yang, T., Lou, K., Song, Y., et al. (2011). A functional variant of IC53 correlates with the late onset of colorectal cancer. Molecular Medicine (Cambridge, Mass.) *17*, 607–618.

Cheng, J.C., Miller, A.L., and Webb, S.E. (2004). Organization and function of microfilaments during late epiboly in zebrafish embryos. Developmental Dynamics : an Official Publication of the American Association of Anatomists *231*, 313–323.

Chew, J., Biswas, S., Shreeram, S., Humaidi, M., Wong, E.T., Dhillion, M.K., Teo, H., Hazra, A., Fang, C.C., López-Collazo, E., et al. (2009). WIP1 phosphatase is a negative regulator of NF-kappaB signalling. Nature Cell Biology *11*, 659–666.

Ching, Y.P., Qi, Z., and Wang, J.H. (2000). Cloning of three novel neuronal Cdk5 activator binding proteins. Gene *242*, 285–294.

Choi, J., Nannenga, B., Demidov, O.N., Dmitry, V., Cooney, A., Brayton, C., Zhang, Y., Mbawuike, I.N., Bradley, A., Appella, E., et al. (2002). Mice Deficient for the Wild-Type Exhibit Defects in Reproductive Organs , Immune Function , and Cell Cycle Control Mice Deficient for the Wild-Type p53-Induced Phosphatase Gene (Wip1) Exhibit Defects in Reproductive Organs , Immune Function , and Cell C.

Christophorou, M. a, Ringshausen, I., Finch, a J., Swigart, L.B., and Evan, G.I. (2006). The pathological response to DNA damage does not contribute to p53-mediated tumour suppression. Nature *443*, 214–217.

Concin, N. (2004). Transdominant TAp73 Isoforms Are Frequently Up-regulated in Ovarian Cancer. Evidence for Their Role as Epigenetic p53 Inhibitors in Vivo. Cancer Research *64*, 2449–2460.

Cordon-cardo, C., Latres, E., Drobnjak, M., Drobujak, M., Oliva, M.R., Pollack, D., Woodruff, J.M., Marechal, V., Chen, J., Brennan, M.F., et al. (1994). Molecular Abnormalities of mdm 2 and p53 Genes in Adult Soft Tissue Sarcomas Molecular Abnormalities of mdm2 and p53 Genes in Adult Soft Tissue Sarcomas ’. 794–799.

Cuenda, A., and Rousseau, S. (2007). p38 MAP-kinases pathway regulation, function and role in human diseases. Biochimica Et Biophysica Acta *1773*, 1358–1375.

Dai, C., and Gu, W. (2010). P53 Post-Translational Modification: Deregulated in Tumorigenesis. Trends in Molecular Medicine *16*, 528–536.

Demidov, O.N., Kek, C., Shreeram, S., Timofeev, O., Fornace, a J., Appella, E., and Bulavin, D.V. (2007). The role of the MKK6/p38 MAPK pathway in Wip1-dependent regulation of ErbB2-driven mammary gland tumorigenesis. Oncogene *26*, 2502–2506.

Donehower, L. a, Harvey, M., Slagle, B.L., McArthur, M.J., Montgomery, C. a, Butel, J.S., and Bradley, a (1992). Mice deficient for p53 are developmentally normal but susceptible to spontaneous tumours. Nature *356*, 215–221.

Dong, G., Loukinova, E., and Chen, Z. (2001). Molecular Profiling of Transformed and Metastatic Murine Squamous Carcinoma Cells by Differential Display and cDNA Microarray Reveals Altered Expression of Multiple Genes Related to Growth , Apoptosis , Angiogenesis , and the NF- κ B Signal Pathway Molecu.

Dosch, R., Wagner, D.S., Mintzer, K. a, Runke, G., Wiemelt, A.P., and Mullins, M.C. (2004). Maternal control of vertebrate development before the midblastula transition: mutants from the zebrafish I. Developmental Cell *6*, 771–780.

Dranovsky, A., Vincent, I., Gregori, L., Schwarzman, A., Colflesh, D., Enghild, J., Strittmatter, W., Davies, P., and Goldgaber, D. (2001). Cdc2 phosphorylation of nucleolin demarcates mitotic stages and Alzheimer ' s disease pathology . *22*, 517–528.

Duffy, K.T., McAleer, M.F., Davidson, W.R., Kari, L., Kari, C., Liu, C.-G., Farber, S. a, Cheng, K.C., Mest, J.R., Wickstrom, E., et al. (2005). Coordinate control of cell cycle regulatory genes in zebrafish development tested by cyclin D1 knockdown with morpholino phosphorodiamidates and hydroxyprolyl-phosphono peptide nucleic acids. Nucleic Acids Research *33*, 4914–4921.

Elenitoba-Johnson, K.S.J., Jenson, S.D., Abbott, R.T., Palais, R. a, Bohling, S.D., Lin, Z., Tripp, S., Shami, P.J., Wang, L.Y., Coupland, R.W., et al. (2003). Involvement of multiple signaling pathways in follicular lymphoma transformation: p38-mitogen-activated protein kinase as a target for therapy. Proceedings of the National Academy of Sciences of the United States of America *100*, 7259–7264.

Engelberg, D. (2004). Stress-activated protein kinases-tumor suppressors or tumor initiators? Seminars in Cancer Biology *14*, 271–282.

Eymin, B., Karayan, L., Seite, P., Brambilla, C., Brambilla, E., Larsen, C.J., and Gazzeri, S. (2001). Human ARF binds E2F1 and inhibits its transcriptional activity. Oncogene *20*, 1033–1041.

Fatyol, K., and Szalay, a a (2001). The p14ARF tumor suppressor protein facilitates nucleolar sequestration of hypoxia-inducible factor-1alpha (HIF-1alpha) and inhibits HIF-1-mediated transcription. The Journal of Biological Chemistry *276*, 28421–28429.

Fiscella, M., Zhang, H., Fan, S., Sakaguchi, K., Shen, S., Mercer, W.E., Vande Woude, G.F., O'Connor, P.M., and Appella, E. (1997). Wip1, a novel human protein phosphatase that is induced in response to ionizing radiation in a p53-dependent manner. Proceedings of the National Academy of Sciences of the United States of America *94*, 6048–6053.

Foster, B. a. (1999). Pharmacological Rescue of Mutant p53 Conformation and Function. Science *286*, 2507–2510.

Fujimoto, H., Onishi, N., Kato, N., Takekawa, M., Xu, X.Z., Kosugi, a, Kondo, T., Imamura, M., Oishi, I., Yoda, a, et al. (2006). Regulation of the antioncogenic Chk2 kinase by the oncogenic Wip1 phosphatase. Cell Death and Differentiation *13*, 1170–1180.

Gilmore, T.D. (1999). Multiple mutations contribute to the oncogenicity of the retroviral oncoprotein v-Rel.

Goldstein, I., Marcel, V., Olivier, M., Oren, M., Rotter, V., and Hainaut, P. (2011). Understanding wild-type and mutant p53 activities in human cancer: new landmarks on the way to targeted therapies. Cancer Gene Therapy *18*, 2–11.

Goloudina, A.R., Tanoue, K., Hammann, A., Fourmaux, E., Le, X., and Bulavin, D.V. (2011). Wip1 promotes RUNX2-dependent apoptosis in p53-negative tumors and protects normal tissues during treatment with anticancer agents.

Granero-Moltó, F., Sarmah, S., O'Rear, L., Spagnoli, A., Abrahamson, D., Saus, J., Hudson, B.G., and Knapik, E.W. (2008). Goodpasture antigen-binding protein and its spliced variant, ceramide transfer protein, have different functions in the modulation of apoptosis during zebrafish development. The Journal of Biological Chemistry *283*, 20495–20504.

Graves, P.R., Yu, L., Schwarz, J.K., Gales, J., Sausville, E. a, O'Connor, P.M., and Piwnica-Worms, H. (2000). The Chk1 protein kinase and the Cdc25C regulatory pathways are targets of the anticancer agent UCN-01. The Journal of Biological Chemistry *275*, 5600–5605.

Gu, W., and Roeder, R.G. (1997). Activation of p53 sequence-specific DNA binding by acetylation of the p53 C-terminal domain. Cell *90*, 595–606.

Gubanova, E., Brown, B., Ivanov, S.V., Helleday, T., Mills, G.B., Yarbrough, W.G., and Issaeva, N. (2012). Downregulation of SMG-1 in HPV-positive head and neck squamous cell carcinoma due to promoter hypermethylation correlates with improved survival. Clinical Cancer Research : an Official Journal of the American Association for Cancer Research *18*, 1257–1267.

Gudkov, A.V., and Komarova, E. a (2003). The role of p53 in determining sensitivity to radiotherapy. Nature Reviews. Cancer *3*, 117–129.

Gudkov, A.V., and Komarova, E. a (2005). Prospective therapeutic applications of p53 inhibitors. Biochemical and Biophysical Research Communications *331*, 726–736.

Gudkov, A.V., and Komarova, E. a (2007). Dangerous habits of a security guard: the two faces of p53 as a drug target. Human Molecular Genetics *16 Spec No*, R67–72.

Harrison, M., Li, J., Degenhardt, Y., Hoey, T., and Powers, S. (2004). Wip1-deficient mice are resistant to common cancer genes. Trends in Molecular Medicine *10*, 359–361.

Hasan, M.K., Yaguchi, T., Sugihara, T., Kumar, P.K.R., Taira, K., Reddel, R.R., Kaul, S.C., and Wadhwa, R. (2002). CARF is a novel protein that cooperates with mouse p19ARF (human p14ARF) in activating p53. The Journal of Biological Chemistry *277*, 37765–37770.

Holloway, B. a, Gomez de la Torre Canny, S., Ye, Y., Slusarski, D.C., Freisinger, C.M., Dosch, R., Chou, M.M., Wagner, D.S., and Mullins, M.C. (2009). A novel role for MAPKAPK2 in morphogenesis during zebrafish development. PLoS Genetics *5*, e1000413.

Hui, L., Bakiri, L., Mairhorfer, A., Schweifer, N., Haslinger, C., Kenner, L., Komnenovic, V., Scheuch, H., Beug, H., and Wagner, E.F. (2007). p38alpha suppresses normal and cancer cell proliferation by antagonizing the JNK-c-Jun pathway. Nature Genetics *39*, 741–749.

Hupp, T.R., Lane, D.P., and Ball, K.L. (2000). Strategies for manipulating the p53 pathway in the treatment of human cancer. The Biochemical Journal *352 Pt 1*, 1–17.

Iida, S., Akiyama, Y., Nakajima, T., Ichikawa, W., Nihei, Z., Sugihara, K., and Yuasa, Y. (2000). Alterations and hypermethylation of the p14(ARF) gene in gastric cancer. International Journal of Cancer. Journal International Du Cancer *87*, 654–658.

Ikegami, R., Hunter, P., and Yager, T.D. (1999). Developmental activation of the capability to undergo checkpoint-induced apoptosis in the early zebrafish embryo. Developmental Biology *209*, 409–433.

Jeong, K., Jeong, J.-Y., Lee, H.-O., Choi, E., and Lee, H. (2010). Inhibition of Plk1 induces mitotic infidelity and embryonic growth defects in developing zebrafish embryos. Developmental Biology *345*, 34–48.

Jiang, H., Luo, S., and Li, H. (2005). Cdk5 activator-binding protein C53 regulates apoptosis induced by genotoxic stress via modulating the G2/M DNA damage checkpoint. The Journal of Biological Chemistry *280*, 20651–20659.

Jiang, H., Wu, J., He, C., Yang, W., and Li, H. (2009). Tumor suppressor protein C53 antagonizes checkpoint kinases to promote cyclin-dependent kinase 1 activation. Cell Research *19*, 458–468.

Joly, J.S., Joly, C., Schulte-Merker, S., Boulekbache, H., and Condamine, H. (1993). The ventral and posterior expression of the zebrafish homeobox gene eve1 is perturbed in dorsalized and mutant embryos. Development (Cambridge, England) *119*, 1261–1275.

Junttila, M.R., Ala-Aho, R., Jokilehto, T., Peltonen, J., Kallajoki, M., Grenman, R., Jaakkola, P., Westermarck, J., and Kähäri, V.-M. (2007). P38Alpha and P38Delta Mitogen-Activated Protein Kinase Isoforms Regulate Invasion and Growth of Head and Neck Squamous Carcinoma Cells. Oncogene *26*, 5267–5279.

Junttila, M.R., and Evan, G.I. (2009). p53--a Jack of all trades but master of none. Nature Reviews. Cancer *9*, 821–829.

Kallioniemi, a, Kallioniemi, O.P., Piper, J., Tanner, M., Stokke, T., Chen, L., Smith, H.S., Pinkel, D., Gray, J.W., and Waldman, F.M. (1994). Detection and mapping of amplified DNA sequences in breast cancer by comparative genomic hybridization. Proceedings of the National Academy of Sciences of the United States of America *91*, 2156–2160.

Kamijo, T., Bodner, S., Kamp, E.V.D., Randle, D.H., and Sherr, C.J. (1999). Tumor Spectrum in ARF -deficient Mice Tumor Spectrum in ARF-deficient Mice 1. 2217–2222.

Kamijo, T., Zindy, F., Roussel, M.F., Quelle, D.E., Downing, J.R., Ashmun, R. a, Grosveld, G., and Sherr, C.J. (1997). Tumor suppression at the mouse INK4a locus mediated by the alternative reading frame product p19ARF. Cell *91*, 649–659.

Kane, D. a, Hammerschmidt, M., Mullins, M.C., Maischein, H.M., Brand, M., van Eeden, F.J., Furutani-Seiki, M., Granato, M., Haffter, P., Heisenberg, C.P., et al. (1996). The zebrafish epiboly mutants. Development (Cambridge, England) *123*, 47–55.

Kane, D. a, and Kimmel, C.B. (1993). The zebrafish midblastula transition. Development (Cambridge, England) *119*, 447–456.

Kane, D. a, McFarland, K.N., and Warga, R.M. (2005). Mutations in half baked/E-cadherin block cell behaviors that are necessary for teleost epiboly. Development (Cambridge, England) *132*, 1105–1116.

Kato, T., Duffey, D.C., Ondrey, F.G., Dong, G., Chen, Z., Cook, J. a, Mitchell, J.B., and Van Waes, C. (2000). Cisplatin and radiation sensitivity in human head and neck squamous carcinomas are independently modulated by glutathione and transcription factor NF-kappaB. Head & Neck *22*, 748–759.

Kimmel, C.B., Ballard, W.W., Kimmel, S.R., Ullmann, B., and Schilling, T.F. (1995). Stages of embryonic development of the zebrafish. Developmental Dynamics : an Official Publication of the American Association of Anatomists *203*, 253–310.

Kirsch, D.G., Santiago, P.M., di Tomaso, E., Sullivan, J.M., Hou, W.-S., Dayton, T., Jeffords, L.B., Sodha, P., Mercer, K.L., Cohen, R., et al. (2010). P53 Controls Radiation-Induced Gastrointestinal Syndrome in Mice Independent of Apoptosis. Science (New York, N.Y.) *327*, 593–596.

Kishimoto, Y. (2004). Zebrafish maternal-effect mutations causing cytokinesis defect without affecting mitosis or equatorial vasa deposition. Mechanisms of Development *121*, 79–89.

Ko, L.J., and Prives, C. (1996). P53: Puzzle and Paradigm. Genes & Development *10*, 1054–1072.

Koch, W.M., Joseph, A., Zahurak, M., Goodman, S.N., William, H., Schwab, D., Yoo, H., Lee, D.J., Arlene, A., and Sidransky, D. (1996). p53 Mutation and Locoregional. *88*,.

Komarov, P.G., Komarova, E. a, Kondratov, R.V., Christov-Tselkov, K., Coon, J.S., Chernov, M.V., and Gudkov, a V. (1999). A chemical inhibitor of p53 that protects mice from the side effects of cancer therapy. Science (New York, N.Y.) *285*, 1733–1737.

Komarova, E. a, and Gudkov, a V. (1998). Could p53 be a target for therapeutic suppression? Seminars in Cancer Biology *8*, 389–400.

Komarova, E. a, and Gudkov, a V. (2000). Suppression of p53: a new approach to overcome side effects of antitumor therapy. Biochemistry. Biokhimiia *65*, 41–48.

Komarova, E. a, and Gudkov, a V. (2001). Chemoprotection from p53-dependent apoptosis: potential clinical applications of the p53 inhibitors. Biochemical Pharmacology *62*, 657–667.

Komarova, E. a, Kondratov, R.V., Wang, K., Christov, K., Golovkina, T.V., Goldblum, J.R., and Gudkov, A.V. (2004). Dual effect of p53 on radiation sensitivity in vivo: p53 promotes

hematopoietic injury, but protects from gastro-intestinal syndrome in mice. Oncogene *23*, 3265–3271.

Korgaonkar, C., Hagen, J., Tompkins, V., Frazier, A.A., Allamargot, C., Quelle, F.W., and Quelle, D.E. (2005). Nucleophosmin (B23) Targets ARF to Nucleoli and Inhibits Its Function. *25*, 1258–1271.

Kubbutat, M., Jones, S., and Vousden, K. (1997). Regulation of p53 stability by Mdm2. Nature.

Kumar, A., Takada, Y., Boriek, A.M., and Aggarwal, B.B. (2004). Nuclear factor-kappaB: its role in health and disease. Journal of Molecular Medicine (Berlin, Germany) *82*, 434–448.

Kuo, M.-L., den Besten, W., Bertwistle, D., Roussel, M.F., and Sherr, C.J. (2004). N-terminal polyubiquitination and degradation of the Arf tumor suppressor. Genes & Development *18*, 1862–1874.

Lachnit, M., Kur, E., and Driever, W. (2008). Alterations of the cytoskeleton in all three embryonic lineages contribute to the epiboly defect of Pou5f1/Oct4 deficient MZspg zebrafish embryos. Developmental Biology *315*, 1–17.

Lammers, T., and Lavi, S. (2007). Role of type 2C protein phosphatases in growth regulation and in cellular stress signaling. Critical Reviews in Biochemistry and Molecular Biology *42*, 437–461.

Lane, D.P. (1998). Killing tumor cells with viruses--a question of specificity. Nature Medicine *4*, 1012–1013.

Lane, D.P., and Hupp, T.R. (2003). Drug discovery and p53. Drug Discovery Today *8*, 347–355.

Lane, D.P., and Lain, S. (2002). Therapeutic exploitation of the p53 pathway. Trends in Molecular Medicine *8*, S38–42.

Lavin, M.F., and Gueven, N. (2006). The complexity of p53 stabilization and activation. Cell Death and Differentiation *13*, 941–950.

Leach, F.S., Tokino, T., Meltzer, P., Burrell, M., Oliner, J.D., Smith, S., Hill, D.E., Sidransky, D., Kinzler, K.W., and Vogelstein, B. (1993). p53 Mutation and MDM2 Amplification in Human Soft Tissue Sarcomas Advances in Brief p53 Mutation and MDM2 Amplification in Human Soft Tissue Sarcomas1. 2231–2234.

Leonova, K.I., Shneyder, J., Antoch, M.P., Toshkov, I. a, Novototskaya, L.R., Komarov, P.G., Komarova, E. a, and Gudkov, A.V. (2010). A small molecule inhibitor of p53 stimulates amplification of hematopoietic stem cells but does not promote tumor development in mice. Cell Cycle (Georgetown, Tex.) *9*, 1434–1443.

Lin, F., Chen, S., Sepich, D.S., Panizzi, J.R., Clendenon, S.G., Marrs, J. a, Hamm, H.E., and Solnica-Krezel, L. (2009). Galpha12/13 regulate epiboly by inhibiting E-cadherin activity and modulating the actin cytoskeleton. The Journal of Cell Biology *184*, 909–921.

Liu, D., Wang, W.-D., Melville, D.B., Cha, Y.I., Yin, Z., Issaeva, N., Knapik, E.W., and Yarbrough, W.G. (2011). Tumor suppressor Lzap regulates cell cycle progression, doming, and zebrafish epiboly. Developmental Dynamics : an Official Publication of the American Association of Anatomists *240*, 1613–1625.

Lu, X., Ma, O., Nguyen, T.-A., Jones, S.N., Oren, M., and Donehower, L. a (2007). The Wip1 Phosphatase acts as a gatekeeper in the p53-Mdm2 autoregulatory loop. Cancer Cell *12*, 342–354.

Lu, X., Nannenga, B., and Donehower, L. a (2005). PPM1D dephosphorylates Chk1 and p53 and abrogates cell cycle checkpoints. Genes & Development *19*, 1162–1174.

Lu, X., Nguyen, T.-A., Moon, S.-H., Darlington, Y., Sommer, M., and Donehower, L. a (2008). The type 2C phosphatase Wip1: an oncogenic regulator of tumor suppressor and DNA damage response pathways. Cancer Metastasis Reviews *27*, 123–135.

MJ, P. (2005). The LxxLL motif: a multifunctional binding sequence in transcriptional regulation. Trends in Biochemical Sciences *30*, 63–66.

Ma, C., Fan, L., Ganassin, R., Bols, N., and Collodi, P. (2001). Production of zebrafish germ-line chimeras from embryo cell cultures. Proceedings of the National Academy of Sciences of the United States of America *98*, 2461–2466.

Mak, G.W.-Y., Chan, M.M.-L., Leong, V.Y.-L., Lee, J.M.-F., Yau, T.-O., Ng, I.O.-L., and Ching, Y.-P. (2011). Overexpression of a novel activator of PAK4, the CDK5 kinase-associated protein CDK5RAP3, promotes hepatocellular carcinoma metastasis. Cancer Research *71*, 2949–2958.

Mak, G.W.-Y., Lai, W.-L., Zhou, Y., Li, M., Ng, I.O.-L., and Ching, Y.-P. (2012). CDK5RAP3 Is a Novel Repressor of p14(ARF) in Hepatocellular Carcinoma Cells. PloS One *7*, e42210.

Matsuo, Y., Amano, S., Furuya, M., Namiki, K., Sakurai, K., Nishiyama, M., Sudo, T., Tatsumi, K., Kuriyama, T., Kimura, S., et al. (2006). Involvement of p38alpha mitogen-activated protein kinase in lung metastasis of tumor cells. The Journal of Biological Chemistry *281*, 36767–36775.

Mayo, L.D., Dixon, J.E., Durden, D.L., Tonks, N.K., and Donner, D.B. (2002). PTEN protects p53 from Mdm2 and sensitizes cancer cells to chemotherapy. The Journal of Biological Chemistry *277*, 5484–5489.

McFarland, K.N., Warga, R.M., and Kane, D. a (2005). Genetic locus half baked is necessary for morphogenesis of the ectoderm. Developmental Dynamics : an Official Publication of the American Association of Anatomists *233*, 390–406.

Momand, J., Jung, D., Wilczynski, S., and Niland, J. (1998). The MDM2 gene amplification database. Nucleic Acids Research *26*, 3453–3459.

Mongelard, F., and Bouvet, P. (2007). Nucleolin: a multiFACeTed protein. Trends in Cell Biology *17*, 80–86.

Montero, J., Kilian, B., Chan, J., Bayliss, P.E., and Heisenberg, C. (2003). Phosphoinositide 3-Kinase Is Required for Process Outgrowth and Cell Polarization of Gastrulating Mesendodermal Cells. Current *13*, 1279–1289.

Montero-Balaguer, M., Lang, M.R., Sachdev, S.W., Knappmeyer, C., Stewart, R. a, De La Guardia, A., Hatzopoulos, A.K., and Knapik, E.W. (2006). The mother superior mutation ablates foxd3 activity in neural crest progenitor cells and depletes neural crest derivatives in zebrafish. Developmental Dynamics : an Official Publication of the American Association of Anatomists *235*, 3199–3212.

Musacchio, A., and Hardwick, K.G. (2002). The spindle checkpoint: structural insights into dynamic signalling. Nature Reviews. Molecular Cell Biology *3*, 731–741.

Negron, J.F., and Lockshin, R. a (2004). Activation of apoptosis and caspase-3 in zebrafish early gastrulae. Developmental Dynamics : an Official Publication of the American Association of Anatomists *231*, 161–170.

Neve, R.M., Holbro, T., and Hynes, N.E. (2002). Distinct roles for phosphoinositide 3-kinase, mitogen-activated protein kinase and p38 MAPK in mediating cell cycle progression of breast cancer cells. Oncogene *21*, 4567–4576.

Oren, M., and Rotter, V. (2010). Mutant p53 gain-of-function in cancer. Cold Spring Harbor Perspectives in Biology *2*, a001107.

Orlowski, R.Z., and Baldwin, A.S. (2002). κ B as a therapeutic target in cancer NF-κ. *8*, 385–389.

Palmero, I., Pantoja, C., and Serrano, M. (1998). p19ARF links the tumour suppressor p53 to Ras. Nature *395*, 125–126.

Pfaff, K.L., Straub, C.T., Chiang, K., Bear, D.M., Zhou, Y., and Zon, L.I. (2007). The zebra fish cassiopeia mutant reveals that SIL is required for mitotic spindle organization. Molecular and Cellular Biology *27*, 5887–5897.

Pike, A.C., Brzozowski, A.M., and Hubbard, R.E. (2000). A structural biologist's view of the oestrogen receptor. The Journal of Steroid Biochemistry and Molecular Biology *74*, 261–268.

Poeta, M.L., Manola, J., Goldwasser, M. a, Forastiere, A., Benoit, N., Califano, J. a, Ridge, J. a, Goodwin, J., Kenady, D., Saunders, J., et al. (2007). TP53 mutations and survival in squamous-cell carcinoma of the head and neck. The New England Journal of Medicine *357*, 2552–2561.

Pomerantz, J., Schreiber-Agus, N., Liégeois, N.J., Silverman, a, Alland, L., Chin, L., Potes, J., Chen, K., Orlow, I., Lee, H.W., et al. (1998). The Ink4a tumor suppressor gene product, p19Arf, interacts with MDM2 and neutralizes MDM2's inhibition of p53. Cell *92*, 713–723.

Pomerantz, R.G., and Grandis, J.R. (2004). The epidermal growth factor receptor signaling network in head and neck carcinogenesis and implications for targeted therapy. Seminars in Oncology *31*, 734–743.

Quelle, D.E., Zindy, F., Ashmun, R. a, and Sherr, C.J. (1995). Alternative reading frames of the INK4a tumor suppressor gene encode two unrelated proteins capable of inducing cell cycle arrest. Cell *83*, 993–1000.

Raingeaud, J., Whitmarsh, A.J., Barrett, T., Dérijard, B., Davis, R.J., Raingeaud, L., Whitmarsh, A.J., Barrett, T., De, B., and Davis, R.J. (1996). MKK3- and MKK6-regulated gene expression is mediated by the p38 mitogen-activated protein kinase signal transduction pathway . These include : MKK3- and MKK6-Regulated Gene Expression Is Mediated by the p38 Mitogen-Activated Protein Kinase Signal Transduc. *16*,.

Ramel, M.-C., Buckles, G.R., Baker, K.D., and Lekven, A.C. (2005). WNT8 and BMP2B co-regulate non-axial mesoderm patterning during zebrafish gastrulation. Developmental Biology *287*, 237–248.

Rayet, Â., and Ge, Â. (1999). Aberrant rel / nfkb genes and activity in human cancer. 6938–6947.

Reim, G., and Brand, M. (2006). Maternal control of vertebrate dorsoventral axis formation and epiboly by the POU domain protein Spg/Pou2/Oct4. Development (Cambridge, England) *133*, 2757–2770.

Riebe, C., Pries, R., Kemkers, A., and Wollenberg, B. (2007). Increased cytokine secretion in head and neck cancer upon p38 mitogen-activated protein kinase activation. International Journal of Molecular Medicine *20*, 883–887.

Ried, T., Petersen, I., Holtgreve-grez, H., Speicher, M.R., Sdirã, E., Manoir, S., and Cremer, T. (1994). Mapping of Multiple DNA Gains and Losses in Primary Small Cell Lung Carcinomas by Comparative Genomic Hybridization Mapping of Multiple DNA Gains and Losses in Primary Small Cell Lung Carcinomas by Comparative Genomic Hybridization1. 1801–1806.

Rivlin, N., Brosh, R., Oren, M., and Rotter, V. (2011). Mutations in the p53 Tumor Suppressor Gene: Important Milestones at the Various Steps of Tumorigenesis. Genes & Cancer *2*, 466–474.

Romani, M., Tonini, G.P., Banelli, B., Allemanni, G., Mazzocco, K., Scaruffi, P., Boni, L., Ponzoni, M., Pagnan, G., Raffaghello, L., et al. (2003). Biological and clinical role of p73 in neuroblastoma. Cancer Letters *197*, 111–117.

Saccani, S., Pantano, S., and Natoli, G. (2002). p38-Dependent marking of inflammatory genes for increased NF-kappa B recruitment. Nature Immunology *3*, 69–75.

Saxena, a, Rorie, C.J., Dimitrova, D., Daniely, Y., and Borowiec, J. a (2006). Nucleolin inhibits Hdm2 by multiple pathways leading to p53 stabilization. Oncogene *25*, 7274–7288.

Scheffner, M., Huibregtse, J.M., Vierstra, R.D., and Howley, P.M. (1993). The HPV-16 E6 and E6-AP complex functions as a ubiquitin-protein ligase in the ubiquitination of p53. Cell *75*, 495–505.

Schmitt, C. a, McCurrach, M.E., de Stanchina, E., Wallace-Brodeur, R.R., and Lowe, S.W. (1999). INK4a/ARF mutations accelerate lymphomagenesis and promote chemoresistance by disabling p53. Genes & Development *13*, 2670–2677.

Schulte-Merker, S., van Eeden, F.J., Halpern, M.E., Kimmel, C.B., and Nüsslein-Volhard, C. (1994). no tail (ntl) is the zebrafish homologue of the mouse T (Brachyury) gene. Development (Cambridge, England) *120*, 1009–1015.

Seaman, W.T., Andrews, E., Couch, M., Kojic, E.M., Cu-Uvin, S., Palefsky, J., Deal, A.M., and Webster-Cyriaque, J. (2010). Detection and quantitation of HPV in genital and oral tissues and fluids by real time PCR. Virology Journal *7*, 194.

Selivanova, G., Kawasaki, T., Ryabchenko, L., and Wiman, K.G. (1998). Reactivation of mutant p53: a new strategy for cancer therapy. Seminars in Cancer Biology *8*, 369–378.

Selivanova, G., and Wiman, K.G. (2007). Reactivation of mutant p53: molecular mechanisms and therapeutic potential. Oncogene *26*, 2243–2254.

Sen, R., and Baltimore, D. (1986). Multiple nuclear factors interact with the immunoglobulin enhancer sequences. Cell *46*, 705–716.

Sherr, C.J. (1998). Tumor surveillance via the ARF-p53 pathway. Genes & Development *12*, 2984–2991.

Sherr, C.J., and Weber, J.D. (2000). The ARF/p53 pathway. Current Opinion in Genetics & Development *10*, 94–99.

Shieh, S., Ahn, J., Tamai, K., Taya, Y., and Prives, C. (2000). The human homologs of checkpoint kinases Chk1 and Cds1 (Chk2) phosphorylate p53 at multiple DNA. *1*, 289–300.

Shimizu, T., Yabe, T., Muraoka, O., Yonemura, S., Aramaki, S., Hatta, K., Bae, Y.-K., Nojima, H., and Hibi, M. (2005). E-cadherin is required for gastrulation cell movements in zebrafish. Mechanisms of Development *122*, 747–763.

Shreeram, S., Demidov, O.N., Hee, W.K., Yamaguchi, H., Onishi, N., Kek, C., Timofeev, O.N., Dudgeon, C., Fornace, A.J., Anderson, C.W., et al. (2006). Wip1 phosphatase modulates ATM-dependent signaling pathways. Molecular Cell *23*, 757–764.

Sibon, O.C., Laurençon, a, Hawley, R., and Theurkauf, W.E. (1999). The Drosophila ATM homologue Mei-41 has an essential checkpoint function at the midblastula transition. Current Biology : CB *9*, 302–312.

Sibon, O.C., Stevenson, V. a, and Theurkauf, W.E. (1997). DNA-replication checkpoint control at the Drosophila midblastula transition. Nature *388*, 93–97.

Sidi, S., Goutel, C., Peyriéras, N., and Rosa, F.M. (2003). Maternal induction of ventral fate by zebrafish radar. Proceedings of the National Academy of Sciences of the United States of America *100*, 3315–3320.

Siegel, R., Naishadham, D., and Jemal, A. (2012). Cancer Statistics , 2012.

Skinner, H.D., Sandulache, V.C., Ow, T.J., Meyn, R.E., Yordy, J.S., Beadle, B.M., Fitzgerald, A.L., Giri, U., Ang, K.K., and Myers, J.N. (2012). TP53 disruptive mutations lead to head and

neck cancer treatment failure through inhibition of radiation-induced senescence. Clinical Cancer Research : an Official Journal of the American Association for Cancer Research *18*, 290–300.

Solnica-Krezel, L. (2005). Conserved patterns of cell movements during vertebrate gastrulation. Current Biology : CB *15*, R213–28.

Solnica-Krezel, L. (2006). Gastrulation in zebrafish -- all just about adhesion? Current Opinion in Genetics & Development *16*, 433–441.

Soussi, T., Ishioka, C., Claustres, M., and Béroud, C. (2006). Locus-specific mutation databases: pitfalls and good practice based on the p53 experience. Nature Reviews. Cancer *6*, 83–90.

de Stanchina, E., McCurrach, M.E., Zindy, F., Shieh, S.-Y., Ferbeyre, G., Samuelson, a. V., Prives, C., Roussel, M.F., Sherr, C.J., and Lowe, S.W. (1998). E1A signaling to p53 involves the p19ARF tumor suppressor. Genes & Development *12*, 2434–2442.

Storck, S., Thiry, M., and Bouvet, P. (2009). Conditional knockout of nucleolin in DT40 cells reveals the functional redundancy of its RNA-binding domains. Biology of the Cell / Under the Auspices of the European Cell Biology Organization *101*, 153–167.

Strom, E., Sathe, S., Komarov, P.G., Chernova, O.B., Pavlovska, I., Shyshynova, I., Bosykh, D. a, Burdelya, L.G., Macklis, R.M., Skaliter, R., et al. (2006). Small-molecule inhibitor of p53 binding to mitochondria protects mice from gamma radiation. Nature Chemical Biology *2*, 474–479.

Tajrishi, M.M., Tuteja, R., and Tuteja, N. (2011). Nucleolin: The most abundant multifunctional phosphoprotein of nucleolus. Communicative & Integrative Biology *4*, 267–275.

Takagi, M., Absalon, M.J., McLure, K.G., and Kastan, M.B. (2005). Regulation of p53 translation and induction after DNA damage by ribosomal protein L26 and nucleolin. Cell *123*, 49–63.

Takekawa, M., Adachi, M., Nakahata, a, Nakayama, I., Itoh, F., Tsukuda, H., Taya, Y., and Imai, K. (2000). p53-inducible wip1 phosphatase mediates a negative feedback regulation of p38 MAPK-p53 signaling in response to UV radiation. The EMBO Journal *19*, 6517–6526.

Tamura, S., Toriumi, S., Saito, J.-I., Awano, K., Kudo, T.-A., and Kobayashi, T. (2006). PP2C family members play key roles in regulation of cell survival and apoptosis. Cancer Science *97*, 563–567.

Tang, R., Dodd, A., Lai, D., Mcnabb, W.C., and Love, D.R. (2007). Validation of Zebrafish (Danio rerio) Reference Genes for Quantitative Real-time RT-PCR Normalization. Acta Biochimica Et Biophysica Sinica *39*, 384–390.

Tao, W., and Levine, a J. (1999). P19(ARF) stabilizes p53 by blocking nucleo-cytoplasmic shuttling of Mdm2. Proceedings of the National Academy of Sciences of the United States of America *96*, 6937–6941.

Tergaonkar, V., Bottero, V., Ikawa, M., Li, Q., and Verma, I.M. (2003). I κ B Kinase-Independent I κ B α Degradation Pathway : Functional NF- κ B Activity and Implications for Cancer Therapy I B Kinase-Independent I B ⎵ Degradation Pathway : Functional NF- B Activity and Implications for Cancer Therapy.

Thoms, H.C., Dunlop, M.G., and Stark, L. a (2007). p38-mediated inactivation of cyclin D1/cyclin-dependent kinase 4 stimulates nucleolar translocation of RelA and apoptosis in colorectal cancer cells. Cancer Research *67*, 1660–1669.

Tominaga, K., Srikantan, S., Lee, E.K., Subaran, S.S., Martindale, J.L., Abdelmohsen, K., and Gorospe, M. (2011). Competitive regulation of nucleolin expression by HuR and miR-494. Molecular and Cellular Biology *31*, 4219–4231.

Ugrinova, I., Monier, K., Ivaldi, C., Thiry, M., Storck, S., Mongelard, F., and Bouvet, P. (2007). Inactivation of nucleolin leads to nucleolar disruption, cell cycle arrest and defects in centrosome duplication. BMC Molecular Biology *8*, 66.

Views, E. (2004). An Arf GFP / GFP Reporter Mouse Reveals that the Arf Tumor Suppressor Monitors Latent Oncogenic Signals In Vivo nd io sc ie nc . N ot fo r d is t rib ut n . sc ie nc . N ot fo rib. 239–240.

Vivo, M., Calogero, R. a, Sansone, F., Calabrò, V., Parisi, T., Borrelli, L., Saviozzi, S., and La Mantia, G. (2001). The human tumor suppressor arf interacts with spinophilin/neurabin II, a type 1 protein-phosphatase-binding protein. The Journal of Biological Chemistry *276*, 14161–14169.

Vogelstein, B., Lane, D., and Levine, a J. (2000). Surfing the p53 network. Nature *408*, 307–310.

Wagner, D.S., Dosch, R., Mintzer, K. a, Wiemelt, A.P., and Mullins, M.C. (2004). Maternal control of development at the midblastula transition and beyond: mutants from the zebrafish II. Developmental Cell *6*, 781–790.

Wagner, E.F., and Nebreda, A.R. (2009). Signal integration by JNK and p38 MAPK pathways in cancer development. Nature Reviews. Cancer *9*, 537–549.

Wang, J., An, H., Mayo, M.W., Baldwin, A.S., and Yarbrough, W.G. (2007a). LZAP, a putative tumor suppressor, selectively inhibits NF-kappaB. Cancer Cell *12*, 239–251.

Wang, J., An, H., Mayo, M.W., Baldwin, A.S., and Yarbrough, W.G. (2007b). LZAP, a putative tumor suppressor, selectively inhibits NF-kappaB. Cancer Cell *12*, 239–251.

Wang, J., He, X., Luo, Y., and Yarbrough, W.G. (2006). A novel ARF-binding protein (LZAP) alters ARF regulation of HDM2. The Biochemical Journal *393*, 489–501.

Wang, Y., Elson, A., and Leder, P. (1997). Loss of p21 increases sensitivity to ionizing radiation and delays the onset of lymphoma in atm-deficient mice. Proceedings of the National ….

Waskiewicz, a J., and Cooper, J. a (1995). Mitogen and stress response pathways: MAP kinase cascades and phosphatase regulation in mammals and yeast. Current Opinion in Cell Biology *7*, 798–805.

Weber, J.D. (2000). p53-independent functions of the p19ARF tumor suppressor. Genes & Development *14*, 2358–2365.

Weber, J.D., Taylor, L.J., Roussel, M.F., Sherr, C.J., and Bar-Sagi, D. (1999). Nucleolar Arf sequesters Mdm2 and activates p53. Nature Cell Biology *1*, 20–26.

Weinberg, R. a (1995). The retinoblastoma protein and cell cycle control. Cell *81*, 323–330.

Westmark, C.J., and Malter, J.S. (2001). Up-regulation of nucleolin mRNA and protein in peripheral blood mononuclear cells by extracellular-regulated kinase. The Journal of Biological Chemistry *276*, 1119–1126.

Wilkins, S.J., Yoong, S., Verkade, H., Mizoguchi, T., Plowman, S.J., Hancock, J.F., Kikuchi, Y., Heath, J.K., and Perkins, A.C. (2008). Mtx2 directs zebrafish morphogenetic movements during epiboly by regulating microfilament formation. Developmental Biology *314*, 12–22.

Wilm, T.P., and Solnica-Krezel, L. (2005). Essential roles of a zebrafish prdm1/blimp1 homolog in embryo patterning and organogenesis. Development (Cambridge, England) *132*, 393–404.

Wong, N., Lai, P., Lee, S.W., Fan, S., Pang, E., Liew, C.T., Sheng, Z., Lau, J.W., and Johnson, P.J. (1999). Assessment of genetic changes in hepatocellular carcinoma by comparative genomic hybridization analysis: relationship to disease stage, tumor size, and cirrhosis. The American Journal of Pathology *154*, 37–43.

Yamashita, M. (2003). Apoptosis in zebrafish development. Comparative Biochemistry and Physiology Part B: Biochemistry and Molecular Biology *136*, 731–742.

Yan, W., Wistuba, I.I., Emmert-Buck, M.R., and Erickson, H.S. (2011). Squamous Cell Carcinoma - Similarities and Differences among Anatomical Sites. American Journal of Cancer Research *1*, 275–300.

Yang, A., Shi, G., Zhou, C., Lu, R., Li, H., Sun, L., and Jin, Y. (2011). Nucleolin maintains embryonic stem cell self-renewal by suppression of p53 protein-dependent pathway. The Journal of Biological Chemistry *286*, 43370–43382.

Yarbrough, W.G., Bessho, M., Zanation, A., Bisi, J.E., and Xiong, Y. (2002). Human Tumor Suppressor ARF Impedes S-Phase Progression Independent of p53 Human Tumor Suppressor ARF Impedes S-Phase Progression Independent of p53 1. 1171–1177.

Yin, Z., Jones, G.N., Towns, W.H., Zhang, X., Abel, E.D., Binkley, P.F., Jarjoura, D., and Kirschner, L.S. (2008). Heart-specific ablation of Prkar1a causes failure of heart development and myxomagenesis. Circulation *117*, 1414–1422.

Zaika, a. I., Slade, N., Erster, S.H., Sansome, C., Joseph, T.W., Pearl, M., Chalas, E., and Moll, U.M. (2002). Np73, A Dominant-Negative Inhibitor of Wild-type p53 and TAp73, Is Up-regulated in Human Tumors. Journal of Experimental Medicine *196*, 765–780.

Zamir, E., Kam, Z., and Yarden, a (1997). Transcription-dependent induction of G1 phase during the zebra fish midblastula transition. Molecular and Cellular Biology *17*, 529–536.

Zhang, Y., and Xiong, Y. (1999). Mutations in human ARF exon 2 disrupt its nucleolar localization and impair its ability to block nuclear export of MDM2 and p53. Molecular Cell *3*, 579–591.

Zhang, Y., and Xiong, Y. (2001). Control of p53 ubiquitination and nuclear export by MDM2 and ARF. Cell Growth & Differentiation : the Molecular Biology Journal of the American Association for Cancer Research *12*, 175–186.

Zhang, Y., Xiong, Y., and Yarbrough, W.G. (1998). ARF promotes MDM2 degradation and stabilizes p53: ARF-INK4a locus deletion impairs both the Rb and p53 tumor suppression pathways. Cell *92*, 725–734.

Zhao, J., Pan, K., Li, J., Chen, Y., Chen, J., Lv, L., Wang, D., Pan, Q., Chen, M., and Xia, J. (2011). Identification of LZAP as a new candidate tumor suppressor in hepatocellular carcinoma. PloS One *6*, e26608.

Zindy, F., Eischen, C.M., Randle, D.H., Kamijo, T., Cleveland, J.L., Sherr, C.J., and Roussel, M.F. (1998). Myc signaling via the ARF tumor suppressor regulates p53-dependent apoptosis and immortalization. Genes & Development *12*, 2424–2433.

Zindy, F., Williams, R.T., Baudino, T. a, Rehg, J.E., Skapek, S.X., Cleveland, J.L., Roussel, M.F., and Sherr, C.J. (2003). Arf tumor suppressor promoter monitors latent oncogenic signals in vivo. Proceedings of the National Academy of Sciences of the United States of America *100*, 15930–15935.